`

Effect of hyperoxia on oscillatory brain states in waking and asleep humans

by

Sayeed Devraj-Kizuk

A thesis submitted in partial fulfillment of the requirements for the degree of

Master of Science

Neuroscience
University of Alberta

Abstract

The major question addressed by neuroscience is how behavior can be explained through knowledge of the brain. Given the unobservable nature of mind, cognitive neuroscientists depend on observations of the electrical activity of the brain gleaned through electroencephalographic (EEG) recordings to track gross changes in brain state across multiple levels of behavioral state – from alert wakefulness to deep sleep. Briefly, shifts towards vigilance or arousal are accompanied by a shift towards faster frequencies of neural oscillations in the brain, whereas shifts towards inactivity are accompanied by a preponderance of slower brain rhythms. Brain processing is highly dependent on oxidative metabolism, however studies in rats have shown that the administration of 100% oxygen gas (hyperoxia) results in a paradoxical shift toward more deactivated brain states during both anesthesia and natural sleep. The research here presented was conducted to ascertain if similar effects of hyperoxia are present in awake and sleeping humans. Experiment 1 administered 100% oxygen gas or normal air to participants who were performing an eyes-opened/eyes-closed resting state task. Hyperoxia was associated with decreases in alpha, beta, and gamma oscillations when the eyes were opened, and decreases in beta and increases in delta oscillations when the eyes were closed. We also observed that hyperoxia increased the magnitude of the eyes-opened/eyes-closed state transition. Experiment 2 administered 100% oxygen gas or normal air to participants who were taking a 90-minute nap. Hyperoxia was associated with minor decreases in alpha oscillations in the Wake and N1 stage and increases in theta oscillations in the N2 stage. Taken together, these studies reveal a more complex influence of hyperoxia on EEG oscillations, where high-frequency oscillations are attenuated in some brain states, and low-frequency oscillations are enhanced in others.

Preface

This work was supported by Natural Science a nd Engineering Research Council of Canada (NSERC) discovery grants 2016-06576 and 04792 to Drs. Clayton T Dickson and Kyle E. Mathewson, respectively. This work was also supported by a Branch Out Neurological Foundation summer scholarship to Wesley Vuong. Sayeed Devraj-Kizuk was also partially supported by the Neuroscience and Mental Health Institute of the University of Alberta.

Acknowledgements

I would like to extend a warm appreciation to members of the Attention Perception and Performance Lab and the Brain Rhythms Lab for helping with experiments, as well as my special thanks to my friends and coworkers Wesley Vuong, Raphael Gastrock, Vanessa Tran, and Joanna Scanlon, and my supervisor Clayton Dickson, without whom this work would not have been possible.

Table of Contents

List of Tables

List of Figures

gas condition and eye condition is plotted at every electrode and frequency. Comparisons which were statistically significant at the 0.05 α level are emphasized. The topographical distribution of the statistical effect in this band as well as the magnitude of the raw power in each condition are plotted for each condition. Error bars represent the within-subject SEM. G) The difference spectra for eyes-closed – eyes-opened power across the hyperoxia and normoxia conditions, for electrode F3. Error bars represent the within-subject SEM. As shown, a larger alpha amplitude difference exists in the hyperoxic state between eyes-closed and eyes-opened conditions.

Figure 2.4. Analysis of changes in detected oscillations across electrodes, frequencies, state, and oxygen conditions. A) The $P_{episode}$ spectra across all electrodes, thresholded with the average power spectrum across the whole experiment. Error bars represent the within-subject SEM. B) The t-statistic for the difference due to hyperoxia on eyes-opened $P_{episode}$ is plotted at each electrode and frequency. Comparisons which were statistically significant at the 0.05 α level are emphasized. The topographical distributions of the statistical effect, as well as the percentage of time oscillations were detected in each condition is plotted for each band. Error bars represent the within-subject SEM. C) The same analysis as for B) is presented for the eyes-closed condition. D) The difference spectrum of hyperoxia – normoxia $P_{episode}$ during the eyes-opened condition, from electrode F3. The shaded error plot represents the 95% CI for the difference. E) The difference spectrum of eyes-closed $P_{episode}$, hyperoxia – normoxia, plotted from electrode PO4 to show the observed increase in the delta band. The error bar represents the 95% CI for the difference. F) The $P_{episode}$ spectra thresholded with the averaged power within each gas condition, rather than across all gas conditions showing that the choice of background spectra did not influence the detection of oscillations of different frequencies. G) The F statistic for the interaction between gas condition and eye condition is plotted at every electrode and frequency.

Comparisons which were statistically significant at the 0.05 α level are emphasized. The topographical distribution of the statistical effect in this band as well as the percentage of time oscillations were detected are plotted for each condition. Error bars represent the within-subject SEM. H) The difference spectra for eyes-closed – eyes-opened $P_{episode}$ across the hyperoxia and normoxia conditions, for electrode F3. This shows a larger difference in the hyperoxia condition. Error bars represent the within-subject SEM.

Figure 2.5 Analysis of detected alpha epoch lengths. A) Bar graphs showing the raw power values within detected segments only (detected power) for the six frequency ranges which showed main effects of gas on detected oscillations. Only the beta frequency range of 21.14 – 35.16 Hz in the eyes-opened condition shows a decrease in power within detected segments. Error bars are within-subject SEM. B) Cycle length distributions for detected cycles from the range of 6.8 : 9.3 Hz. Closing the eyes results in longer cycle lengths, for both normoxia and hyperoxia conditions. C) Empirical cumulative distribution function estimated from the pooled cycle length distributions across subjects. Hyperoxia cdfs were significantly more extreme than normoxia cdfs.

Figure 3.1. Experimental procedure. Participants completed two sessions exactly one week apart. Within each session, participants were given 2 minutes to breathe the gas, and then were instructed to attempt to sleep for 90 minutes. The order of the gas condition was counterbalanced between subjects.

Figure 3.2. Expert and algorithmic scoring. A) The scored sleep patterns for our 9 participants for the expert scorer (black) and the BOSC algorithm (red). B) Example 5-second segments of raw EEG data, corresponding to four 5-second segments from one session of one participant which were determined by both the expert and algorithmic scorers to be the awake, N1, N2, and

SWS sleep stages. C) The sleep pattern for one subject's hyperoxia session is shown larger. D) The centered power for that session is shown, averaged across midline electrodes (Oz, Pz, Cz, and Fz). It can be seen that deeper sleep stages correspond to increased power in slower EEG frequencies. E) The detection values are shown for every datapoint in the time and frequency domains, including all detections from the midline electrodes (Oz, Pz, Cz, and Fz). It can be seen that deeper sleep stages correspond to increased detection of slower EEG frequencies. F) The chin EMG RMS for that session is shown. G) The EOG RMS for that session is shown, averaging across the horizontal and vertical electrode dipoles.

Figure 3.3. Physiological Measurements. A) The effect of hyperoxia on the SpO2 change, post-gas-delivery minus pre-gas delivery, is shown. Hyperoxia increased SpO2 values for almost all participants and led to a significant increase across subjects ($t(21) = 6.63$, $p<0.001$). B) The effect of hyperoxia on the heart rate is shown for all collected participants, averaged across the entire session. Hyperoxia decreased heart rate significantly across all subjects ($t(21) = 4.47$, $p<0.001$). C) The effect of hyperoxia on the breathing rate is shown for all collected participants, averaged across the entire session. Hyperoxia had no significant impact on breathing rate across all subjects ($t(21) = 0.63$, *n.s.*).

Figure 3.4. Sleep timing measurements. A) The effect of hyperoxia on the total time spent asleep is shown for the 9 subjects who successfully entered slow wave sleep. There was no effect of hyperoxia on sleep time across all participants ($t(8) = 0.74$, *n.s.*). B) The effect of hyperoxia on the time each subject took to reach the SWS stage is shown. There was no effect of hyperoxia on SWS onset time across all participants ($t(8) = -0.02$, *n.s.*). C) The effect of hyperoxia on the time each subject spent in each sleep stage while asleep is shown, including REM. There was no

effect of hyperoxia on sleep stage time across all participants, for any of the SWS ($t(8) = 0.05$, *n.s.*), N2 ($t(8) = 0.87$, *n.s.*), N1 ($t(8) = -0.29$, *n.s.*), or REM ($t(8) = 0.34$, *n.s.*) stages.

Figure 3.5. Sleep oscillation power measurements. A) The t-statistic for the effect of hyperoxia on the power of oscillations is plotted at every electrode and every frequency, and for each of the four stages of interest (SWS, N2, N1, and Wake). Comparisons which were statistically significant at the 0.05 α-level are emphasized. B) The topographical distribution of the raw-power difference is shown for each of the four sleep stages, at a single frequency of interest for each stage. Significant electrodes are plotted in green. C) The raw power spectra for both the normoxia and hyperoxia conditions are shown, for each sleep stage, and at a single electrode of interest. It can be observed how the sleep stage affects the overall shape of the spectral density distribution. D) The effect of hyperoxia on raw oscillation power is shown for each subject, and at a single frequency and electrode of interest. As this frequency and electrode were chosen post-hoc, the difference should be considered an overestimation of the real effect of hyperoxia at a given stage. At the electrodes and frequencies chosen, significant effects of hyperoxia were observed at the SWS ($t(8) = 2.7668$, $p = 0.024418$), N2 ($t(8) = 2.9305$, $p = 0.018983$), N1 $t(8) = 2.8607$, $p = 0.02113$), and Wake ($t(8) = 2.596$, $p = 0.031814$) stages.

Figure 3.6. Sleep oscillation $P_{episode}$ measurements. A) The t-statistic for the effect of hyperoxia on the detection of oscillations in plotted at every electrode and every frequency, and for each of the four stages of interest (SWS, N2, N1, and Wake). Comparisons which were statistically significant at the 0.05 α-level are emphasized. B) The topographical distribution of the $P_{episode}$ difference is shown for each of the four sleep stages, at a single frequency of interest for each stage. Significant electrodes are plotted in green. C) The $P_{episode}$ spectra for both the normoxia and hyperoxia conditions are shown, for each sleep stage, and at a single electrode of interest. It

can be observed how the sleep stage affects the overall shape of the oscillation detection distribution. D) The effect of hyperoxia on oscillation detections is shown for each subject, at a single electrode of interest, but using pre-determined ranges for the spindle (11.5-16 Hz), theta (3.5-7 Hz), and alpha (7-14 Hz) frequency bands. As the frequency band and electrode were chosen post-hoc, the difference should be considered an overestimation of the real effect of hyperoxia at a given stage. At the electrodes and frequencies chosen, significant effects of hyperoxia were observed at the SWS ($t(8) = 2.65$, $p = 0.03$), and N1 $t(8) = 2.32$, $p = 0.049$) stages, whereas trending effects were found at the N2 ($t(8) = -1.93$, $p = 0.09$) and REM ($t(8) = 1.94$, $p = 0.088$) stages.

1. GENERAL INTRODUCTION

Part A) Oscillatory brain states

1.1.1 State dependent brain activity

Oscillations are an integral part of our world, and thus of the design and function of our brains. Much of life on this planet undergoes alternations throughout the day between more active and more inactive patterns of movement, goal-seeking, foraging etc., which can be understood as regular alternations in observable behavior yoked to the oscillatory revolution of the earth on its axis. In addition, the patterns of brain activity associated with these shifts in behavioral state are made up of different patterns of 'neural' oscillations, wherein populations of neurons synchronize their firing to the same rhythm, generating an electrical wave large enough to be detected by a nearby electrode (Lopes da Silva, 1991). These electrical oscillations are usually larger in amplitude and slower in frequency when very large numbers of neurons synchronize their firing across many brain regions, which is characteristic of inactive behavioral states (Knyazev, 2012). Conversely, active behavioral states are associated with low amplitude, fast oscillations generated locally within many neural populations (Von Stein & Sarnthein, 2000). Lastly, the daily transitions between fast and slow oscillatory states are actually made up of a complex set of nested circadian and ultradian rhythms (Shannahoff-Khalsa, 2007), which as we will see in the example of REM and NREM sleep, play a major role in the evolution of brain state across the day-night cycle.

One of the main benefits of neurophysiology is that shifts in behavioral state can be correlated with changes in the electrical activity produced by the brain. Using electrodes placed either on the surface of the scalp, or inside the skull, an investigator can deliver an environmental stimulus to a subject, and then measure the response of nearby neurons. Carefully employing this

technique, investigators have discovered that the dynamics of neural oscillations in the brain are intrinsically linked to behavioral state, such that shifts towards vigilance or arousal are accompanied by a shift towards faster frequencies, and shifts towards inactivity are accompanied by a preponderance of slow brain rhythms (Steriade, 2005). This discovery suggests that neural oscillations are intrinsically related to the neural mechanisms which transition between and maintain brain states (Lopes da Silva, 1991).

The discovery of a neural correlate of behavioral state has resulted in a trend in recent years towards measuring spontaneous brain activity pre-stimulus, as opposed to stimulus-evoked activity (Busch & VanRullen, 2010; Busch, Dubois, & VanRullen, 2009; Gonçalves et al., 2006; Hanslmayr et al., 2007; Klimesch, Sauseng, Hanslmayr, Gruber, & Freunberger, 2007; Romei et al., 2008; Sauseng, Klimesch, Gerloff, & Hummel, 2009), and this reflects a growing understanding that the brain's response to an external stimulus is very much influenced by its internal state. Furthermore, the preponderance of articles from the last decade or so relating integrative, global aspects of neural functioning to interactions among oscillations in multiple frequency bands reflects a growing understanding that neural oscillations, and especially their relationship to one another, are crucial to communication on the whole-brain scale (Donner & Siegel, 2011; Fries, 2005, 2015; Jensen, Gips, Bergmann, & Bonnefond, 2014; Pomper, 2014).

1.1.2 Importance of oscillations and synchronization

One of the reasons that the body shows such a variety of endogenous rhythms may be to allow the nervous system to synchronize its operations with external periodicities in the environment as well as other internal periodicities (Buzsáki & Draguhn, 2004). Oscillatory systems share information through a process known as synchronization, where the phases of the two connected oscillators align, if certain conditions are met. These conditions vary according to

the type of oscillator in the brain (Osipov, Kurths, & Zhou, 2009). In one formulation, proposed by György Buszáki in 2006 neural oscillations in the brain create a 'tensegrity' equilibrium state (Buzsáki, 2006), by which he means a system of oscillators that exert synchronizing force on each other, but are not capable of synchronizing fully, and thereby reach some form of equilibrium state.

A system of oscillators connected to each other will tend to synchronize their periods (Osipov et al., 2009). If the periods are harmonics of each other, the two oscillators synchronize, however, if the periods are nonharmonic (Buszáki suggests that in humans, the periods are related by a factor of e, or ~2.72), then they will exert an influence on each other but not reach full synchronization. If one oscillator is driven externally, the increased energy will draw the equilibrium state into a state that is dominated by that oscillator. When the external drive (stimulus) is removed, the oscillator returns to its previous level of firing, and the chaos state returns. This tensegrity principle allows brain states, as defined by a preponderance of a certain kind of neural oscillation, to develop and dissipate rapidly, though the relative power of various neural oscillators.

Evidence for oscillation synchronization can be found in the corticothalamic system in sleep (Steriade, 2003). Two distinct types of delta oscillations (1 – 4 Hz) are generated in the brain, one by the thalamus and one by the cortex, and they appear to synchronize their phases, demonstrating the ability of low-frequency oscillations to communicate information quickly across large distances. When TC neurons are hyperpolarized during the descent into deep sleep, the thalamic delta oscillation to predominates over the spindle (11.5 – 16 Hz) oscillation, demonstrating the property of oscillatory power "trading off" between frequency bands as brain states change. Slow oscillations produced by the cortex during deep sleep also have the property

of grouping thalamic NREM oscillations and fast oscillations by the phase of the slow oscillation.

Another piece of evidence comes from research on visual processing. Gamma oscillations (30 – 200 Hz) are thought to allow local, and perhaps distant, neural assemblies to 'bind' their processing of distinct features of a single visual object into a single interacting cell assembly (Benchenane, Tiesinga, & Battaglia, 2011; Buzsáki & Schomburg, 2015; Roux & Uhlhaas, 2014). A recently proposed framework (Jensen et al., 2014) suggests that the power of high-frequency gamma oscillations in the brain is modulated by the phase of lower-frequency alpha oscillations (7 – 14 Hz) such that gamma power is totally suppressed and reset at a certain phase of the alpha rhythm. The phase of the alpha oscillation then, in this framework, serves to provide a temporal window for visual processing, resetting the mechanisms of visual processing and feature-binding with every new period of the alpha oscillation (Bonnefond & Jensen, 2013; Gips, van der Eerden, Jensen, & Foxe, 2016; Jensen et al., 2014).

Part B) Neural oscillations in Cognitive Neuroscience

Hans Berger, the inventor of EEG, observed in 1929 that simply by having his subject close his eyes he could elicit a consistent oscillation, larger in amplitude and slower in frequency than the preceding activity, and with a regular period of ~100 ms, and he called this the "alpha oscillation". In contrast, when the eyes were opened, the "beta" oscillation predominated, which was faster, lower in frequency, and in general more disorganized. In 1934, a well-known physiologist (Adrian & Matthews, 1934a) repeated Berger's experiments and described the alpha rhythm as:

> a pulsating activity which develops in the occipital lobe and involves a considerable number of neurones working synchronously … [which] can only occur in a group of

> neurones when the conditions of excitation are uniform throughout the group. When this obtains the neurones will all discharge at the same frequency and they may come to work in phase with one another as a result of their interconnection (pp. 371-372).

Decades later, Lopes da Silva (1991) published an influential review describing how the cortical alpha oscillation is generated by the pulvinar nucleus of the thalamus and then projected through TC neurons to disparate locations in the cortex, and then spread further through cortico-cortical connections. Drawing further on evidence that theta oscillations in the hippocampus and spindle oscillations in the thalamus both serve a "gating function" by blocking transmission between the cortex and the midbrain, but also that cortical beta and gamma oscillations synchronize in response to stimulation, he concluded that "oscillatory mechanisms have emerged as the mechanism of choice for a neural mass … to switch between different behavioral modes." (p. 91).

Research into the functional significance of neural oscillations in humans makes extensive use of electroencephalography (EEG) and magnetoencephalography (MEG) because of the high temporal resolution (up to a millisecond) offered by these techniques (Lopes da Silva, 2013). Most studies observe either spontaneous resting-state activity, or stimulus-evoked activity through the event-related synchronization or desynchronization (ERS/ERD) technique (Neuper, Wörtz, & Pfurtscheller, 2006). This technique uses well-validated tasks from cognitive psychology to induce cognitive events and measures the associated shifts in neural oscillations. In human EEG research, there are five commonly used frequency bands of neural oscillations: delta (1 – 4 Hz), theta (~ 3.5 – 7 Hz), alpha (~ 7 – 14 Hz), beta (~ 15 – 30 Hz), and gamma (~ 30 – 200 Hz), each of which likely reflect several different neural processes using similar frequency channels.

1.2.2 Delta oscillations

Delta oscillations (0.5 – 3.5 Hz) in humans are observed primarily during the deepest stages of sleep, but also during states of severe brain damage and early in development (Knyazev, 2012). Three types of "slow-waves" (0.1 – 3.5 Hz) dominate the deepest stages of sleep, the slow oscillation (< 1 Hz) and the two types of delta oscillation (1 – 3.5 Hz), clock-like delta recorded from the thalamus and cortical delta. During sleep, clock-like delta oscillations appear to be associated with the disconnection of the brain from sensory stimulation during the descent into deep sleep (Steriade, 2003), and EEG (cortical) delta oscillations appear to be associated with autonomic events as well as the length of time a person stayed awake, leading Knyazev (2012) to suggest that delta oscillations represent evolutionary ancient metabolic and homeostatic processes. In contrast, delta oscillations during sleep have been linked to some aspects of memory consolidation (Walker & Stickgold, 2004), memory reactivation (Batterink, Creery, & Paller, 2016; Wilson & McNaughton, 1994), and waking task requirements (Poe, Walsh, & Bjorness, 2010). The slow oscillation is generated in the cortex and likely has the property of modulating other slow waves during slow-wave sleep (Steriade, 2003).

One recent review of event-related delta oscillations found that increased delta power was associated with concentration, working memory, cognitive control, and semantic processing, supporting a role for cortical delta oscillations in the inhibition of sensory disruptions to internal concentration (Harmony, 2013). Another recent review (Güntekin & Başar, 2016) supports this by showing that delta oscillations are also associated with emotional processing and cognitive dysfunction, and also play a role in the multi-band interactions involved in sensory neural processing.

1.2.3 Theta oscillations

Theta oscillations (~3.5 – 7 Hz) have been observed in two situations, during attentional and learning processes while awake (frontal-midline theta), and during REM sleep while asleep (hippocampal theta). Hippocampal theta has been observed primarily in rats, is driven by the medial septum, and modulates most neurons in the HC (Brown, Basheer, McKenna, Strecker, & McCarley, 2012), whereas frontal-midline theta is an EEG waveform observed mainly in humans, localized around frontal electrodes, and may not necessarily be related to hippocampal theta (Mitchell, McNaughton, Flanagan, & Kirk, 2008). Hippocampal theta is known to modulate gamma oscillations during REM sleep (Buzsáki, 1998), and has been suggested to play a role in synaptic consolidation of memories (Diekelmann & Born, 2010).

Source localizations of the frontal-midline theta rhythm has placed generators in the prefrontal cortex and the anterior cingulate (Asada, Fukuda, Tsunoda, Yamaguchi, & Tonoike, 1999; Srinivasan, Winter, & Nunez, 2006). The frontal-midline theta rhythm has been linked to a variety of cognitive processes such as selective attention processes (Başar, Başar-Eroglu, Karakaş, & Schürmann, 2001; Landau & Fries, 2012), cortico-hippocampal communication (Miller, 2013), and memory (Hanslmayr, Staresina, & Bowman, 2016; Rizzuto, Madsen, Bromfield, Schulze-Bonhage, & Kahana, 2006). To summarize, the activation of theta oscillations is associated most strongly in human EEG studies with learning and memory processes.

1.2.4 Alpha oscillations

Considering Adrian's original description, it is not surprising that alpha was long considered to reflect 'cortical idling' (Pfurtscheller, Stancák, & Neuper, 1996), however recent investigations have demonstrated that alpha oscillations may play a functional role in visual attention (Mathewson et al., 2011a; Romei et al., 2008; Thut, Nietzel, Brandt, & Pascual-Leone,

2006). Alpha oscillations are theorized to rhythmically inhibit visual processing (Kizuk & Mathewson, 2017; Mathewson, Gratton, Fabiani, Beck, & Ro, 2009; Spaak, de Lange, & Jensen, 2014), allowing the brain to reduce the impact of stimulation from unattended areas. Alpha oscillations have also been linked to working memory (Klimesch, 2012; Roux & Uhlhaas, 2014), sensory gating (Foxe & Snyder, 2011; Jensen & Mazaheri, 2010), temporal prediction (Samaha, Bauer, Cimaroli, & Postle, 2015) and suppression of somatosensory stimulation (Haegens, Luther, & Jensen, 2012; Mazaheri, Nieuwenhuis, Van Dijk, & Jensen, 2009).

1.2.5 Beta oscillations

Beta-band (~15 – 30 Hz) oscillations are observed during active wakefulness and in the absence of alpha oscillations, however, they seem to play similar roles to alpha oscillations in other modalities. For example, beta-oscillations are observed in the somatosensory cortex during somatosensory stimulation, as well as the preparation and execution of movements, and motor imagery (Neuper et al., 2006). It has been suggested that beta oscillations represent a very similar rhythmic inhibition to that proposed for alpha oscillations, only for the somatosensory system instead of the visual system (Pomper, 2014; Pomper, Keil, Foxe, & Senkowski, 2015a). In fact, one theoretical framework (Bastos et al., 2015; Fries, 2005; Michalareas et al., 2016) does not make a discrimination between alpha and beta oscillations, instead referring to a ‘alpha-beta band’ consisting of 8-20 Hz (Fries, 2015).

In addition, a role has been proposed for beta in the integration of processing from disparate neural populations (Donner & Siegel, 2011; Pomper et al., 2015a) such as happens during decision making. The exact function and correlates of beta oscillations are still unclear, but for our purposes we will treat beta oscillations similarly to alpha oscillations, as an indicator of attention and wakefulness, with respect to the tactile and somatosensory modalities.

1.2.6 Gamma oscillations

Gamma oscillations (30 – 200 Hz) are difficult to study in human scalp recordings due to the fact that the skull filters out these low amplitude oscillations, so we do not measure them in our studies. However, they seem to be elementary processes observed during a wide variety of behaviors (Schürmann, Başar-Eroglu, & Başar, 1997). Gamma oscillations subserve more local interactions than slower rhythms, for example local computation within a column of the cat visual cortex (Gray, König, Engel, & Singer, 1989), but have also been shown to participate in multi-band interactions in complex neural processes such as feature-binding (Tononi, Edelman, & Sporns, 1998), working memory (Lundqvist et al., 2016; Roux & Uhlhaas, 2014), visual processing (Jensen et al., 2014; Spaak, Bonnefond, Maier, Leopold, & Jensen, 2012) and interareal communication (Fries, 2015; Michalareas et al., 2016). After a concise review, Başar and colleagues (2001) conclude: "Rather than being highly specific correlates of a single process, gamma oscillations might be important building blocks of electrical activity of the brain" (p. 244).

1.2.7 Measuring neural oscillations

The process of measuring neural oscillations (with EEG) begins with establishing a connection between the scalp and a lattice grid of electrodes (usually numbering from 16 to 256), while ensuring that the conductance between the scalp and the electrodes is not impeded by hair, sebum, etc. Once a connection is established, the grid of electrodes allows the researcher to measure the voltage of the electric field projected onto the scalp by underlying neural processes. The signal from every electrode is subtracted by the signal from a reference electrode often located behind the mastoid processes or at the top of the head, which removes the influence of non-brain related signals caused by the activity of the head and facial muscles. A variety of

techniques exist for removing additional components of noise, including regression-based approaches (Gratton, Coles, & Donchin, 1983), and independent component analysis (Makeig & Onton, 2011). These techniques can be applied to the scalp electrodes, or to auxiliary electrodes placed around the eyes or on the face. The voltages coming from the scalp are digitized at a certain sample rate in time, so that a 1000 Hz sample rate will produce one discrete value every millisecond. This is an important detail in EEG research because the Nyquist Frequency – the maximum frequency of oscillation which can be measured – is defined as one half of the sampling rate.

In order to turn the preprocessed EEG signal into a representation of oscillatory activity, a method called the fast-fourier transform (FFT) is often used (Cohen, 2014). In non-mathematical terms, the FFT transforms a signal into a collection of sinusoids which, if superimposed, would perfectly recreate the original signal. A drawback of the FFT procedure is that it assumes that the signal is made up of perfect sinusoids, which are continuous in time, and always have the same amplitude and frequency. Neural oscillations, however, are observed to be far more irregular in amplitude, duration, and frequency (Adrian & Matthews, 1934b). To measure neural oscillations more accurately, researchers also often use a Morlet wavelet, which is a sinusoid that is tapered at either side by multiplying with a gaussian distribution and is limited to a certain number of cycles. Researchers can use these wavelets to estimate oscillatory activity at every moment in time, by convolving the wavelet (say, 100 time-points long) with every 100 time-point segment of the recording. Whichever method is used, the result is a representation of the activity of the brain as a collection of sinusoidal waveforms, whose squared amplitudes are a measure of the oscillatory contribution to the signal at that frequency, and if a

wavelet is used, at that time. This measure is called spectral power, and in EEG research usually has the units of microvolts squared $\mu V^2/Hz$.

While spectral power is useful for detecting changes in the observed spectral profile in response to a stimulus, it has the disadvantage of being unable to distinguish between neural oscillations per se and transient or inconsistent fluctuations in the EEG signal caused by artifacts or event-related potentials (Luck, 2005). Furthermore, spectral power is known to be inversely related to the frequency of the oscillation, such that a unit increase or decrease in power will be less noticeable at low frequencies and more marked at high frequencies, making results from different frequency bands difficult to compare. The Better OSCillation (BOSC) detection method was developed by Caplan and colleagues (Caplan, Madsen, Raghavachari, & Kahana, 2001; Hughes, Whitten, Caplan, & Dickson, 2012) to avoid this issue by subjecting the measure of spectral power to two thresholds, a power threshold to ensure that the amplitude of the oscillation is significantly higher than that expected from the non-oscillatory background activity, and a duration threshold to ensure that only consistent oscillations are considered. These thresholds result in a binary value of detected or undetected for every sampled time-point, which are averaged in a window of time to return the $P_{episode}$; a value between 0 and 1 which represents the proportion of time a significantly large and consistent neural oscillation of a given frequency was detected in that time. The $P_{episode}$ measure has the advantage of separating legitimately oscillatory activity from transient, non-oscillatory waveforms, but has the disadvantage of being unable to distinguish between relative amounts of supra-threshold power, and so both spectral power and $P_{episode}$ are used in our studies.

Part C) Oxygen

1.3.1 Brain oxygen metabolism

The brain is one of the most metabolically active organs in the human body, accounting for approximately 20% of the body's energy requirements (Raichle & Gusnard, 2002). It is well known that neuroimaging techniques such as fMRI and PET rely on detecting changes in blood flow, reflecting the changing need for both oxygen and glucose in activated and deactivated areas (Raichle & Mintun, 2006). The utilization of glucose for energy is totally dependent on the availability of oxygen in the brain (Sokoloff et al., 1977), and therefore oxygen metabolism is a crucial physiological parameter influencing human neurological function.

1.3.2 Psychological effects of oxygen

Popular culture is developing an interest in the terms and constructs of cognitive psychology. So-called "brain training" businesses, for example, sell their products on promises of improvements to attention and memory (e.g. Lumosity) or relaxation and anxiety (e.g. Muse), and the increasing interest in meditation both in the research and private sectors suggests that people are increasingly motivated by the idea of controlling and improving their mental states. A recent expression of this trend is the "oxygen bar" which markets highly concentrated oxygen to consumers, generally promising improvements in stress, attention, energy, and the like. While some evidence exists that participants in randomized control trials do not self-report any changes in stress, attention, or energy (Walsh, Thimmesch, D'Achiardi, & Pierce, 2011), it is an interesting question whether a direct measure of attentional state through neural oscillations could more conclusively validate these claims, or indeed the claims of any number of products which promise improvements to attention.

While it is well known that a lack of oxygen (hypoxia) in the brain leads to cognitive impairments (Areza-Fegyveres, Kairalla, Carvalho, & Nitrini, 2010), the literature is less definite as to whether excess oxygen (hyperoxia) leads to cognitive enhancement. A series of papers

reported enhancements in cognitive function (Moss, Scholey, & Wesnes, 1998) and word memory (Scholey, Moss, Neave, & Wesnes, 1999; Scholey, Moss, & Wesnes, 1998) in participants breathing oxygen compared to participants breathing regular air. In one study (Winder & Borrill, 1998), participants were randomly assigned in a 2x2 factorial design to receive a drink sweetened with either 50g of glucose or 4g of aspartame, and subsequently to receive either 100% oxygen or regular air for 1 min, and then to perform a battery of memory tasks, with the hypothesis that the combination of oxygen and glucose would result in the largest memory improvement. In fact, only the addition of oxygen improved memory, whereas glucose had no effect in that experiment. Hyperoxia has also been shown by others to decrease n-back response times in elderly subjects (Kim et al., 2013) and to increase n-back accuracy in intellectually and developmentally disabled individuals (Kim et al., 2015).

1.3.3 Neural effects of oxygen

Despite the widespread use of supplemental oxygen in surgery and medical therapy (Kumaria & Tolias, 2009; Loredo, Ancoli-Israel, Kim, Lim, & Dimsdale, 2006; Owens, 2013), the effect that hyperoxia has on neural oscillation in the brain has only recently begun to be studied. Wu and colleagues., (2014) have demonstrated that hyperoxia does increase resting state BOLD response in the default mode network (DMN), while decreasing BOLD response in visual cortices, and Croal and colleagues, (2015) also reported a decrease in MEG alpha activity. Considering that alpha oscillations have in the past been inversely linked to BOLD response (Goldman, Stern, Engel, & Cohen, 2002; Gonçalves et al., 2006; Jann et al., 2009), and positively linked to visual cortex activity (Dougherty, Cox, Ninomiya, Leopold, & Maier, 2015; Harvey et al., 2013), these results suggest that a reduction in alpha activity would not be unexpected in the EEG, and this appears to be the case. Seo, Bahk, Jun, & Chae, (2007) reported

decreases in beta and gamma activity in subjects who had their eyes-opened, but Kaskinoro, Maksimow, Laitio, Scheinin, & Jääskeläinen, (2010) who instructed their participants to keep their eyes closed, reported only trending decreases in alpha activity, also reported by Seo and colleagues, (2007). Both studies also reported increases in slow, delta activity. More recently, Sheng, Liu, Mao, Ge, & Lu, (2017) administered hyperoxia to participants while they were performing a sustained attention task, and found that hyperoxia suppressed alpha and beta power. The consistently observed decreases in beta and alpha activity and increases in delta activity in these studies suggests that it could be reasonable to expect a change in cognitive state as a consequence of oxygen administration. Moreover, the somewhat consistent decrease in alpha activity across the three EEG studies suggests a specific measure of the claims of oxygen bars to 'improve attention'.

Part D) Sleep

1.4.1 The definition of sleep

Sleep is characterized by a combination of electrophysiological, behavioral, and physiological attributes which differentiate it from other unconscious states. For example, patients anesthetized with xenon gas demonstrate the muscle atonia and lack of responsiveness that behaviorally characterizes sleep, but lack other characteristics, such as the ability to be roused by sensory stimulation (Lee-Chiong, 2005). Over the last few decades, electrophysiological studies have revealed that the sleeping brain is in fact undergoing a complex sequence of nested oscillatory mechanisms; exhibiting far more complexity than is apparent from overt behavior (Steriade & Amzica, 1998; Steriade, 2003). The goal of the cognitive neuroscience of sleep is to understand sleep function by studying these underlying oscillatory mechanisms and state transitions (Poe et al., 2010).

1.4.2 Sleep architecture

Sleep onset in humans is partially governed by an oscillatory (circadian) pacemaker located in the suprachiasmatic nucleus of the hypothalamus (Brown et al., 2012), which operates in conjunction with a homeostatic process which keeps track of "sleep debt" and influences the body to make up lost sleep (Ferrara & De Gennaro, 2001; Ferrara, De Gennaro, & Bertini, 1999). Sleep onset is regulated by the ventrolateral preoptic nucleus of the hypothalamus, which has mutually inhibitory projections with nuclei in the ascending reticular activating system (ARAS), a midbrain system that maintains consciousness (Steriade, 2005). Within a sleeping period, there is also a more rapid alternation between two oscillatory sleep states: a high-frequency but non-oscillatory state termed Rapid Eye Movement (REM) and a low-frequency and highly oscillatory state termed Non-Rapid Eye Movement (NREM) sleep. NREM sleep always occurs first in the sleep session and is further comprised of a descent through three increasingly low-frequency stages. REM sleep occurs 60-90 minutes after the start of the sleep session and increases in frequency towards the end of the sleep session. Although physiological signs of sleep are intensified, the neural activity during REM sleep is high-frequency, reminiscent of waking brain activity. In addition, both REM sleep and NREM sleep are characterized by distinct oscillatory waveforms in the EEG, such as sleep spindles, sawtooth waves, PGO waves, and slow oscillations (Lee-Chiong, 2005).

1.4.3 The function of sleep

Rhythmic alternations in brain state such as sleep reflect processes whereby the nervous system synchronizes its operations with important periodicities in the environment. This mechanism is highly conserved; all organisms studied that live longer than one day display some form of behavioral quiescence synchronized with the day/night cycle (Siegel, 2005), and

humans, other mammals, and birds all show a pattern of alternations between several sleep stages (Campbell & Tobler, 1984). Despite the apparent complexity in the architecture of sleep, there is no clear "essential function" that these various oscillatory mechanisms perform, and it has even been argued that sleep has only the trivial function of forcing animals to conserve energy (Rial et al., 2007). Some arguments against this view are that sleep deprivation leads to death in most mammals (Campbell & Tobler, 1984; Lee-Chiong, 2005), and that REM sleep and NREM sleep seem to be phylogenetically dissociated from one another. For example, reptiles such as turtles have been shown to not exhibit any form of REM sleep, but birds do (Siegel, 2008). This suggests that REM sleep conferred an evolutionary advantage onto these animals. Furthermore, sleep loss in humans has been evaluated for its importance for bodily restoration (Siegel, 2005), neural restoration and detoxification (Cirelli & Tononi, 2008), as well as cognitive and memory processes (Buzsáki, 1998; Diekelmann & Born, 2010; Paller & Voss, 2004; Stickgold, 2005). Further controversy surrounds the function of the individual sleep states, REM and NREM sleep. REM sleep has been linked to learning and memory (Diekelmann & Born, 2010; Siegel, 2001; Walker & Stickgold, 2004), whereas NREM sleep has been linked to restorative functions as well as modulation of synaptic plasticity (Knyazev, 2012; Lee-Chiong, 2005).

1.4.4 Sleep oscillations and sleep stages

NREM sleep is characterized by three stages, which are described by their electrophysiological as well as physiological and behavioral characteristics. The first stage of sleep is called NREM1 (N1), and is characterized by less muscle activity, slow rolling eye movements, and the presence of slower, theta waves (4 - 7Hz). The next stage (N2) is characterized by the presence of highly characteristic waveforms called K complexes – a sharp negative inflection followed by a positive inflection – and sleep spindles – a short train of 11.5-

15 Hz waves, usually following a K complex. The N3 or Slow Wave Sleep (SWS) stage is the deepest stage of sleep and is characterized by large amplitude, 0.5-2 Hz oscillations, and little to no eye movements or EMG activity. Lastly, there is the rapid-eye-movement (REM) stage, a somewhat paradoxical stage that appears to be a deep sleep stage, as evidenced by little to no EMG activity, but involves sharp eye movements in quick succession, as well as "saw-tooth" waves, which consist of trains of 2-6 Hz activity maximal over central electrode sites. In addition to these, we also define an 'awake' stage as the time not spent in any of the four sleep stages during a sleeping period. Wakefulness is characterized in the EEG by the presence of consistent alpha waves, any high-frequency (>30) oscillations, blinks, stair-case eye movements, and high amplitude EMG activity.

The alternation between forebrain states observed across NREM and REM is controlled by increasing activity in a pair of nuclei located in the midbrain, the lateral dorsal tegmental nucleus (LDT) and pedunculopontine tegmental nucleus (PPT). These cholinergic and so-called "REM-on" nuclei project separately to the forebrain and hindbrain to produce REM sleep phenomena – paralysis of skeletal musculature and activation of the cortical regions. "REM-off" nuclei which allow for switching back into NREM states during sleep are located nearby in pontine regions s (Lee-Chiong, 2005).

The function that these various stages perform is not precisely known, just as it is not clear what the function of sleep is generally. One likely reason for the difficulty is what has already been addressed; sleep is a continuous, state-dependent process of brain activity, and the ability to use of neural oscillations to examine these types of research questions is a somewhat recent development.

1.4.5 Relevance of oxygen to sleep

Recent findings have produced new insights on the potential impacts that hyperoxia may have on EEG oscillations during sleep. In rats, urethane anesthesia produces a model of sleep that demonstrates spontaneous alternations in oscillatory states (Clement et al., 2008). These alternating states overlapped well with natural sleep recordings in terms of oscillatory characteristics and the timing of state transitions, but were not exactly alike, and so were classified as "activated" (high frequency, small amplitude) and "deactivated" (low frequency, high amplitude) states, analogous to the REM and NREM states of natural sleep. This model allowed a more precise characterization of the timing of sleep state transitions, and the precise oscillatory characteristics of these states. For example, it was shown that in the activated states, theta frequency activity in hippocampal recording sites was greatest in power, but as the rat transitioned into the deactivated state low frequency oscillations in the neocortex became greatest in power. Extending these results, Whitten, Martz, Guico, Gervais, & Dickson (2009) showed that these activated and deactivated states are strongly coupled to thermoregulation, such that the high amplitude deactivated state can be induced by lowering body temperature, and conversely that the activated state can be induced by raising body temperature. An additional finding was that replacing the normal air with highly concentrated oxygen – a normal practice in animal surgeries – briefly dissociated this relationship between body temperature and sleep states, suggesting an independent manipulator of oscillatory sleep stages. Lastly, it was discovered that when 100% oxygen was administered to the anesthetized rats a disruption in the sleep state transitions occurred whereby the high-frequency "activated" state was totally abolished, producing a constant low-frequency "deactivated" state. This relationship between hyperoxic gas and oscillatory sleep state led to the hypothesis that the oscillatory sleep stages observed under urethane anesthesia may be related to, or caused by, irregularities in the

breathing patterns of the anesthetized animals. This, however, was found not to be the case. Rats under urethane anesthesia display the same patterns as observed in natural sleep: shallower and more irregular breathing in the activated (REM) stage and deeper and more regular breathing in the deactivated (NREM) stage (Pagliardini, Funk, & Dickson, 2013).

A recent experiment in the Dickson lab directly compared the impact of hyperoxia on sleep stage transitions in both urethane anesthetized and naturally sleeping rats (Hauer et al., 2018). In the anesthetized rats, it was again observed that administering oxygen resulted in a steadily deactivated state, with very little oscillatory pattern present in the recording. Furthermore, the average epoch length differed between the two conditions, with animals under hyperoxia having shorter waking periods than animals under normoxia. In naturally sleeping rats, the impact of oxygen on NREM and REM states was in a similar direction but not as extreme, and there was no effect on epoch length (Hauer et al., 2017). Hyperoxia did not produce any differences in the total time spent asleep, but significantly more time was spent in the NREM stage compared to the REM stage. These findings suggest that the effect of oxygen on the sleep states of rats under urethane anesthesia is comparable to the effect that oxygen has in natural sleep.

Research aims

Given these findings in animals, one interesting question is whether hyperoxia would similarly impact sleep stages in humans. We conducted two studies to assess the impact of hyperoxia on neural oscillations in humans, the first in awake, resting participants, and the second in sleeping participants, to assess more conclusively whether hyperoxia in fact has any impact on neurological function in humans. A definitive answer to this question, when combined with future research linking the neurological changes to behavioral improvements, will have

considerable impact, confirming hyperoxia as a proven physiological enhancer of cognitive function.

1.5.1 Test whether hyperoxia can produce reliable changes in awake human EEG oscillations that are consistent with reported effects in humans

Our experimental approach to study the impact of hyperoxia on resting state EEG made use of an eyes-open/eyes-closed resting state task, which serves several important functions. First, previous reports of hyperoxia in humans have demonstrated decreases in alpha activity with the eyes opened (Seo et al., 2007; Sheng et al., 2017), but other studies have shown no significant effect with the eyes closed. Examining the effect of hyperoxia in both these conditions will allow us to determine if the disparate effects observed in the literature are due to this instruction. Secondly, it is well-known that the closing of the eyes results in a large increase in the power of alpha-band oscillations in the human EEG (Adrian & Matthews, 1934a; Berger, 1929), and this is one of the largest and most easily reproducible oscillatory state transitions in human oscillation research. We hypothesized that the administration of hyperoxia might disrupt this state transition, analogously to the disruption observed between NREM and REM oscillatory states in sleeping rats. Lastly, the presence of an eyes-closed condition will allow us to compare the impact of hyperoxia on waking oscillatory states (chapter 2) with the impact of hyperoxia on asleep oscillatory states (chapter 3) while controlling for differences such as eye movements and visual processing. Our experiment was careful to control for physiological differences that may be produced by oxygen administration, including heart rate and breathing rate, and will directly measure the extent to which the excess oxygen is taken up into the blood, in order to be as certain as possible that the effects of hyperoxia on oscillatory measures are due to differences in neural activity, and not external factors.

In the context of the previous human EEG studies discussed above, we hypothesized in this experiment that hyperoxia would lead to a general "slowing" of the spectrum, increasing the power of slow oscillations and decreasing the power of fast oscillations. Specifically, we hypothesized that hyperoxia would induce changes in the oscillatory characteristics of resting state EEG, especially in the alpha-band. In the context of the previous research discussed in sleeping rats, we also hypothesized a possible increase in delta oscillations.

1.5.2 Test whether oxygen can produce reliable changes in human EEG sleep oscillations that are consistent with reported effects in animals

The second experiment was a similar comparison between neural oscillations in hyperoxia and normoxia, but in sleeping participants. Previous research on auditory processing during sleep has shown that it is possible to encourage participants to fall asleep while EEG recording is taking place, and that it is possible to reliably record event-related potentials (Atienza, Cantero, & Escera, 2001) and measure sleep stages (Strauss et al., 2015; Winter, Kok, Kenernans, & Elton, 1995).

One recent study (Ong et al., 2016) used a 90-minute napping period, and was able to record reliable measures of slow and theta oscillations, and we adopted the same 90-minute napping design for our study. In order to maximize sleep propensity, we set up a naturalistic sleep environment inside the EEG recording chamber and encouraged participants to fall asleep during the recording period. Based on the previous results observed in the rat model, we hypothesized that hyperoxia would lead to increased time spent in the stages characterized by slower oscillations, namely SWS, and less time in the stages characterized by faster activity, namely REM and N1. We also hypothesized that participants may spend increased time in SWS overall, keeping in mind that this was not found in naturally sleeping rats. Lastly, we

hypothesized that hyperoxia would impact the oscillatory characteristics of the EEG during sleep, producing more consistent and larger amplitude slow-wave oscillations.

2. ELECTROPHYSIOLOGICAL CORRELATES OF HYPEROXIA DURING RESTING-STATE EEG IN AWAKE HUMAN SUBJECTS

2.1 Introduction

Over the past decade, recreational use of oxygen (O_2) has increased, and oxygen providers have suggested therapeutic benefits of using O_2 to reduce stress, boost energy, and increase alertness, yet, there is little evidence to validate these benefits (Walsh et al., 2011). Both hypoxic and hyperoxic states can be induced in the body by respectively decreasing or increasing the fractional O_2 concentration (normally 21%) in inhaled gas. Intermittent exposure to hypoxia has been associated with global impairments in executive functioning (Saunamäki, Himanen, Polo, & Jehkonen, 2009), sleep disturbances (Hamrahi, Stephenson, Mahamed, Liao, & Horner, 2001), cardiovascular and metabolic problems (Lévy et al., 2008; Marin, Carrizo, Vicente, & Agusti, 2005) and the induction of neuronal apoptosis (Xu et al., 2004). Given that hypoxia is associated with physiological and brain function impairments, is the opposite true for hyperoxia? That is, are there neural and cognitive benefits of inducing a short term hyperoxic state?

In view of the fact that the brain has high metabolic requirements, and since metabolic O_2 consumption in the brain appears to correspond very well to the degree of neuronal/functional activation on a moment to moment basis (Magistretti & Allaman, 2015; Raichle & Mintun, 2006), it stands to reason that providing additional oxidative substrate to the brain might well produce measurable changes in its functional electrophysiological state. Previous work has shown that hyperoxia induces changes in basic physiological parameters such as breathing and heart rate and in turn, these changes may directly or indirectly affect brain state or function (Berssenbrugge, Dempsey, Iber, Skatrud, & Wilson, 1983; Colrain, Trinder, Fraser, & Wilson, 1987; Desai, Tailor, & Bhatt, 2015; Pack, Cola, Goldszmidt, Ogilvie, & Gottschalk, 1992;

Tsanov, Chah, Reilly, & O'Mara, 2014; Yackle et al., 2017). Indeed, hyperoxia is also known to induce changes in cerebral blood flow (Bergø & Tyssebotn, 1995; Bew, Field, Droste, & Razis, 1994; Busija, Orr, Rankin, Liang, & Wagerle, 1980; Floyd et al., 2003; Kety & Schmidt, 1948; Lund et al., 1999; Watson, Beards, Altaf, Kassner, & Jackson, 2000), which might also be expected to result in a functional change in the operation of the brain even given the fact that cerebral blood flow and brain state can show independence from each other, despite their typical tight correspondence (Bangash et al., 2008; Braun et al., 1997; Hajak et al., 1994; Hofle et al., 1997). In terms of pathological influences, there are also deleterious consequences of hyperoxia due to the production of reactive oxidative species (ROS), however, the exposure times necessary to observe these effects are quite long (~ 6 hours in normobaric conditions).

We have previously observed that providing 100% oxygen to spontaneously breathing urethane-anesthetized and naturally sleeping rats with implanted cortical and hippocampal electrodes shifts forebrain states towards more deactivated slow-wave (≤1Hz) patterns (Hauer et al., 2018; Whitten et al., 2009). This suggests that ongoing oscillatory EEG measures of brain state may be an effective assay for the effects of hyperoxia and that (perhaps paradoxically) excess oxygen may promote EEG rhythms that are typically associated with decreased levels of arousal. Two human studies appear to indicate this as well. In the first, breathing 100% oxygen appeared to increase coupling in the "default mode network" (Wu et al., 2014), a group of brain regions that show more activation during baseline, sleeping and anesthetized conditions, as compared to instances of alert processing (Raichle, 2015). In the second, increasing inhaled oxygen content to 35% produced an increase in delta (1-4Hz) activity together with a decrease in both beta and gamma power (Seo et al., 2007). In a further independent study, however, no significant EEG changes were observed following a one-hour period of breathing 100% O_2

(Kaskinoro et al., 2010). In another, Croal et al., (2015), reported decreases in occipital lobe alpha and beta oscillations using MEG, but without any concomitant changes in cerebral blood flow. In all these studies, however, behavioural state was not controlled and the influence of physiological variables such as respiratory and heart rate changes were not taken into account. A recent study, however, reported decreases in EEG alpha activity during sustained-attention and task-evoked conditions, comparing 5-minute interleaved oxygen and control blocks (Sheng et al., 2017). While this study did control behavioural state under alert, sustained attention conditions, there has still been no systematic evaluation of the impact of hyperoxia on EEG oscillations in resting-state conditions.

In the present study, we examined short term (15 minute) influence of breathing 100% oxygen on resting-state EEG during wakefulness in two simple situations that produce prominent state-dependent differences in the production of alpha activity: eyes-opened and eyes-closed conditions. We ensured that oxygen saturation was maximised during the hyperoxic condition and we also monitored both respiratory and cardiac rhythms during our manipulations. We show that hyperoxia has a state-dependent and complex influence on brain activity that may indicate enhanced attention during eyes-opened conditions while promoting the initiation of sleep when the eyes are closed.

2.2 Method

2.2.1 Procedure

Figure 2.1 illustrates the experimental protocol used. The experiment consisted of 4 blocks wherein either 100% oxygen or regular air was administered at a controlled flow rate for ~15 minutes each. The order of the gases provided was counterbalanced across subjects. Within each block, participants completed an alternating eyes-opened/eyes-closed resting-state condition, again in an ABAB design, for 3 minutes each. The eyes-closed condition was always

the first and third trial, and the eyes-opened task was always the second and fourth trial. There were ~3 minutes between each block to allow for blood oxygenation measurements. Participants were blind both to the design of the study as well as their condition. We collected data from 26 right handed participants (Mean age = 22.2, range = 18 – 38, 18 female), all of whom had normal or corrected vision and were screened for relevant medical or neurological illnesses. All participants gave informed consent and were compensated for their time. The Health Research Ethics Board at the University of Alberta approved all experimental procedures.

2.2.2 EEG data recording and preprocessing

EEG data was recorded with a 32-channel EEG system inside a radio-frequency attenuated chamber. Standard procedures for reducing electrical impedance between the skin and electrodes were followed. We additionally had vertical and horizontal EOG electrodes placed around the eyes, a respiration belt transducer to measure respiratory rate, a pulse oximeter to measure heart rate, and a second oximeter to measure oxygen saturation levels in the blood (SpO_2), all synchronized with the EEG data. 100% Oxygen or room air was delivered through an unsealed gas delivery mask, allowing 2 minutes before the start of each 15-minute block to allow the oxygen to be taken up by the body. Pulse oxygenation level was measured at the start and end of this 2-minute period.

All data was processed in MATLAB using EEGLAB toolbox functions (Delorme & Makeig, 2004). Raw traces were segmented into 180 second epochs locked to the onset of each trial corresponding to the following conditions: normoxia eyes-opened, normoxia eyes-closed, hyperoxia eyes-opened, and hyperoxia eyes-closed, resulting in four 3-minute epochs within each condition, and 16 trials total per participant. An additional 9s was taken before and after each trial to avoid edge artifacts. Eye movements were corrected with a regression-based procedure (Gratton et al., 1983). No other form of artifact correction was used.

2.2.3 Time frequency Analysis

We transformed our 3-minute segments into time-frequency space by convolving the data with a Morlet wavelet 6 cycles in length and for 100 logarithmically sampled frequencies from 1 – 50Hz. These raw power values were log-transformed and averaged within each segment, resulting in four trial averages within each condition. These trial averages were then themselves averaged, resulting in a measure of the average raw power at each frequency, for each of the 4 conditions, for each electrode, and for each participant.

In addition to the analysis of the oscillatory power, we used the BOSC (Better OSCillation detection) method, introduced by Caplan et al., (2001) and recently revised by Whitten et al., (2011). The BOSC method is designed to detect consistent oscillatory activity in EEG signals by modelling the functional form of the non-rhythmic background activity and employing two thresholding procedures to ensure the presence of oscillatory activity, using one threshold for amplitude and one for duration. Our procedure was as follows. The average wavelet power across the entire experimental session was used to estimate the parameters of the spectral background function (a natural property of autocorrelated time-series signals such as EEG (Schlesinger & West, 1988)) and was assumed to be described by the equation $\text{Power}(f) = Af^{\alpha}$. The session-averaged wavelet spectrum was log-transformed, and a linear regression of these values on frequency in log-log space was computed, resulting in an intercept, corresponding to log(A), and a slope, corresponding to -α. It is possible to consider this fitted value (Power(*f*)) as the mean of the theoretical $\chi^2_{(2)}$ distribution for expected power values, allowing us to create probability distribution functions for the background power at every frequency. The power threshold, P_T, is chosen such that observed power values exceeding the 95th percentile of this distribution were considered oscillatory. The duration threshold, D_T, was set such that the

wavelet power must have exceeded the power threshold for at least 3 cycles of the given frequency. The end result was a binary value of "detected" or "undetected" for every point in time-frequency space, which is summarized by the "$P_{episode}$", the proportion of time oscillations of a given frequency are detected in a given period. The four trials per condition were averaged, resulted in one value of $P_{episode}$ for each frequency, condition, electrode, and participant.

The raw power and $P_{episode}$ values were averaged across all participants and across all electrodes to demonstrate the gross differences between the four conditions. Examining eyes-closed and eyes-opened trials separately, we performed a cluster-based statistical analysis of the effect of hyperoxia across frequencies and electrodes. The effect of hyperoxia was assessed at every electrode and every sampled frequency by a two-tailed uncorrected paired t-test with an alpha set to 0.05. In order to minimize false alarms, only effects that consistently spanned across several clustered electrodes were considered. We defined an electrode cluster as a spatial array of at least three mutually adjacent electrodes showing significant differences in a common direction. Based on this criterion, bands of frequencies were identified which indicated an effect of hyperoxia, and the t-statistics for each electrode were averaged across the frequencies within the band and plotted as a scalp topography. The electrode with the largest t-statistic was selected to represent the locus of the statistical difference on the scalp, and a final uncorrected two-tailed paired t-statistic for the mean power or $P_{episode}$ difference within this frequency range and at this single electrode was calculated and reported. The difference spectra, hyperoxia minus normoxia, was also computed and plotted, to present at a single electrode the magnitude and variability of the difference hyperoxia produces across the spectrum. The electrode with the largest t-statistic was chosen to represent this difference, but in some cases was chosen to best reflect the most theoretically interesting results for that condition.

In addition to examining the effect of hyperoxia on the eyes-opened and eyes-closed trials separately, we were also interested in the effect of hyperoxia on the transition between one eye-condition to the next. The average wavelet power was computed within each of the four oxygen conditions (2 trials of hyperoxia, 2 trials of normoxia), instead of across the whole session, to estimate separate P_T thresholds within each oxygen condition and recompute the $P_{episode}$ measure for each eye-condition. This analysis allowed the relative power and $P_{episode}$ to be compared within oxygen blocks without being affected by the variability between the blocks. At every electrode and frequency, a two-way repeated-measures ANOVA was performed, with an alpha set to 0.05, and using the uncorrected F-statistic for the eye by oxygen interaction as our indication of significance across electrodes. The same statistical analyses was performed as described above using this F-statistic.

We performed two additional analyses with the aim of examining in more detail how the patterns of oscillatory activity were changing between the gas conditions. The first consisted of a restricted power analysis where time points not classified as "detected" within a given frequency were excluded from the estimation oscillatory power. Oscillation power is often interpreted as reflecting the amplitude of an oscillation, however, this is not necessarily true. As the proportion of an EEG signal which is oscillatory ($P_{episode}$) increases or decreases, the estimation of power across that signal will also increase or decrease, although the amplitude of the oscillations are in fact identical. We returned to the frequency bands which showed a significant effect of hyperoxia on the $P_{episode}$ within an eye condition, and re-estimated the power in these ranges by averaging across only detected oscillations within a trial, and then averaging this value across the 4 trials per condition as above to obtain one measure of the "detected raw power" within each condition which is not affected by differences in the prevalence of oscillations between

conditions. This measure was calculated at frequencies and electrodes already shown in the previous analyses so as to present the most comparable data to our more standard analyses. An uncorrected two-tailed paired t-test was performed on the detected power within this range and the means, standard deviations, and t-statistics for this test are reported.

We lastly examined whether the differences observed due to both factors could be explained by changes in the length, measured in cycles, of the detected oscillatory epochs. The number of cycles was defined as the duration that an individual oscillatory segment remained over the power threshold P_T, and excluding durations less than 3 cycles for failing to meet the minimum duration threshold D_T. This analysis was restricted to the alpha range represented in Figure 2.3G because that is the only range which contains enough separate oscillatory epochs to allow a stable estimation of the number of cycles. The number and duration of detected oscillatory epochs were identified within the aforementioned frequency range, and at the electrode with the largest test statistic for the interaction presented in Figure 2.3G. The oscillatory epoch counts were pooled both across trials and across participants, due to the low numbers of oscillatory epochs per subject (typically less than 30). Histograms of the number of cycles from the eyes-opened and eyes-closed conditions were plotted, overlaid so as to demonstrate the shift in the alpha distribution that is caused by closing the eyes. The MATLAB function ecdf() – which uses the Kaplan-Meier nonparametric method for empirically estimating the cdf of a population from observed data – was used to estimate the cumulative distribution function (cdf) for these four distributions. Two-sample Kolmogorov-Smirnov (KS) tests were used to test if the hyperoxia distribution would be shifted towards longer or shorter number of cycles than the normoxia distribution in both the eyes-closed and eyes-opened conditions.

2.3 Results

2.3.1 Physiological measurements

Exposure to hyperoxia elevated pulse oxygen saturation levels significantly across participants (Figure 2.2A), demonstrating that the oxygen delivery was effective in our participants ($t(25) = 9.75$, $p < 0.001$). The experiment consisted of 4 blocks wherein either 100% oxygen or regular air was administered at 3 l/min for ~15 minutes each. Consistent with the literature, hyperoxia had a slight but non-significant slowing effect on breathing rate in eyes-opened ($t(25) = .968$, *n.s.*) and eyes-closed conditions ($t(25) = .701$, *n.s.*; Figure 2.2B), and significantly lowered heart rate in both the eyes-opened ($t(25) = 4.87$, $p < 0.001$) and eyes-closed ($t(25) = 3.06$, $p < 0.01$) conditions (Figure 2.2C). We performed a homoscedastic two-sample uncorrected t-test on the SpO2 difference, hyperoxia minus normoxia, between hyperoxia-first subjects and normoxia subjects, resulting in a trend for a larger difference in normoxia-first subjects (2.9 %) than hyperoxia-first subjects (2.2 %), but this was not significant ($t(12) = 1.96$, $p = 0.073$). We also performed the same test on the difference in breathing rate and heart rate which showed that the counterbalancing order did not alter the effect of hyperoxia on breathing rate (eyes-opened: $t(12) = 0.77$, $p = 0.46$; eyes-closed: ($t(12) = 1.00$, $p = 0.34$), however counterbalancing order did significantly alter the effect of hyperoxia on heart rate in the eyes-closed condition ($t(12) = 2.82$, $p = 0.016$) and showed a trend in the eyes-open condition ($t(12) = 2.02$, $p = 0.066$), although due to the presence of a significant outlier in one subject (See Figure 2.2C) these effects may not be reliable. For every statistical test of observed spectral differences described below, a correlation was made between the observed difference and the measures of breathing rate, heart rate, and SpO_2. No spectral differences were found to be correlated to the effect of hyperoxia on any of these measures. All relevant interactions between observed spectral differences and the counterbalancing order are described below.

2.3.2 Power Analyses

Across all electrodes, a large decrease in power was observed in the alpha band in the eyes-opened condition compared to the eyes-closed condition (Figure 2.3A), as would be expected from previous research on alpha oscillations (Haegens, Cousijn, Wallis, Harrison, & Nobre, 2014). We performed a statistical analysis to isolate clusters of frequencies and electrodes showing reliable power differences (Bew et al., 1994; Desai et al., 2015; Kety & Schmidt, 1948; Pack et al., 1992; Tsanov et al., 2014) between the hyperoxia and normoxia conditions. In the eyes-opened condition, hyperoxia was associated with decreases in power in the alpha (7.95 – 9.66 Hz) and beta (17.38 – 21.98 Hz) frequency ranges, as shown in the electrode by frequency heatmap plot in Figure 2.3B. Test statistics whose probability is below the 0.05 alpha level are emphasized in darker colours. The decrease in alpha power was focused around fronto-central electrode sites (electrode F3: $M_{hyp} = 5.8215$, $M_{norm} = 5.8542$; $M_{diff} = 0.0328$, $SD_{diff} = 0.0748$; $t(25) = -2.23$, $p = 0.035$). A two-factor repeated-measures ANOVA found a main effect of hyperoxia on alpha power ($F(1,12) = 7.38$, $p = 0.019$), as well as an interaction between the effect of hyperoxia and the counterbalancing order ($F(1,12) = 13.84$, $p < 0.01$) although there was no main effect of counterbalancing order ($F(1,12) = 0.099$, *n.s.*). The decrease in beta power was focused around left-frontal sites. (electrode F3: $M_{hyp} = 5.1584$, $M_{norm} = 5.1900$; $M_{diff} = 0.0316$, $SD_{diff} = 0.0684$; $t(25) = -2.36$, $p = 0.027$). A two-factor repeated-measures ANOVA found a main effect of hyperoxia on beta power ($F(1,12) = 5.39$, $p = 0.039$), as well as an interaction between the effect of hyperoxia and the counterbalancing order ($F(1,12) = 8.59$, $p = 0.013$) although there was no main effect of counterbalancing order ($F(1,12) = 1.71$, *n.s.*). The difference spectra, hyperoxia – normoxia, shows the impact of hyperoxia on the oscillations at electrode F3. The shaded lines represent the 95% CI for the difference. Frequencies in the alpha and beta frequency ranges which reached significance at this level are indicated in red on the x-

axis (listed above; Figure 2.3D). In the eyes-closed condition, hyperoxia was not associated with any reliable changes in power (Figure 2.3E).

Figure 2.3F shows the power in the eyes-opened and eyes-closed conditions after the average power within the entire oxygen block was subtracted out. It can be observed that within the hyperoxia blocks, the difference in power between eyes-closed and eyes-opened was more pronounced. We isolated the clusters of electrodes and frequencies which reliably showed this interaction between the magnitude of the eyes-opened and eyes-closed difference and the oxygen condition, revealing one band in the alpha range from 7.64 – 8.94 Hz, as shown in the electrode by frequency heatmap in Figure 2.3G. This interaction was present in a large group of frontal electrode sites. (electrode F3: $M_{Hypdiff} = 0.2496$, $M_{Normdiff} = 0.2032$; $SD_{hypdiff} = 0.2305$, $SD_{normdiff} = 0.1983$; $F(1,25) = 6.1031$, $p = 0.021$). A three-factor repeated-measures ANOVA found a main effect of eye condition on alpha power ($F(1,12) = 24.19$, $p < 0.001$), as well as interactions between the effect of hyperoxia and the counterbalancing order ($F(1,12) = 9.95$, $p < 0.01$) and between hyperoxia, eye condition, and counterbalancing order ($F(1,12) = 5.03$, $p = 0.044$). The interaction between hyperoxia and eye condition was trending in this case ($F(1,12) = 3.91$, $p = 0.07$). The two difference spectras, eyes-closed – eyes-opened, were plotted for both the hyperoxia and normoxia conditions at electrode F3 (Figure 2.3I). Error bars represent the within-subject SEM, removing the variance associated with differences between individuals (Loftus & Masson, 1994). The frequencies in the alpha range for which the oxygen by eye interaction reaches significance at the 0.05 alpha level are indicated in red on the x-axis (indicated above).

2.3.3 BOSC and $P_{episode}$ Analyses

Because spectral power reflects a smeared average across frequency bands and is not necessarily a robust method for detecting oscillations per se (Caplan et al., 2001), we used the Better OSCillation (BOSC) detection method which has been validated for state-dependent

alternations in alpha detections (Whitten et al., 2011). Across all electrodes, a large (~20%) decrease in the number of detected alpha oscillations was observed in the eyes-opened condition compared to the eyes-closed condition (Figure 2. 4A), similar to the power results. We performed the same statistical analysis to isolate clusters of frequencies and electrodes showing reliable differences in $P_{episode}$ between the hyperoxia and normoxia conditions. In the eyes-opened condition, hyperoxia was associated with decreases in $P_{episode}$ in the alpha (6.80 – 10.06 Hz), beta (14.30 – 19.55 Hz), and gamma (21.14 – 35.16 Hz) frequency ranges, as shown in the electrode by frequency heatmap plot in Figure 2.4B. Test statistics which are below the 0.05 alpha level are emphasized in darker colours. The decrease in alpha power was again focused around frontal electrode sites and was significant in a larger number of sites than in the power analysis. (electrode F3: M_{hyp} = 8.00, M_{norm} = 9.62; M_{diff} = 1.61, SD_{diff} = 2.78; $t(25)$ = -2.74, p = 0.0067. The decrease in beta power was focused around left-frontal sites. (electrode F3: M_{hyp} = 2.18, M_{norm} = 2.74; M_{diff} = 0.56, SD_{diff} = 0.91; $t(25)$ = -3.13, p = 0.0044). A two-factor repeated-measures ANOVA found a main effect of hyperoxia on beta power ($F(1,12)$ = 7.29, p = 0.019), as well as an interaction between the effect of hyperoxia and the counterbalancing order ($F(1,12)$ = 6.35, p = 0.027) but no main effect of counterbalancing order ($F(1,12)$ = 0.72, *n.s.*). The decrease in gamma power was focused around a range of sites over the left-frontal, central, and posterior regions (electrode Pz (M_{hyp} = 0.70, M_{norm} = 1.00; M_{diff} = 0.31, SD_{diff} = 0.60; $t(25)$ = -2.60, p = 0.015). The difference spectra, hyperoxia – normoxia, shows the impact of hyperoxia on the oscillations at electrode F3. Error bars represent the 95% CI for the difference. Frequencies in the alpha, beta, and gamma frequency ranges which reached significance at this level are indicated in red on the x-axis (listed above; Figure 2.4D).

In the eyes-closed condition, hyperoxia was associated with increases in $P_{episode}$ in the delta (1.73 – 2.10 Hz), and theta (4.25 – 4.60 Hz) frequency ranges, and with a decrease in the beta (15.46 – 19.55 Hz) frequency ranges, in contrast to the lack of differences found in the power analysis (Figure 2.4E). Test statistics whose probability were below the 0.05 alpha level are emphasized in darker colours. The increase in detected delta oscillations was focused around right-posterior electrode sites (electrode PO4: $M_{hyp} = 0.76$, $M_{norm} = 0.36$; $M_{diff} = 0.40$, $SD_{diff} = 0.56$; $t(25) = 3.63$, $p = 0.0013$). The increase in detected theta oscillations was focused around a small cluster of right-frontal sites (electrode F8: $M_{hyp} = 0.75$, $M_{norm} = 0.46$; $M_{diff} = 0.29$, $SD_{diff} = 0.46$; $t(25) = 3.22$, $p = 0.0036$). A two-factor repeated-measures ANOVA found a main effect of hyperoxia on theta power ($F(1,12) = 9.65$, $p = 0.0091$), as well as an interaction between the effect of hyperoxia and the counterbalancing order ($F(1,12) = 8.18$, $p = 0.014$) although there was no main effect of counterbalancing order ($F(1,12) = 1.75$, *n.s.*). The decrease in detected beta oscillations was focused around frontal and central electrode sites (electrode C4: $M_{hyp} = 3.92$, $M_{norm} = 4.44$; $M_{diff} = 0.52$, $SD_{diff} = 1.05$; $t(25) = -2.52$, $p = 0.018$). The difference spectra subtracting hyperoxia from normoxia, shows the impact of hyperoxia on the oscillations at electrode F3. Error bars represent the 95% CI for the difference. Frequencies in the alpha, beta, and gamma frequency ranges which reached significance at this level are indicated in red on the x-axis (listed above; Figure 2.4G).

Figure 2.4H shows the $P_{episode}$ in the eyes-opened and eyes-closed conditions when the power threshold was estimated within an oxygen condition rather than across the whole experimental session. In this case, the oscillation detection procedure does not seem to depend as strongly as the power analysis on the choice of baseline. We isolated the clusters of electrodes and frequencies which reliably showed an interaction between the magnitude of the eyes-opened

and eyes-closed difference and the oxygen condition, revealing one band in the alpha range (6.80 – 9.30 Hz), and one band in the gamma range (23.78 – 42.76 Hz), as shown Figure 2.4I. The interaction in the alpha range was present across most of the scalp and especially in frontal and central electrode sites (electrode F3: $M_{Hypdiff} = 13.43$, $M_{Normdiff} = 10.19$; $SD_{hypdiff} = 12.83$, $SD_{normdiff} = 11.33$; $F(1,25) = 10.58$, $p = 3.0\times10^{-5}$). A three-factor repeated-measures ANOVA found a main effect of eye condition on alpha power ($F(1,12) = 23.79$, $p < 0.001$), as well as two interactions between the eye condition and the effect of hyperoxia ($F(1,12) = 6.24$, $p = 0.028$), and between the eye condition, effect of hyperoxia, and the counterbalancing order ($F(1,12) = 7.78$, $p = 0.016$). The interaction in the gamma range was present across a large group of electrodes centered on left-central electrode sites (electrode FC1: $M_{Hypdiff} = 0.026$, $M_{Normdiff} = -0.42$; $SD_{hypdiff} = 1.09$, $SD_{normdiff} = 1.47$; $F(1,25) = 5.50$, $p = 0.036$). The two difference spectras, eyes-closed – eyes-opened, were plotted for both the hyperoxia and normoxia conditions at electrode F3 (Figure 2.4K). Error bars represent the within-subject SEM. Frequencies in the alpha and gamma range for which the oxygen by eye interaction reaches significance at the 0.05 alpha level are indicated in red on the x-axis.

2.3.4 Analyses of detected alpha epochs

For periods of detected oscillatory activity in our frequency bands of interest, we computed the mean raw power to determine if there were any differences in the amplitude of the signals as an effect of hyperoxia (Figure 2.5A). For five out of our six bands, although differences had been observed in the number of detected oscillations, no change in detected power was observed between hyperoxia and normoxia conditions. For the remaining band, however (21.14 – 35.16 Hz) in the eyes-opened condition, the decrease in detected oscillations was accompanied by a decrease in detected power.

We also characterized the actual number of cycles in each detected alpha epoch to determine if hyperoxia had any effect on epoch lengths. Figure 2.5B shows the histograms of the pooled number of cycles from the alpha range frequencies shown in Figure 2.4I showing a significant interaction between eye and oxygen condition. Only detected segments from electrode F3 were included. For both hyperoxia and normoxia conditions, opening the eyes leads to a larger proportion of short (3-6 cycle) oscillatory periods, while closing the eyes increases the proportion of long (7-25 cycle) oscillatory periods. Figure 2.5C shows the empirical cumulative distribution function (cdf) derived from the pooled number of cycles. This figure similarly shows that closing the eyes leads to a cdf which is more shifted to the longer cycle lengths. This effect is larger for hyperoxia than normoxia. The KS test revealed that the hyperoxia eyes-opened condition was significantly "smaller" than the distribution for the normoxia condition ($p = 3.08x10^{-7}$), whereas the hyperoxia eyes-closed condition was significantly "larger" than the distribution for the hyperoxia eyes-opened condition ($p = 1.17x10^{-7}$).

2.4 Discussion

Oxygen is used in many clinical settings and its popularity for recreational administration is rising. Our aim was to evaluate possible attentional benefits of short-term oxygen administration through an eyes-closed and eyes-opened resting-state EEG task. Under short-term hyperoxia, we observed changes in blood O_2 saturation as well as in heart rate and, and no reduction in breathing rate. In addition, in the brain, there were state-dependent decreases across several high EEG frequency bands, including low alpha, high alpha, beta, and gamma, as well as increases in low frequency bands including delta and theta. Finally, our results also demonstrate interactions between the oxygen and eye-conditions, which suggests that the effects of oxygen on cortical activity may be state-specific.

Our experiment measured SpO_2, breathing rate, and heart rate. Breathing is often ignored in studies that examine cognitive tasks under hyperoxia. Monitoring of breathing is useful to elucidate whether changes in spontaneous brain activity are due to oxygen manipulations per se or instead influenced by fluctuating CO_2 levels, which can be affected by breathing. Poikliocapnic hyperoxia results in an immediate decrease in minute ventilation in the first minute of exposure followed by a sustained increased in minute ventilation above baseline breathing (Marczak & Pokorski, 2004); this increase in minute ventilation results from an increase in both breathing rate and tidal volume. Despite changes in minute ventilation, changes in alveolar CO_2 across hyperoxia exposure do not differ when compared to the same duration of exposure to room air. Since we observed increases in SpO_2, but little change in breathing rate between the oxygen conditions, the changes in brain activity observed is more likely due to oxygen manipulation rather than change in central CO_2. It should be noted, however, that we cannot rule out an effect of central CO_2 and/or changes in cerebral blood flow as contributors to our findings although a recent MRI experiment found no evidence that short-term hyperoxia causes such changes (Croal et al., 2015) and a variety of sleep studies using PET have shown evidence of uncoupling of cerebral blood flow and EEG measures of brain state (Bangash et al., 2008; Braun et al., 1997; Hajak et al., 1994; Hofle et al., 1997). Our finding of decreased heart rate with oxygen administration is consistent with the literature and suggests that oxygen influences the parasympathetic nervous system (Shibata, Iwasaki, Ogawa, Kato, & Ogawa, 2005; Waring et al., 2003). The reduction in parasympathetic activity is potentially mediated by a reduced input from peripheral chemoreceptors to the medulla oblongata (Lahiri, Mokashi, Mulligan, & Nishino, 1981).

One last consideration on the physiological variables is the question of whether it can be assumed that oxygenation of the blood as evidenced in the difference in SpO_2 levels (Figure 2.2A) translates to oxygenation of neural tissue. One commonly reported effect of hyperoxia is cerebral vasoconstriction (Hafner et al., 2015) leading to a reduction in cerebral blood flow (Floyd et al., 2003). At least in patients with obstructive respiratory disorders, hyperoxia is well-known to cause hypercarbia (Dunn, Nelson, & Hubmayr, 1991). In healthy participants, Croal et al., (2015) used an isocapnic hyperoxic stimulus to measure the effect of hyperoxia on MEG activation, and found that hyperoxia produced decreases in alpha and beta signalling similar to those reported in our study. However, much larger decreases in the same areas were in fact produced with pure hypercarbia. In order to fully elucidate what exactly in the brain causes the reduction in high-frequency oscillations which we have reported here, it would be necessary to not only measure end-tidal O_2 and CO_2 to monitor changes in alveolar gas exchange, but also to have a measure of the relative oxygenation in the brain before and after hyperoxia.

Based on the known associations of alpha with visual and visuo-spatial attention (Jensen & Mazaheri, 2010; Kizuk & Mathewson, 2017; Klimesch, Sauseng, & Hanslmayr, 2007; Mathewson et al., 2011b; Thut et al., 2006), we would hypothesize that fewer alpha detections and lower power during eyes-opened conditions with hyperoxia would produce a beneficial effect for these processes. Similar to the functional role of alpha in visual and other sensory modalities, a suppression of beta activity is often associated with the role of sensory gating in the somatosensory system and anticipatory selective attention (Neuper et al., 2006; Pomper, Keil, Foxe, & Senkowski, 2015b). Our finding of a robust difference in beta activity between normoxia and hyperoxia when the eyes were open but less so when the eyes were closed could suggest that the impact of oxygen affects beta during alert, attentional states, and has little effect

with a disengaged state with the eyes-closed. This decrease in alpha and beta activity under hyperoxia during alert states lends credence to reports of noticeable attentional changes when using recreational oxygen, given the growing literature on beta activity and cognitive functioning. Engel & Fries (2010) propose that a functional role of beta activity is the maintenance of the current cognitive state of the participant. Under this framework, the decreases in the observed beta activity under hyperoxia could reflect increased cognitive control and attentional flexibility, which users of recreational oxygen interpret as improving their attention. Perhaps paradoxically, although supported by previous studies which likely recorded under eyes-closed conditions (Seo et al., 2007; Wu et al., 2014), hyperoxia appeared to enhance delta and theta activities while decreasing gamma, a result that would likely indicate promotion of the initial stages (i.e., N1) of sleep (Borbély & Tobler, 2011; Greene & Frank, 2010).

The eyes-closed and eyes-opened resting-state EEG task allowed us to compare within and across different attentional states. As expected, opening and closing the eyes produced clear differences in both the power and the $P_{episode}$ (frequency of detection) of alpha oscillations. When the eyes were open, the detections of alpha, beta, and gamma bandwidth oscillations decreased when hyperoxia was administered, whereas when the eyes were closed, the detections of delta and theta bandwidth oscillations increased with hyperoxia, along with a decrease in gamma detections. Hyperoxia was associated with a more notable decrease in alpha power and both alpha and gamma detections when the eyes were opened compared to when they were closed. In addition, we observed that hyperoxia contributes to the magnitude of the transition between eyes-opened (engaged) and eyes-closed (disengaged) oscillatory states. There was a significant interaction between oxygen and eye effects such there was a significantly larger transition during hyperoxia in both the power and detection of alpha oscillations across the eyes closed/opened

condition than during normoxia. Indeed, when we computed the average number of contiguous cycles of alpha using BOSC, we observed that not only did closing the eyes produce longer bursts of alpha activity, but that hyperoxia was associated with a more exaggerated transition across the behavioural condition.

While different oscillatory states are associated with specific cognitive functions, our task did not specifically test a cognitive function, rather it simply demonstrated that there are oscillatory changes that occur under short-term hyperoxia in resting state conditions. Sheng et al., (2017) recently demonstrated that hyperoxia was associated with reductions in alpha and beta power during both a sustained attention task and a visual ERP task. Our results similarly showed that hyperoxia was associated with decreases in alpha and beta power as well as proportion of detections during a resting state task when the eyes were opened but extended this to the comparison of eyes-closed condition in which this decrease was lessened.

That said, there are other factors which may have influenced our findings. In particular, the fronto-temporal localization of the beta and gamma decrease under hyperoxia suggests that decreased scalp and eye muscular activity could be contributing in whole or in part to our results. This lays the foundation for future research to explore the potential of transient administration of oxygen on attentional tasks, to see if these changes in oscillatory dynamics correlate with behavioural performance. Such studies should be careful to measure muscular contributions to oscillation measures using EMG. Another limitation of our study was that our SpO_2 measurement was not continuously assessed during the trials, but rather at the beginning and ends of each block. Thus, we were only able to examine differences in SpO_2 across different blocks. Lastly, we were unable to assess whether participant entered into light stages of sleep

during the eyes-closed condition, which may have contributed to the enhancements seen in delta and theta bands.

Conclusion

Here we manipulated oxygen administration in eyes-opened and eyes-closed resting states while monitoring for respiration and other physiological responses like heart rate and SpO_2. Modest EEG changes were seen in both resting state conditions during hyperoxia that may be associated with increased alertness during eyes-opened conditions and paradoxically perhaps, the initiation of sleep states during eyes-closed conditions. In addition, we found that oxygen enhanced the changes typically seen when comparing eyes-opened to eyes-closed conditions, especially in the alpha band. Our results demonstrate that in comparable conditions to that provided by recreational oxygen providers, the administration of hyperoxic gas could potentially have the attentional benefits specified during eyes-opened wakefulness and may also differentially promote relaxation and sleep during eyes-closed conditions. Future studies are needed to evaluate the precise impact of hyperoxia on neural oxygenation, and to further evaluate the effects of oxygen on attentional processing, behavioural performance, and behavioural state.

2.5 Figure Captions

Figure 2.1 Experimental procedure. Participants completed four 3-minute trials, two eyes-opened and two eyes-closed, within each gas block. Participants completed four gas blocks in total, two hyperoxia and two normoxia conditions, interleaved. Block order was counterbalanced across subjects.

Figure 2.2 Physiological measurements. A) SpO2 measurements for the baseline period (red) and for the average of the two measurements at the beginning and end of each gas block (blue). B) Breathing rate differences between hyperoxia and normoxia conditions. No significant within-subjects difference was observed. Dark line is grand average, error bars are within-subject SEM. C) Heart rate differences between hyperoxia and normoxia conditions. Heart rate was significantly lower in the hyperoxia condition for both eyes-opened ($p < 0.001$) and eyes-closed ($p < 0.01$) conditions.

Figure 2.3 Analysis of power changes across electrodes, frequencies, state, and oxygen conditions. A) The raw power spectra of each condition averaged across all electrodes. Shaded lines represent the within-subject SEM. B) The t-statistic for the difference due to hyperoxia on eyes-opened power is plotted at each electrode and frequency. Comparisons which were statistically significant at the 0.05 α level are emphasized. Topographical distributions of the statistical effects, as well as the magnitude of power in each condition is plotted for each band. Error bars represent the within-subject SEM. C) The t-statistic for the difference due to hyperoxia on eyes-closed power is plotted at every electrode and frequency, showing no clusters of significant differences. D) The difference spectrum of hyperoxia – normoxia power for the eyes-opened condition, from electrode F3. The shaded line plots the 95% CI for the difference. E) Power spectra for each condition after subtracting the overall average power across conditions, accentuating the differences due to gas. F) The F statistic for the interaction between

gas condition and eye condition is plotted at every electrode and frequency. Comparisons which were statistically significant at the 0.05 α level are emphasized. The topographical distribution of the statistical effect in this band as well as the magnitude of the raw power in each condition are plotted for each condition. Error bars represent the within-subject SEM. G) The difference spectra for eyes-closed – eyes-opened power across the hyperoxia and normoxia conditions, for electrode F3. Error bars represent the within-subject SEM. As shown, a larger alpha amplitude difference exists in the hyperoxic state between eyes-closed and eyes-opened conditions.

Figure 2.4 Analysis of changes in detected oscillations across electrodes, frequencies, state, and oxygen conditions. A) The $P_{episode}$ spectra across all electrodes, thresholded with the average power spectrum across the whole experiment. Error bars represent the within-subject SEM. B) The t-statistic for the difference due to hyperoxia on eyes-opened $P_{episode}$ is plotted at each electrode and frequency. Comparisons which were statistically significant at the 0.05 α level are emphasized. The topographical distributions of the statistical effect, as well as the percentage of time oscillations were detected in each condition is plotted for each band. Error bars represent the within-subject SEM. C) The same analysis as for B) is presented for the eyes-closed condition. D) The difference spectrum of hyperoxia – normoxia $P_{episode}$ during the eyes-opened condition, from electrode F3. The shaded error plot represents the 95% CI for the difference. E) The difference spectrum of eyes-closed $P_{episode}$, hyperoxia – normoxia, plotted from electrode PO4 to show the observed increase in the delta band. The error bar represents the 95% CI for the difference. F) The $P_{episode}$ spectra thresholded with the averaged power within each gas condition, rather than across all gas conditions showing that the choice of background spectra did not influence the detection of oscillations of different frequencies. G) The F statistic for the interaction between gas condition and eye condition is plotted at every electrode and frequency.

Comparisons which were statistically significant at the 0.05 α level are emphasized. The topographical distribution of the statistical effect in this band as well as the percentage of time oscillations were detected are plotted for each condition. Error bars represent the within-subject SEM. H) The difference spectra for eyes-closed – eyes-opened $P_{episode}$ across the hyperoxia and normoxia conditions, for electrode F3. This shows a larger difference in the hyperoxia condition. Error bars represent the within-subject SEM.

Figure 2.5 Analysis of detected alpha epoch lengths. A) Bar graphs showing the raw power values within detected segments only (detected power) for the six frequency ranges which showed main effects of gas on detected oscillations. Only the beta frequency range of 21.14 – 35.16 Hz in the eyes-opened condition shows a decrease in power within detected segments. Error bars are within-subject SEM. B) Cycle length distributions for detected cycles from the range of 6.8 : 9.3 Hz. Closing the eyes results in longer cycle lengths, for both normoxia and hyperoxia conditions. C) Empirical cumulative distribution function estimated from the pooled cycle length distributions across subjects. Hyperoxia cdfs were significantly more extreme than normoxia cdfs.

2.6 Figures

Figure 2.1

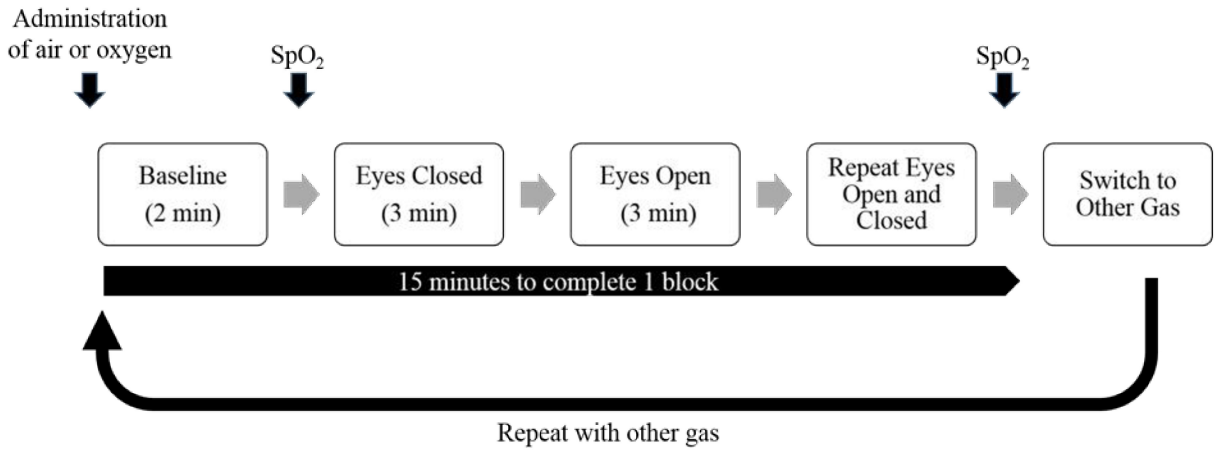

Figure 2.2

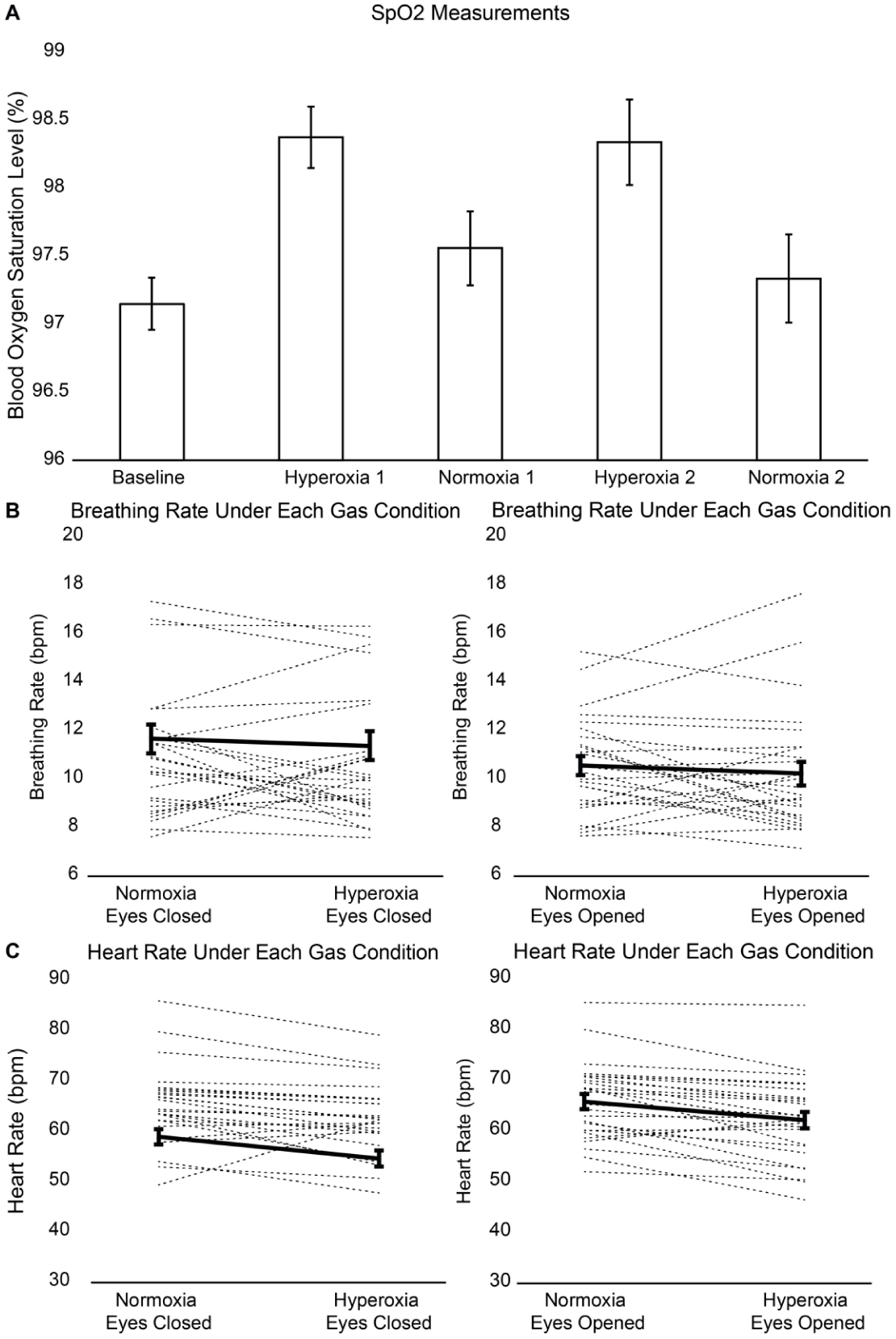
A
SpO2 Measurements
Blood Oxygen Saturation Level (%)
99
98.5
98
97.5
97
96.5
96
Baseline
Hyperoxia 1
Normoxia 1
Hyperoxia 2
Normoxia 2
B
Breathing Rate Under Each Gas Condition
Breathing Rate (bpm)
20
18
16
14
12
10
8
6
Normoxia
Eyes Closed
Hyperoxia
Eyes Closed
Breathing Rate Under Each Gas Condition
Normoxia
Eyes Opened
Hyperoxia
Eyes Opened
C
Heart Rate Under Each Gas Condition
Heart Rate (bpm)
90
80
70
60
50
40
30
Normoxia
Eyes Closed
Hyperoxia
Eyes Closed
Heart Rate Under Each Gas Condition
Normoxia
Eyes Opened
Hyperoxia
Eyes Opened

Figure 2.3-

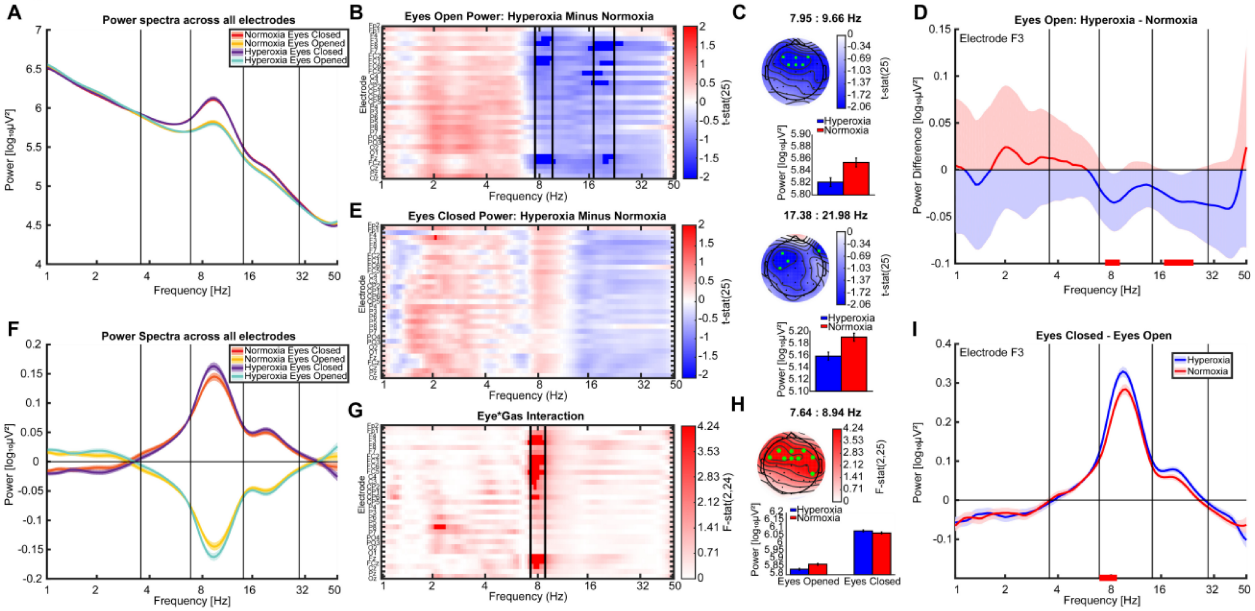
A
Power spectra across all electrodes
Normoxia Eyes Closed
Normoxia Eyes Opened
Hyperoxia Eyes Closed
Hyperoxia Eyes Opened
Power [log10μV²]
Frequency [Hz]
B
Eyes Open Power: Hyperoxia Minus Normoxia
Electrode
Frequency (Hz)
t-stat(25)
C
7.95 : 9.66 Hz
t-stat(25)
Hyperoxia
Normoxia
Power [log10μV²]
17.38 : 21.98 Hz
D
Eyes Open: Hyperoxia - Normoxia
Electrode F3
Power Difference [log10μV²]
Frequency [Hz]
E
Eyes Closed Power: Hyperoxia Minus Normoxia
F
Power Spectra across all electrodes
G
Eye*Gas Interaction
F-stat(2,24)
H
7.64 : 8.94 Hz
F-stat(2,25)
Eyes Opened
Eyes Closed
I
Eyes Closed - Eyes Open

Figure 2.4

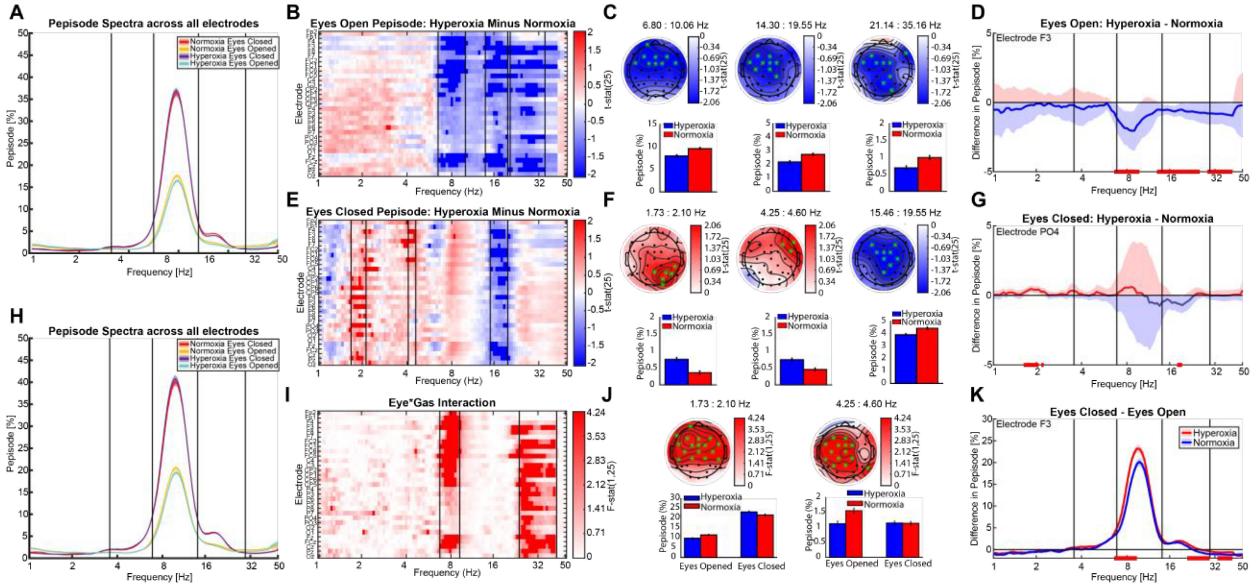
A
Pepisode Spectra across all electrodes
Normoxia Eyes Closed
Normoxia Eyes Opened
Hyperoxia Eyes Closed
Hyperoxia Eyes Opened
Pepisode [%]
Frequency [Hz]
B
Eyes Open Pepisode: Hyperoxia Minus Normoxia
Electrode
Frequency (Hz)
t-stat(25)
C
6.80 : 10.06 Hz
14.30 : 19.55 Hz
21.14 : 35.16 Hz
t-stat(25)
Hyperoxia
Normoxia
Pepisode (%)
D
Eyes Open: Hyperoxia - Normoxia
Electrode F3
Difference in Pepisode [%]
Frequency [Hz]
E
Eyes Closed Pepisode: Hyperoxia Minus Normoxia
F
1.73 : 2.10 Hz
4.25 : 4.60 Hz
15.46 : 19.55 Hz
G
Eyes Closed: Hyperoxia - Normoxia
Electrode PO4
H
Pepisode Spectra across all electrodes
I
Eye*Gas Interaction
F-stat(1,25)
J
1.73 : 2.10 Hz
4.25 : 4.60 Hz
Eyes Opened
Eyes Closed
K
Eyes Closed - Eyes Open
Electrode F3

Figure 2.5

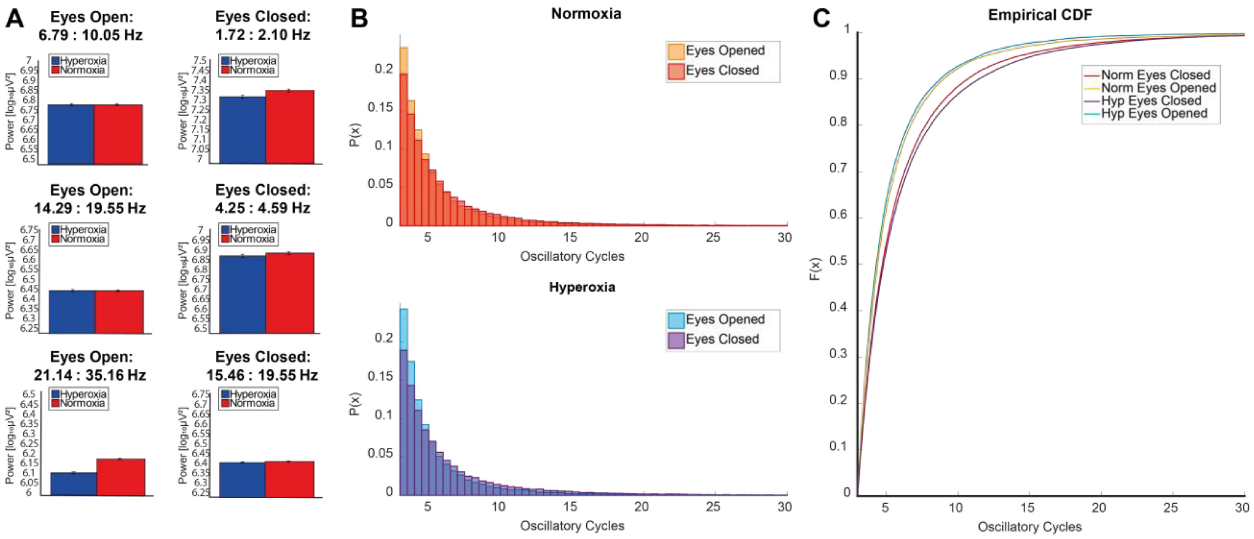
A
Eyes Open:
6.79 : 10.05 Hz
Eyes Closed:
1.72 : 2.10 Hz
Eyes Open:
14.29 : 19.55 Hz
Eyes Closed:
4.25 : 4.59 Hz
Eyes Open:
21.14 : 35.16 Hz
Eyes Closed:
15.46 : 19.55 Hz
Hyperoxia
Normoxia
Power [log10μV²]
B
Normoxia
Eyes Opened
Eyes Closed
P(x)
Oscillatory Cycles
Hyperoxia
C
Empirical CDF
Norm Eyes Closed
Norm Eyes Opened
Hyp Eyes Closed
Hyp Eyes Opened
F(x)

3. ELECTROPHYSIOLOGICAL CORRELATES OF HYPEROXIA DURING MID-DAY NAPS IN HUMAN SUBJECTS

3.1 Introduction

Energy metabolism in the brain is a crucial aspect of brain function (Magistretti & Allaman, 2015; Raichle & Gusnard, 2002), which depends on the aerobic metabolism of pyruvate (Bélanger, Allaman, & Magistretti, 2011; Raichle, 2010) and is thus highly dependent on a high degree of oxygen saturation (>95%) in the blood.

For example, even intermittent reductions (85-90%) in arterial oxygen saturation (Mehta, Vasu, Phillips, & Chung, 2013) caused by respiratory diseases such as obstructive sleep apnea (OSA) can result in deleterious effects on metabolic (Lévy et al., 2008) and cardiovascular health (Marin et al., 2005; Mortola, 2007), cognition (Areza-fegyveres et al., 2010; Saunamäki et al., 2009), and sleep itself (Hamrahi et al., 2001; Polotsky et al., 2006).

By contrast, hyperoxia is commonly used in medical settings for the management of circulatory shock (Hafner et al., 2015), stroke (Kumaria & Tolias, 2009; Shi, Qi, Luo, Ji, & Liu, 2016) as well as therapeutically for conditions such as chronic obstructive pulmonary disease (COPD) (Owens, 2013; Stoller, Panos, Krachman, Doherty, & Make, 2010), to counter any oxygen debt caused by the injury or disease and – apart from some concerns with the generation of free radicals (Hafner et al., 2015) – is generally believed to have no negative impact on the body under short durations (Bitterman, 2009).

Hyperoxia has been studied for the treatment of sleep apnea, and while hyperoxia improved nocturnal oxygenation as well as the standard continuous positive airway pressure (CPAP) treatment, it did not similarly improve sleep quality (Loredo et al., 2006) and has been also been shown to have no effect on sleep in patients with COPD and controls (Fleetham et al.,

1982). However, these papers only measured self-reports of sleep quality, not full polysomnographic recordings using EEG.

Recent investigations have found that in rats showing spontaneous rhythmic alternations of forebrain state under either urethane anesthesia (activated/deactivated) or natural sleep (REM/NREM) (Clement et al., 2008; Whitten, Martz, Guico, Gervais, & Dickson, 2009) hyperoxia promoted the deactivated or NREM state over the activated or REM state (Hauer et al., 2018). These results suggest that hyperoxia may disrupt sleep states in humans, potentially even abolishing REM sleep. Considering that neural activity usually corresponds very well to the rate of oxygen metabolism (Raichle & Mintun, 2006), a well-controlled, high-density investigation of the effect of oxygen on the human EEG during sleep seems to be required. Further support for the hypothesis that hyperoxia may affect sleep oscillations comes from similar studies that have conclusively shown an effect of hyperoxia on the oscillatory brain activity of *awake* human subjects (Croal et al., 2015; Kaskinoro, Maksimow, Laitio, Scheinin, & Jääskeläinen, 2010; Seo, Bahk, Jun, & Chae, 2007; Vuong, Kizuk, Maclean, Dickson, & Mathewson, *under review*; Wu et al., 2014). One recent MRI study reported that hyperoxia was associated with increased signal from the default mode network (DMN) and attentional networks (AN), and decreased signal in visual cortices (Wu et al., 2014). A series of EEG experiments have also found decreases in high-frequency neural oscillations with the eyes opened, (Croal et al., 2015; Seo et al., 2007; Sheng et al., 2017), as well as a non-significant trend for a decrease in alpha activity with the eyes closed (Kaskinoro et al., 2010). In our own lab, we recently conducted a high-density resting-state EEG study evaluating the effect of hyperoxia in both eyes-closed and eyes-opened conditions (Vuong et al., *under review*), and we found that under eyes-opened conditions, alpha, beta, and gamma oscillations decreased, while under eyes-closed

conditions, only beta oscillations decreased. We also observed an *increase* in delta oscillations with hyperoxia under eyes-closed conditions, suggesting that slower frequencies could be enhanced by hyperoxia during sleep.

Our aim in this investigation is to observe the effect of supplemental oxygen administration on sleeping brain activity. We monitored oxygen saturation and respiratory and cardiac rhythms to ensure that our results could not be attributed to systemic physiological changes. We predicted hyperoxia would enhance NREM activity by increasing the amount of time spent in the NREM state, increasing slow oscillations, and increasing the epoch length of the slow wave sleep (SWS) sleep stage and potentially depressing the incidence of REM. Using an exploratory, high-resolution approach, we show that, contrary to expectations, hyperoxia is not associated with any major changes during sleep.

3.2 Methods

3.2.1 Procedure

Our experiment consisted of a "napping task" where a mattress, pillow and blanket were brought inside the EEG chamber, and participants attempted to sleep for a 90-minute recording period. Either normal air or 100% concentrated oxygen was delivered continuously, beginning 2 minutes before the start of the session, so as to allow the gas to be taken up by the body, and ending after the session was completed. Blood oxygenation levels were measured both at the start and end of the 2-minute baseline block, and at the end of the 90-minute session (Figure 3.1). Participants who passed the screening procedures were asked to complete two separate sessions spaced exactly one week apart. All sessions began between 12:00 – 14:00pm . At the beginning of each session, participants were asked to fill out a questionnaire that assessed their current day-time sleepiness. Participants answered questions from the Epworth Sleepiness Scale, Stanford

Sleepiness Scale, and questions that assessed an individual's sleep hygiene. Participants were randomly placed into one of two counterbalancing orders; the first counterbalancing order received regular air during the first session and 100% oxygen on the second session, and the second counterbalancing group had the opposite order of gas administration for the two days. Participants were blind to which gas they were receiving for each session. Four participants were excluded for only completing one out of the two sessions.

We collected data from 26 members of the university community in total (mean= 24.1, range = 20 – 33, 16 female). Eligibility for the experiment was determined for each participant with the Pittsburgh Sleep Quality Index (PSQI). Only participants who scored less than 5 according to the PSQI scoring criteria were eligible to participate in the study. All participants were right handed; had normal or corrected vision; were absent of medical conditions including a history of neurological problems, respiratory disease, cardiac disease, and pulmonary hypertension; were not smokers; did not have allergies; did not take antihistamine medications (i.e. Benadryl, Chlor-Timeton, Dimetane, etc.), and were not pregnant. Five questions from the Horne and Osteberg (1976) Morningness-Eveningness Questionnaire were administered for analysis purposes. All participants gave informed consent and were compensated at a rate of $10/hr to be a research subject. The internal Health Research Ethics Board at the University of Alberta approved all experimental procedures.

3.2.2 EEG recording and setup

EEG data was collected using a 32-channel low-impedance EEG system (actiCAP passive electrodes kept below 5 kΩ), referenced to an electrode attached to the left mastoid, and offline re-referenced to the average of the left and right mastoid. In addition to the 31 EEG sensors, 2 reference electrodes, and the ground electrode, vertical and horizontal bipolar EOG

was recorded, and two more of the same electrodes were placed on the mastibular and submastibular area to record EMG data. We also used a respiration belt transducer to measure breathing rate, as well as two different pulse oximeters to measure heart rate and blood oxygenation level. The experiment took place in a dim, sound and radio frequency-attenuated chamber with the lights off. Following EEG set-up, a mattress, a pillow, and a blanket were provided to help participants maintain a comfortable temperature. Regular air or 100% O_2 (Praxair) was delivered at 3 L/min through an unsealed, disposable plastic gas mask placed over top of the EEG set-up. Participants were asked to lie down in a comfortable prone position, either on their side or their back. Prior to the start of the napping task, the participant's baseline SpO2 measurement was taken. Following this, there was a two-minute period to allow the participants to inhale the gas for the current session. SpO_2 was again measured after this period. Finally, the lights were turned off and participants were asked to close their eyes and attempt to sleep. EEG recording began immediately and lasted for 90 minutes. Participants were awoken after the EEG recording period was terminated. SpO2 was then measured a third time. This procedure was repeated one week later at the exact same time of day for the second session.

3.2.3 Physiological data processing

Raw heart beat and breathing traces were segmented into 5-minute epochs locked to the onset of the EEG recording period. The average breathing and heart rate within each session for each individual were obtained by convolving the data with a Morlet wavelet six cycles in length and for 100 logarithmically sampled frequencies from 1 – 100 cycles per minute (0.0167 – 1.67 Hz). These raw power values were averaged across the 5 second segments, and the frequency with the maximum power is determined for every segment in the 90-minute session (1080 in total). These heart rates and breathing rates were then averaged to give a single value for every

participant, which were compared across gas sessions. The SpO_2 differences for each participant in each gas session were obtained by subtracting the resting SpO_2 from the average of the two measurements at the start and end of the napping task (Figure 3.1).

3.2.4 Time frequency analysis

Raw EEG traces were analyzed as one continuous trace across the 90-minute recording session. A baseline of at least 30s was recorded from before the start of the session, as well as an additional 30s after the session to help correct for edge artifacts. Each trace was transformed into time-frequency space by convolving with a Morlet wavelet with a window of 6 cycles and for frequencies sampled in 100 logarithmic steps covering the bandwidth from 0.1 to 50 Hz. The raw power values were averaged in 5-second windows, resulting in a total of 1080 timepoints for each session (Figure 3.2D).

In addition to the analysis of raw oscillatory power, we also made use of the BOSC (Better OSCillation detection) technique, whereby the wavelet power at each frequency is subjected to a thresholding procedure that requires it to exceed a power threshold (P_T), for a continuous number of cycles (D_T). We set our D_T to 3 continuous cycles. The P_T was determined by first computing the average log-transformed wavelet power spectrum across the whole 90-minute trial. This average signal was then used to fit the background noise spectrum with a linear regression in log-log space. The fitted model provides a theoretical X^2 probability distribution for expected power values at that frequency and electrode, and the P_T is set to the 95^{th} percentile of this distribution, replicating previous applications of the BOSC technique. This estimation was done at each electrode, for each 90-minute recording, as was assumed to take the form of colored noise, where power scales with frequency by the 1/f relationship. The application of these two thresholds resulted in a binary value of ‘detected’ or ‘undetected’ for each frequency and time-

point that does not discriminate between relative amounts of supra-threshold power (Whitten, Hughes, Dickson, & Caplan, 2011; Caplan et al., 2001, 2003).

The $P_{episode}$ was first computed within consecutive 5 second windows of the entire 90-minute trial, for each electrode and frequency, by coding detected values as 1 and undetected value as 0 and averaging across the 5-second window. This resulted in 1080 values ranging between 0 and 1, which can be interpreted as the proportion of time oscillations of that frequency were detected in that 5-second window. These windows always matched up (in groups of 6) exactly with the 30 second blocks used for scoring of sleep stages. The $P_{episode}$ values were then further averaged across all times when the participant was scored to be in one of the five sleep stages by the expert scorer. This resulted in 5 $P_{episode}$ spectras corresponding to the times during the trial that participants were in the Wake, N1, N2, REM, or SWS stage. Figure 3.2 shows how the EEG-derived measures from one subject's session tracked with the manual scoring of sleep stage. The oscillatory power (Figure 3.2D) and $P_{episode}$ (Figure 3.2E) spectrograms show how compared to the average across the entire session, more higher frequency oscillations are detected during wake stages, and more lower frequencies oscillations are detected during SWS and N2 stages.

The same analyses in all cases were performed on unthresholded power data as well as the $P_{episode}$ data. Power data was matched to the manually scored sleep stages and averaged to produce analogous spectra within each sleep stage to the $P_{episode}$ spectra.

3.2.5 Manual scoring of sleep stages

All sleep scoring was conducted by a commercially available service (Sleep Strategies, Vancouver, BC, Canada). In addition, we employed two locally trained scorers with moderate experience. In a subset of these data, we validated scoring using a third, and more extensively

trained scorer. Traces used for scoring consisted of raw EEG data that was filtered with a low pass of 30 Hz and a high pass of 0.1 Hz. Specifically, data from electrodes Oz, Pz, Cz, Fz, the two EOG electrodes, and the EMG electrode were used to score sleep stages. The data was broken up using 30 second epoch windows for manual scoring of the data by eye according to standard protocols provided by the American Academy of Sleep Medicine (AASM, 2013). The manual scoring procedure considers information from EEG electrodes, EOG eye movements, and EMG muscle activity to determine sleep stage. Only one stage was assigned to a given 30 second epoch. If more than one stage appeared in a 30s period, the predominant stage was scored. The time spent asleep was calculated as the total time of the trial scored as sleep (N1, N2, REM, and SWS) divided by the total trial time. The proportion of sleep time spent in each stage was computed for each subject as the total time spent in each sleep stage (N1, N2, REM, SWS) divided by the sum of those four times. If the scorer found a subject who entered the SWS stage for less than 5 minutes in the entire sessions, in either the hyperoxia or the normoxia session, that subject was excluded. Out of the 26 participants initially collected, four failed to return for the second session, and 13 failed to enter the SWS stage during both sessions. This resulted in a final number of 9 subjects (mean = 24.6, range: 21 – 31, 5 female) that were used in all EEG data analysis. The mean epoch duration for each stage was computed as the average number of 30s epochs continuously scored as one of the five stages. All sleep timing measures were computed for each subject and compared between gas sessions.

3.2.6 Algorithmic scoring of sleep stages

One of the advantages of BOSC is that it provides a binary representation of the prevalence of neural oscillations. Considering that most of the criteria for sleep stage scoring are based on the presence or absence of specific oscillatory signals (alpha waves, sleep spindles,

slow waves), we created a simple algorithmic staging procedure which would in theory replicate the judgements of human scorers while circumventing the subjectivity inherent in manual scoring. Our algorithm was based on a simple set of conditions where the detected oscillations within each 5-second window and from multiple pre-determined frequency bands were compared to values derived from the literature (Lee-Chiong, 2005) to determine the sleep stage. These conditions are summarized in Table 1. For every 5-second period, the $P_{episode}$ values were compared to each of these mutually exclusive rules. If one matches, that window is scored as that stage. If none match, the stage is scored as N1 by default. If a window is scored as an arousal, then the window is treated as awake in subsequent analysis. The BOSC scores were not used to subdivide power and $P_{episode}$ values by sleep stage as they were only computed for the purposes of making a comparison with our commercially derived scores (Figure 3.2A). This comparison was made by determining the proportion of scored windows (out of 1080) that matched the manual scoring service, and as well for each of our three local scorers. We removed all windows that the expert scorer scored as REM sleep for this comparison, because REM was observed in very few subjects.

3.3 Results

3.3.1 Physiological measurements

Figure 3.3A summarizes our physiological measures. Hyperoxia was associated with significantly increases in oxygen saturation across all participants ($t(21) = 6.63$, $p < 0.01$), demonstrating that the oxygen delivery was effective. This was also true for the nine participants who successfully entered slow-wave sleep in both sessions ($t(8) = 4.16$, $p = 0.002$). Consistent with both the literature and our previous experiments, exposure to hyperoxia significantly

lowered heart rate across participants (t(21)=-4.47, p<0.001) but had no significant effect on breathing rate (t(21)=-0.63, 0.53.)

3.3.2 Effect of Oxygen on sleep timings

The concordances for our three scorers, as compared to the expert scorer, are shown in table 2 for all subjects. A concordance rate of 85% is generally considered acceptable for two properly trained sleep scorers. None of the three scorers met this criterion, with our algorithm matching the expert score 61% of the time, averaged across subjects and both sessions, which was worse than one of the novice scorers (80%) and comparable to the other novice scorer (62%).

Hyperoxia did not produce any reliable differences in the total time spent asleep (Figure 3.3B), although it can be observed that there was significant variability in how much time participants actually slept during the 90-minute period (Figure 3.2A). Hyperoxia also did not produce any change in the proportion of sleep time spent in any of the four sleep stages (SWS: Normoxia = 31%, Hyperoxia = 31%, t(8) = 0.05, p= 0.96; N2: Normoxia = 52%, Hyperoxia = 48%, t(8) = 0.87, p = 0.41; N1: Normoxia = 12%, Hyperoxia = 13%, t(8) = -0.29, p = 0.78; REM: Normoxia = 8 %, Hyperoxia = 13 %, t(5) = -1.01, p = 0.36), and did not affect the time it took for participants to enter the SWS stage (Normoxia = 31.03 min, Hyperoxia = 31.14 min, t(8) = -0.02, p = 0.99). In order to most closely replicate previous reports of NREM enhancement by hyperoxia (Hauer et al., 2018), we also calculated the total time spent in all NREM states compared to REM states (which was 100% for 4 subjects), and this was also not significant (Normoxia = 95% , Hyperoxia = 91%, t(8) = 1.01, p = 0.34).

There were also no differences in the mean epoch length for any of the five stages (SWS: Normoxia = 88 s, Hyperoxia = 137 s, t(8) = -1.00, p= 0.34; N2: Normoxia = 183 s, Hyperoxia =

205 s, t(8) = -0.71, p = 0.50; N1: Normoxia = 108 s, Hyperoxia = 79 s, t(8) = -1.56, p = 0.16; REM: Normoxia = 108 s, Hyperoxia = 79 s, t(5) = 0.40, p = 0.70; Wake: Normoxia = 126 s, Hyperoxia = 148 s, t(8) = -1.40, p = 0.20).

3.3.3 Effect of Oxygen on sleep power

We performed a two-tailed uncorrected paired t-test for the effect of hyperoxia on raw oscillatory power at every electrode and every sampled frequency, and for every sleep stage excluding REM, as shown in the electrode by frequency heatmap plots in Figure 3.5A. Due to the large number of comparisons being made, we focused our analyses on groups of nearby electrodes.

Figure 3.2B shows how the power spectrum changes with sleep state, shifting towards lower frequencies as deeper stages of sleep are entered. In the waking stage, hyperoxia was associated with a significant decrease in the power of low-frequency alpha oscillations (7.27 Hz) at two occipital electrodes (Oz: t(8)=-2.31, p= 0.050; and O2: t(8)=-2.57, p= 0.033). Figure 3.5C shows the topographical distribution of the raw power difference (hyperoxia – normoxia) at selected frequencies for all four sleep stages. Electrodes which were significant at the 0.05 α-level are emphasized in green. Because of the large number of comparisons being made, we also evaluated whether hyperoxia also led to a decrease in alpha power across a predetermined alpha range of 7-14 Hz. When this full range was considered however, the comparison was no longer significant (Oz: t(8) = -0.87, p = 0.41). In the N1 stage, hyperoxia was also associated with a decrease in the power of alpha oscillations (7.19 - 8.15 Hz), however this was only significant at one electrode (O2, t(8) =- 2.63, p = 0.030). Again, when the full alpha range was considered, this comparison was also not significant (Oz: t(8) = -1.37, p = 0.21). In the N2 stage, hyperoxia was associated most strongly with an increase in the power of theta oscillations (6.33 - 7.19 Hz),

centered around electrode Fz (t(8) = -3.14, p = 0.014). As well, when the full theta range (3.5 - 7 Hz) was considered, the comparison remained significant (Fz: t(8) = -3.17, p = 0.013). Contrary to our predictions, in the SWS stage hyperoxia was associated with a decrease in the power of delta oscillations (1.45: 1.53 Hz) centered around electrode Fz (t(8) = -2.60, p = 0.032) as well as a decrease in the power of theta oscillations (6.61: 1.53 Hz) also centered around this same electrode (t(8) = -2.60, p = 0.032). When the full slow-wave range (0.1 – 2 Hz) was considered, the comparison was only trending (Fz: t(8) = -1.91, p = 0.09), but when the full theta range was considered, this comparison remained significant (Fz: t(8) = -2.32, p = 0.05).

3.3.4 Effect of Oxygen on sleep $P_{episode}$

While spectral power is often useful for detecting overall changes in the relative frequency of EEG signals, it is not always a robust method for distinguishing neural oscillations from other, non-oscillatory components in the EEG (Caplan et al., 2001). We used the Better OSCillation (BOSC) detection method to detect signals which passed certain thresholds for consistent oscillatory activity. The resulting $P_{episode}$ measure (percent detected per unit time) only reflects the contribution of neural oscillations, and unlike spectral power, is scaled evenly across frequencies, allowing for more accurate comparisons between different frequency ranges.

We performed a two-tailed uncorrected paired t-test for the effect of hyperoxia on detected oscillations at every electrode and every sampled frequency, and for every sleep stage excluding REM, as shown in the electrode by frequency heatmap plots in Figure 3.6A. Due to the large number of comparisons being made, we focused our analyses on groups of nearby electrodes, and we averaged $P_{episode}$ values across pre-determined ranges, in addition to the most significant frequencies. Figure 3.6C shows the topographical distribution of the raw power

difference (hyperoxia – normoxia) at selected frequencies for all four sleep stages. Electrodes which were significant at the 0.05 α-level are emphasized in green.

In the waking stage, hyperoxia was associated with a significant decrease in the $P_{episode}$ of low-frequency alpha oscillations (7.49 Hz) at two occipital electrodes, (Oz: t(8) = -2.33, p = 0.049; and O2: t(8) = -2.69, p = 0.027), however, when we compared the average alpha $P_{episode}$ across these two electrodes, and across the full alpha range (7 - 14 Hz), the decrease in alpha with hyperoxia was not significant (t(8) = -0.40, p = 0.54). In the N1 stage, hyperoxia was also associated with a decrease in the power of alpha oscillations (8.49 - 8.85 Hz), however this was only significant at two electrodes (P4: t(8) = -3.06, p = 0.015; and CP2: t(8) = -2.43, p = 0.041). When the full alpha range was considered however, we only observed a trending decrease across both electrodes (t(8) = -2.06, p = 0.074). In the N2 stage, hyperoxia was associated most strongly with an increase in the $P_{episode}$ of theta oscillations (6.33 - 7.19 Hz), with a focal point in the left parietal region (PO4 (t(8) = -3.14, p = 0.014 ; P6 (t(8) = -3.14, p = 0.014 ; P8 (t(8) = -3.14, p = 0.014). When the full theta range was considered (3.5 - 7 Hz), these increases were only trending across all three electrodes (t(8) = 1.87, 0.098). In the SWS stage, hyperoxia was associated with a decrease in the power of oscillations in the sleep spindle range (12.30 - 15.30 Hz) at a single electrode O2 (t(8) = -3.04, p = 0.016). When the full spindle range was considered (11.5 - 15 Hz), the comparison remained significant at electrode O2 (t(8) = -3.30, p = 0.011). In the SWS and N2 stages, the decreases in slow wave and theta oscillations observed in the power measure were not detectable in the $P_{episode}$ measure, suggesting that these decreases were due to some non-oscillatory contribution.

3.4 Discussion

Our aim in this study was to evaluate the effect of respired 100% oxygen gas on sleep oscillations and natural sleep patterns during a 90-minute nap. Under hyperoxia, we observed an increase in blood oxygen saturation and a decrease in heart rate, but no significant changes in breathing rate. Previous reports indicate that hyperoxia causes hyperventilation (Dean, Mulkey, Henderson, Potter, & Putnam, 2004), but we did not observe any changes in breathing rate across subjects, either in this experiment or our previous study in awake humans (Kizuk et al., *under review*). While it is clear that hyperoxic conditions were achieved in our study, changes in EEG measures were modest at best, and changes in overall sleep patterns were not observed.

3.4.1 Hyperoxia does not enhance NREM sleep states during mid-day nap conditions

Contrary to our hypothesis, hyperoxia was not associated with any changes to the proportion of time spent asleep, the proportion of time spent in NREM sleep or any individual sleep stage and was not associated with any changes in epoch length. Our lab (Hauer et al., 2018) previously found that rats anesthetized with urethane and then given 100% oxygen experienced disruptions to state alternations, with the ‘deactivated’ (NREM) state overtaking the ‘activated’ (REM) state. In naturally sleeping rats, the effect was not as strong, but there was still a significant boost to NREM states; hyperoxic rats spent 96% of their sleep time in NREM and normoxic rats spent 90%. One reason we may have not observed this difference is that our 90-minute design was focused on the timings and oscillations within a single sleep cycle. If the effect of hyperoxia is not actually an enhancement of NREM states but instead a disruption of REM states, then it is reasonable to speculate that a longer design would show markedly reduced REM epochs.

We also did not find any conclusive evidence that hyperoxia affects low-frequency NREM oscillations during sleep. Although we observed decreases in the slow-wave and theta bands (Figure 3.4A) in the power measure, this decrease was not present in the $P_{episode}$ measure. The $P_{episode}$ measure is the proportion of time that a neural oscillation of a given power and a given length is detected within a given period of time. For our study, we chose a short duration threshold of 3 cycles, and so increases or decreases that are present in the power measure, but not the $P_{episode}$ measure, may appear oscillatory for a short period of time, but are not consistent oscillations. Given that the $P_{episode}$ measure has been shown in the past to robustly isolate well-known brain rhythms from the non-oscillatory background (Hughes et al., 2012; Whitten et al., 2011), we can say with a reasonable degree of certainty that the power decreases observed in the N2 and SWS stages likely only represent transient fluctuations in the EEG that were not corrected for by our other procedures. In support of our original hypothesis, we did observe an increase in theta oscillations in both the power (Figure 3.4A) and the $P_{episode}$ (Figure 3.5A) during N2, although the effect was only trending across the full theta range. This may suggest that hyperoxia did enhance the initiation of the deeper stages of NREM sleep (N2 and SWS), although this interpretation would seem to be contradicted by the lack of a similar increase in the SWS stage.

3.4.2 Hyperoxia disrupts alpha oscillations but increases sleep spindles

Consistent with previous research on hyperoxia in awake humans, we found some evidence for a decrease in alpha oscillations in the Wake and N1 stages, although this effect was only significant two electrodes at most, and only applied to a very narrow range of alpha oscillations. In our lab, we previously reported that hyperoxia affects the state transition caused by opening and closing the eyes (Kizuk et al., *under review*). Closing the eyes causes an

immediate increase in alpha oscillations (from ~20% to ~40%) and we found that hyperoxia increased the magnitude of this transition by 3-4%. Importantly, the locus of the effect in terms of frequency was not at the alpha peak frequency, but rather in the lower 7 - 9 Hz range. Considering that hyperoxia seems to have more of an effect on alpha oscillations when the eyes were opened compared to closed, it is perhaps not surprising that the effect of hyperoxia is even weaker in the light stages of sleep. However, the consistent localization of the effect in topographical space in both the power and $P_{episode}$ measures, and the consistent frequencies between this study and our previous work suggest that hyperoxia does in fact decrease alpha oscillations, both while awake and in the light stages of sleep.

The only significant change we found to $P_{episode}$ in the SWS stage was an increase in sleep spindles (Figure 3.5A, far right). This effect was only found at one electrode, however it remained significant across the entire pre-determined spindle range. Although sleep spindles are usually considered to be more prevalent in N2 than SWS (See Gennaro & Ferrara, 2003 for an overview), it is interesting to note that both alpha oscillations (Larson et al., 1998; F. H. Lopes da Silva, van Lierop, Schrijer, & Storm van Leeuwen, 1973) and sleep spindles (Steriade, 2000; Steriade & Amzica, 1998; Steriade, 2003) are thought to be generated by thalamocortical GABAergic reticular neurons. Recently, a team of researchers exposed rats to hyperoxia and hypercapnia while recording MRI data, and found that hyperoxia caused an increase in signal in the thalamus, as well as the caudate, hippocampus, and cortex (Lu et al., 2009). This, combined with previous reports that alpha waves are inversely correlated with thalamic glucose metabolism (Larson et al., 1998) and thalamic signaling (Goldman et al., 2002), suggest that the effect of hyperoxia on both alpha in awake subjects and spindles in sleeping subjects could be due to an

increase in thalamic glucose metabolism, caused by the increased availability of oxidative resources.

Interestingly, Goldman and colleagues found that hypercapnia (5% CO_2 and 95% O_2) also increased activity in the thalamus, caudate, and cortex, but not the hippocampus, and they also found that the hemodynamic responses to hyperoxia were maximal in subcortical areas, while the response to hypercapnia was maximal in the cortex. Furthermore, it has previously been reported that hypercapnia normalizes the effects of hyperoxia on the brain (Macey, Woo, & Harper, 2007), but this effect actually specifically did not occur in the thalamus. In our previous work, the effect of hyperoxia was compared to the effect of hypercapnia, and it was observed that the effect was reversed from that seen in hyperoxia; hypercapnia decreased the proportion of time that rats spent in 'deactivated' state during sleep. Future studies should be careful to consider that subcortical recordings and scalp EEG recordings may be affected by different components of the body and brain's homeostatic response to hyperoxia.

Given that hyperoxia was found to disrupt high-frequency activity in awake human subjects (Kizuk et al., *under review*), and to enhance low-frequency activity in sleeping rats (Hauer et al., 2018), it was hypothesized that a similar disruption of low-frequency activity would be observed in the sleeping human. This was found not to be the case. Another possibility is that the decrease in alpha waves observed with hyperoxia in awake humans and the increase in NREM activity with hyperoxia in sleeping rats are mediated by the disparate effects of hyperoxia on rat and human physiology and are not necessarily related. Hyperoxia has been shown to induce a plethora of changes in physiological variables including increasing blood CO_2 concentrations (Lu et al., 2009), decreasing CBF (Lu et al., 2009; Watson et al., 2000), increasing vasoconstriction (Floyd et al., 2003), and increasing free radicals (Bitterman, 2009;

Hafner et al., 2015). It is certainly possible that the true effects of respired 100% O_2 on the rat homeostatic response, and consequently the true levels of blood oxygen and carbon dioxide concentrations in the brain, are dissimilar between rats and humans. Future experiments could explore methods of finding (in)consistencies between the effect of hyperoxia on the rat and the effect of hyperoxia on the human in other conditions than resting state or sleep, by measuring EEG to analyze oscillatory state, and controlling for as many physiological variables as possible, using the same measures and units between the species.

3.4.3 Algorithmic scoring of sleep stage

Based on the observation that sleep states are primarily scored by estimating by eye the relative prevalence of different types of oscillations, we hypothesized than an algorithmic scoring procedure based on BOSC detections might be able to replicate the accuracy of human scorers, while removing the subjectivity inherent in the procedure. While our procedure does correspond more closely to the typical scoring procedure and output than previous attempts at algorithmic scoring (Dunai, Wilkinson, & Trinder, 1996), it was not successful in replicating the accuracy of the expert scorer (61% concordance). We did observe however that the accuracy of an algorithm consisting of five simple decision rules was equivalent to a novice scorer with two months of training (62%). These results emphasize the difficulty in obtaining accurate determinations of sleep state during manual scoring. Our algorithm was designed to replicate the subjective judgements of previous human scorers, although another approach would have been to statistically determine the values which produced maximal concordance with the expert rater, preferably on a very large number of subjects. Future studies could attempt to improve on the procedure by training a version of this algorithm on many sleep datasets, and then testing it on newly collected data.

3.4.4 Limitations of the research

There are a few limitations to our design which may have influenced the results. Firstly, the exploratory nature of our analysis procedure, especially the electrode by frequency heatmap plots in Figure 3.4A and Figure 3.5A, required us to make many statistical comparisons at once. In addition, because both frequency and electrode location are sampled variables of a continuous distribution, neighboring values are very highly auto-correlated, and this precludes the use of a correction method for multiple comparisons such as the Bonferroni method. We attempted to reduce the impact of this issue by giving more weight to effects which were consistent across multiple electrodes and frequencies, however several of our effects are only significant in one or two electrodes and may not represent reproducible effects.

Secondly, the magnitude of oscillatory power measured in different stages may be affected by whether the participant spent a significant portion of their sleep time in that stage, and whether that proportion differs greatly between their two sessions. An inspection of the sleep scores for each participant from Figure 3.2A shows that not all subjects slept a similar amount in both conditions, and so differences in power might not necessarily reflect the amplitude of oscillations, but rather the amount of time the participant spent in a particular stage. For example, it might be the case that the oscillation power after 10 minutes of slow wave sleep is higher than after 5 minutes, and thus the power differences would not reflect a change in the oscillatory amplitude per se. The $P_{episode}$, as a binary measure, should be less susceptible to this type of bias, but it is still affected by power as detected oscillations must reach a certain threshold, which might only occur after a certain number of minutes in a particular sleep stage. It may also be the case that oscillatory differences due to hyperoxia are simply not detectable in the shorter periods of SWS observed in many of these participants. To fully address this issue, as well as the issue of

whether hyperoxia affects REM states rather than NREM states, future studies could examine the effect of hyperoxia on full-night polysomnographic recordings in humans.

Both the power and $P_{episode}$ measures are dependent on an estimation of the spectral background for each subject, due to the 1/f relationship between oscillation frequency and amplitude. Since different participants spend more time in sleep, characterized by larger amplitude slow oscillations, and others spend more time awake, characterized by smaller amplitude fast oscillations, the spectral background will have a different slope in these two groups, because it is calculated from the entire 90-minute session. Thus, it may be the case that the measure of power is not as comparable across our participants as in more tightly controlled situations. Directly measuring what the form the background estimation takes in different participants undergoing various brain states and state transitions will allow us to determine the extent, or lack thereof, of this confound.

Lastly, there are some limitations on the physiological variables used in both studies. The difference in SpO_2 levels is specifically a measurement of the concentration of bound hemoglobin in the blood. Neural oxygenation, however, is dependent on the amount of free oxygen dissolved in the blood, and therefore the SpO_2 levels, especially when fully saturated under hyperoxia (Figure 2.2A and 3.3A) may underestimate neural oxygenation. Hyperoxia has been reported to cause considerable changes to the circulatory system in the brain, including cerebral vasoconstriction (Hafner et al., 2015), changes in cerebral blood flow (Floyd et al., 2003), and hypercarbia in patients with COPD (Dunn et al., 1991). Dean et al., (2004) present evidence that in some patients, hyperoxia leads to the activation of CO_2 chemoreceptors through a process known as hyperoxic hyperventilation, thus potentially mimicking the effect of hypercapnia. To that effect, Croal et al., (2015) have reported decreases in alpha and beta MEG

signalling during hypercapnia which were larger in magnitude but similar in location to those found during hyperoxia. Hyperventilation was not found in our results (Figure 3.3C), however it is possible that there was an increase in tidal volume with no corresponding increase in respiration rate. Future studies would thus benefit from measurements of both end-tidal O_2 and CO_2 to monitor changes in alveolar gas exchange, as well as some measure of O_2 and CO_2 concentration in the brain before and after hyperoxia.

In this study we examined the effect of 100% respired oxygen gas on neural oscillations and brain state transitions during sleep in humans, while monitoring for changes in respiratory and cardiac rhythms. We found no evidence that hyperoxia influences NREM sleep states or sleep oscillations. We did find that hyperoxia may decrease alpha oscillations in sleeping participants, although the significance of the effect is marginal. Overall, our results suggest that previous reports of hyperoxia enhancing NREM sleep in rats and disrupting alpha waves in humans may be mediated by separate mechanisms. Future studies with more physiological controls are required to fully evaluate the effect that hyperoxia has on the brain during sleeping and waking brain states in both rats and humans.

3.5 Table and Figure Captions

Table 3.1. BOSC algorithm conditions: the conditions for 4 sleep states (excluding REM and including arousals) are shown. The detected oscillations ($P_{episode}$) for each frequency band must agree with all the conditions listed to be scored as that stage. If no condition is listed for a given frequency band, that sleep stage does not depend on that band. If no set of matching conditions is found, the stage is scored as N1.

Table 3.2. Sleep stage scoring concordances: concordances for all three sleep stage scorers (Novice 1, Novice 2, BOSC) and for every participant. Novice 1 performed the most accurately (~80%) while the Novice 2 and BOSC scorers performed less accurately (~60%).

Figure 3.1. Experimental procedure. Participants completed two sessions exactly one week apart. Within each session, participants were given 2 minutes to breathe the gas, and then were instructed to attempt to sleep for 90 minutes. The order of the gas condition was counterbalanced between subjects.

Figure 3.2. Expert and algorithmic scoring. A) The scored sleep patterns for our 9 participants for the expert scorer (black) and the BOSC algorithm (red). B) Example 5-second segments of raw EEG data, corresponding to four 5-second segments from one session of one participant which were determined by both the expert and algorithmic scorers to be the awake, N1, N2, and SWS sleep stages. C) The sleep pattern for one subject's hyperoxia session is shown larger. D) The centered power for that session is shown, averaged across midline electrodes (Oz, Pz, Cz, and Fz). It can be seen that deeper sleep stages correspond to increased power in slower EEG frequencies. E) The detection values are shown for every datapoint in the time and frequency domains, including all detections from the midline electrodes (Oz, Pz, Cz, and Fz). It can be seen that deeper sleep stages correspond to increased detection of slower EEG frequencies. F) The chin EMG RMS for that session is shown. G) The EOG RMS for that session is shown,

averaging across the horizontal and vertical electrode dipoles.

Figure 3.3. Physiological Measurements. A) The effect of hyperoxia on the SpO2 change, post-gas-delivery minus pre-gas delivery, is shown. Hyperoxia increased SpO2 values for almost all participants and led to a significant increase across subjects ($t(21) = 6.63$, $p < 0.001$). B) The effect of hyperoxia on the heart rate is shown for all collected participants, averaged across the entire session. Hyperoxia decreased heart rate significantly across all subjects ($t(21) = 4.47$, $p < 0.001$). C) The effect of hyperoxia on the breathing rate is shown for all collected participants, averaged across the entire session. Hyperoxia had no significant impact on breathing rate across all subjects ($t(21) = 0.63$, *n.s.*).

Figure 3.4. Sleep timing measurements. A) The effect of hyperoxia on the total time spent asleep is shown for the 9 subjects who successfully entered slow wave sleep. There was no effect of hyperoxia on sleep time across all participants ($t(8) = 0.74$, *n.s.*). B) The effect of hyperoxia on the time each subject took to reach the SWS stage is shown. There was no effect of hyperoxia on SWS onset time across all participants ($t(8) = -0.02$, *n.s.*). C) The effect of hyperoxia on the time each subject spent in each sleep stage while asleep is shown, including REM. There was no effect of hyperoxia on sleep stage time across all participants, for any of the SWS ($t(8) = 0.05$, *n.s.*), N2 ($t(8) = 0.87$, *n.s.*), N1 ($t(8) = -0.29$, *n.s.*), or REM ($t(8) = 0.34$, *n.s.*) stages.

Figure 3.5. Sleep oscillation power measurements. A) The t-statistic for the effect of hyperoxia on the power of oscillations is plotted at every electrode and every frequency, and for each of the four stages of interest (SWS, N2, N1, and Wake). Comparisons which were statistically significant at the 0.05 α-level are emphasized. B) The topographical distribution of the raw-power difference is shown for each of the four sleep stages, at a single frequency of interest for each stage. Significant electrodes are plotted in green. C) The raw power spectra for both the

normoxia and hyperoxia conditions are shown, for each sleep stage, and at a single electrode of interest. It can be observed how the sleep stage affects the overall shape of the spectral density distribution. D) The effect of hyperoxia on raw oscillation power is shown for each subject, and at a single frequency and electrode of interest. As this frequency and electrode were chosen post-hoc, the difference should be considered an overestimation of the real effect of hyperoxia at a given stage. At the electrodes and frequencies chosen, significant effects of hyperoxia were observed at the SWS ($t(8) = 2.77$, $p = 0.024$), N2 ($t(8) = 2.93$, $p = 0.019$), N1 $t(8) = 2.86$, $= 0.021$), and Wake ($t(8) = 2.60$, $p = 0.032$) stages.

Figure 3.6.Sleep oscillation $P_{episode}$ measurements. A) The t-statistic for the effect of hyperoxia on the detection of oscillations in plotted at every electrode and every frequency, and for each of the four stages of interest (SWS, N2, N1, and Wake). Comparisons which were statistically significant at the 0.05 α-level are emphasized. B) The topographical distribution of the $P_{episode}$ difference is shown for each of the four sleep stages, at a single frequency of interest for each stage. Significant electrodes are plotted in green. C) The $P_{episode}$ spectra for both the normoxia and hyperoxia conditions are shown, for each sleep stage, and at a single electrode of interest. It can be observed how the sleep stage affects the overall shape of the oscillation detection distribution. D) The effect of hyperoxia on oscillation detections is shown for each subject, at a single electrode of interest, but using pre-determined ranges for the spindle (11.5-16 Hz), theta (3.5-7 Hz), and alpha (7-14 Hz) frequency bands. As the frequency band and electrode were chosen post-hoc, the difference should be considered an overestimation of the real effect of hyperoxia at a given stage. At the electrodes and frequencies chosen, significant effects of hyperoxia were observed at the SWS ($t(8) = 2.65$, $p = 0.03$), and N1 $t(8) = 2.32$, $p = 0.049$)

stages, whereas trending effects were found at the N2 ($t(8) = -1.93$, $p = 0.09$) and REM ($t(8) = 1.94$, $p = 0.088$) stages.

3.6 Tables and Figures

Table 3.1

	ALPHA DETECTIONS	THETA DETECTIONS	SLOW-WAVE DETECTIONS	THETA : ALPHA	EMG
AWAKE	>0.5	<0.15	<0.5		
N1	<0.5		<0.5		
N2		>0.15	<0.5	>0.5	
SWS		>0.15	>0.5		
AROUSALS	>0.9				>250

Table 3.2

	Novice 1		Novice 2		BOSC	
	Normoxia	Hyperoxia	Normoxia	Hyperoxia	Normoxia	Hyperoxia
Participant 1	0.81	0.83	0.59	0.43	0.78	0.80
Participant 2	0.88	0.69	0.53	0.57	0.64	0.55
Participant 3	0.88	0.87	0.73	0.71	0.71	0.83
Participant 4	0.80	0.87	0.80	0.59	0.60	0.50
Participant 5	0.83	0.89	0.78	0.30	0.61	0.67
Participant 6	0.53	0.58	0.52	0.59	0.37	0.46
Participant 7	0.80	0.82	0.62	0.65	0.53	0.53
Participant 8	0.83	0.84	0.67	0.66	0.55	0.73
Participant 9	0.84	0.83	0.86	0.67	0.55	0.56

Figure 3.1

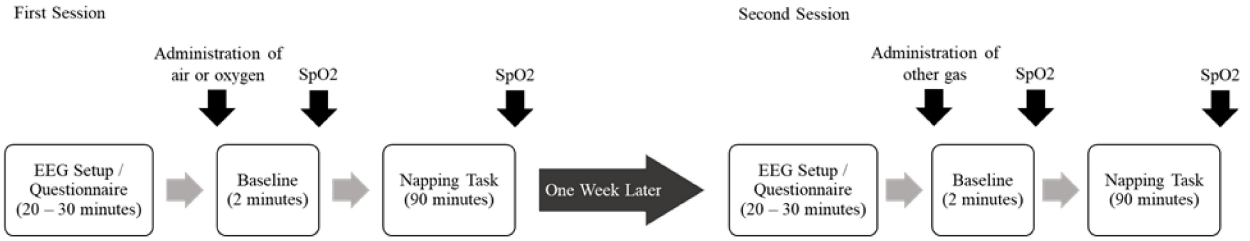
First Session
Administration of air or oxygen
SpO2
SpO2
EEG Setup / Questionnaire (20 – 30 minutes)
Baseline (2 minutes)
Napping Task (90 minutes)
One Week Later
Second Session
Administration of other gas
SpO2
SpO2
EEG Setup / Questionnaire (20 – 30 minutes)
Baseline (2 minutes)
Napping Task (90 minutes)

Figure 3.2

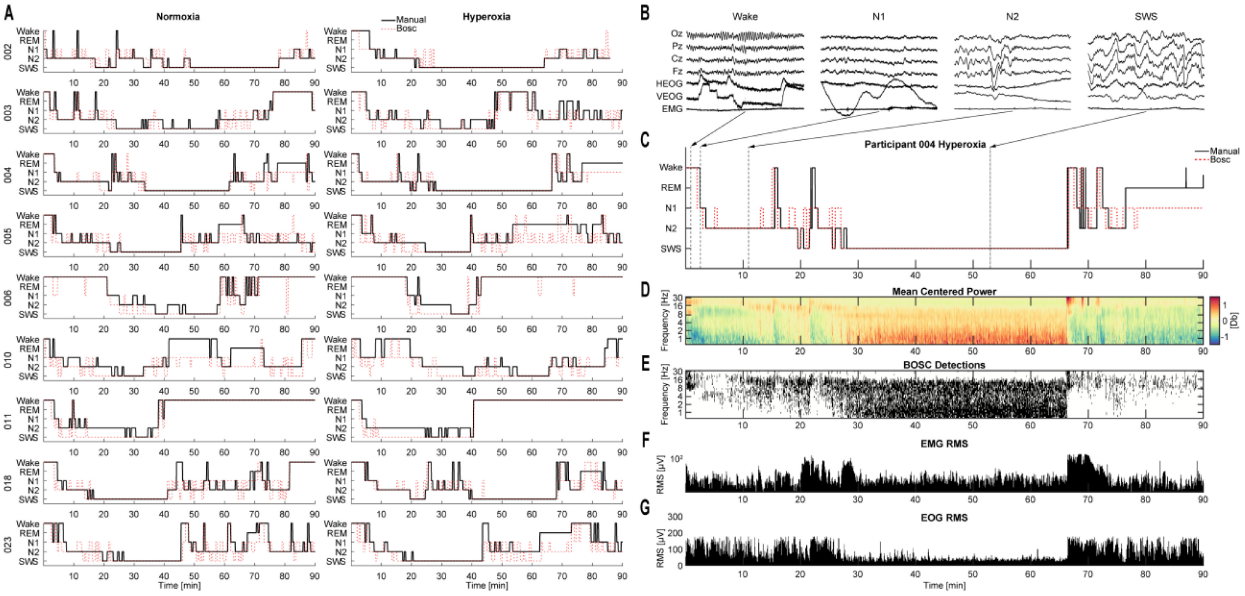
A
Normoxia
Hyperoxia
Manual
Bosc
Wake
REM
N1
N2
SWS
002
003
004
005
006
010
011
018
023
Time [min]
B
Wake
N1
N2
SWS
Oz
Pz
Cz
Fz
HEOG
VEOG
EMG
C
Participant 004 Hyperoxia
Manual
Bosc
D
Mean Centered Power
Frequency [Hz]
[Db]
E
BOSC Detections
F
EMG RMS
RMS [μV]
G
EOG RMS
Time [min]

Figure 3.3———

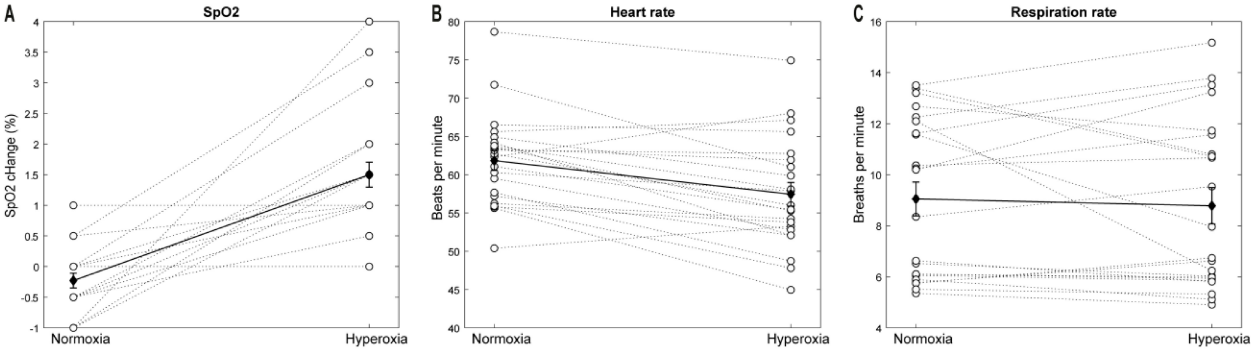
A
SpO2
SpO2 change (%)
Normoxia
Hyperoxia
B
Heart rate
Beats per minute
Normoxia
Hyperoxia
C
Respiration rate
Breaths per minute
Normoxia
Hyperoxia

Figure 3.4

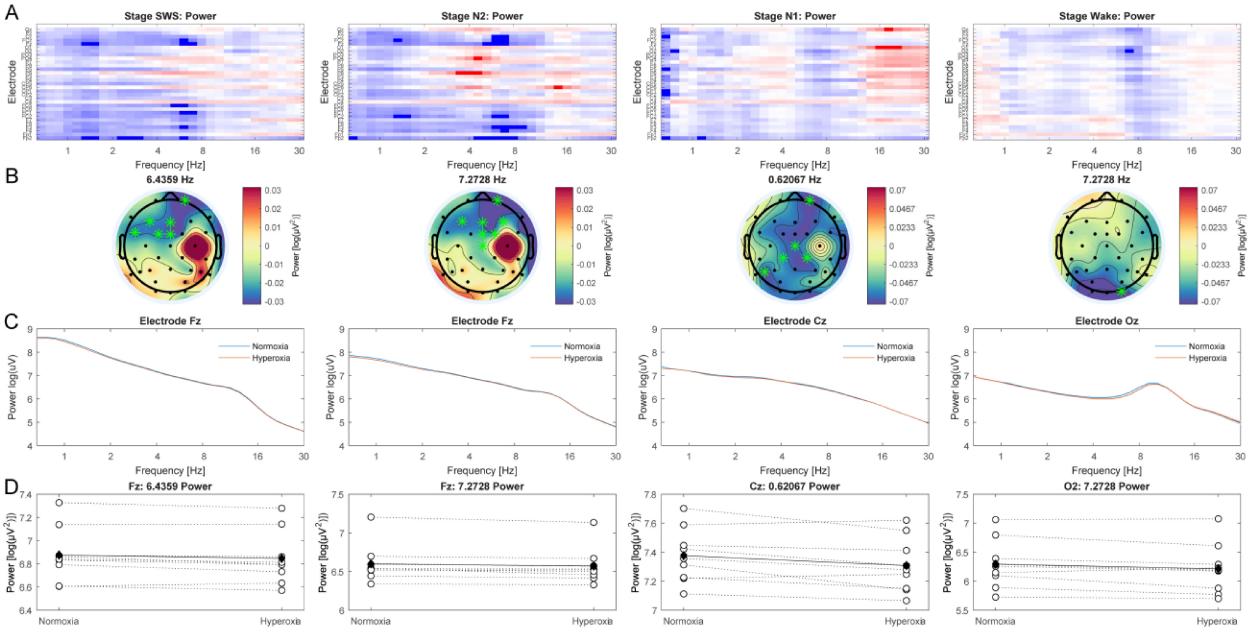
A
Stage SWS: Power
Stage N2: Power
Stage N1: Power
Stage Wake: Power
Electrode
Frequency [Hz]
B
6.4359 Hz
7.2728 Hz
0.62067 Hz
7.2728 Hz
Power [log(uV^2)]
C
Electrode Fz
Electrode Fz
Electrode Cz
Electrode Oz
Normoxia
Hyperoxia
Power log(uV)
Frequency [Hz]
D
Fz: 6.4359 Power
Fz: 7.2728 Power
Cz: 0.62067 Power
O2: 7.2728 Power
Power [log(uV^2)]
Normoxia
Hyperoxia

Figure 3.5

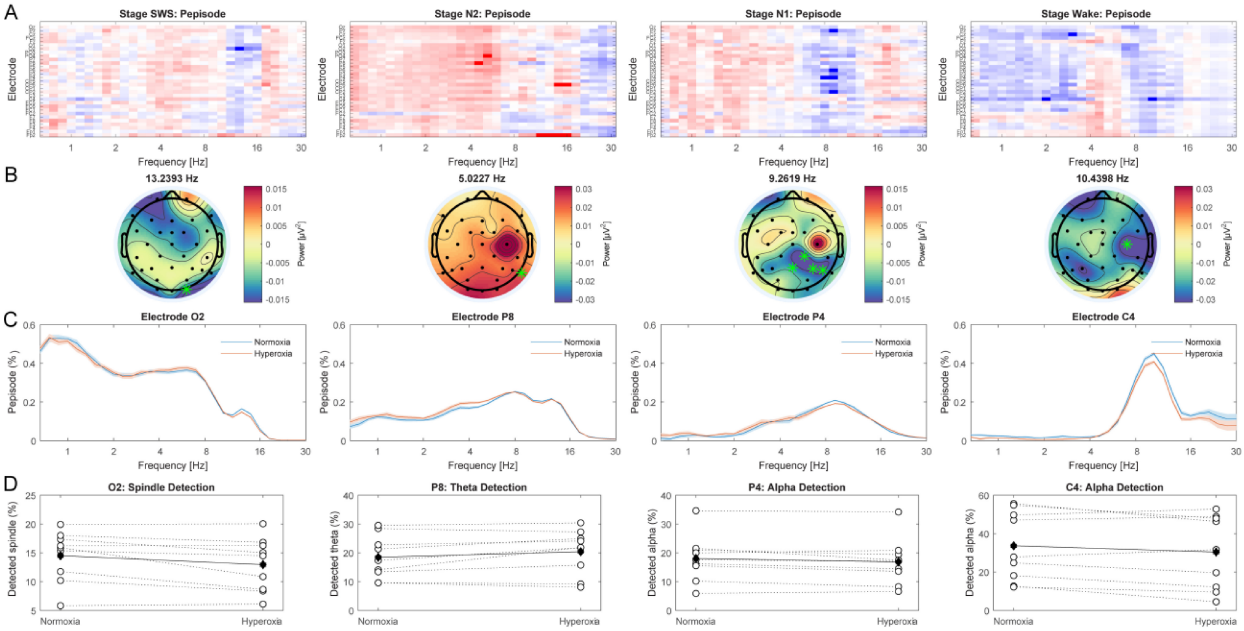
A
Stage SWS: Pepisode
Stage N2: Pepisode
Stage N1: Pepisode
Stage Wake: Pepisode
Electrode
Frequency [Hz]
B
13.2393 Hz
5.0227 Hz
9.2619 Hz
10.4398 Hz
Power (μV²)
C
Electrode O2
Electrode P8
Electrode P4
Electrode C4
Pepisode (%)
Normoxia
Hyperoxia
D
O2: Spindle Detection
P8: Theta Detection
P4: Alpha Detection
C4: Alpha Detection
Detected spindle (%)
Detected theta (%)
Detected alpha (%)

4. GENERAL DISCUSSION

4.1 Aims and predictions

In this thesis, I examined the effect of respired 100% oxygen gas on the resting-state EEG in awake humans and on the sleep stage patterns and neural oscillations in sleeping humans. The primary aim of this research is to demonstrate that hyperoxia influences neural oscillations, and that these results differ by brain state. These investigations were motivated by a recent discovery that hyperoxia enhanced low-frequency 'deactivated' activity in the anesthetized and sleeping rat (Hauer et al., 2018). Based on previous EEG studies in humans, we predicted that hyperoxia would produce a generalized 'slowing' of the EEG spectrum, with high-frequency oscillations being attenuated, and low-frequency oscillations being enhanced. What we found instead was that hyperoxia does seem to disrupt high-frequency alpha and beta waves but may or may not be associated with any enhancement of low-frequency oscillations in waking or sleeping humans.

4.2 Summary of Experiment 1 Results

In experiment 1, I examined the relationship between oxygen administration and EEG oscillations in awake humans, who were performing an eyes-opened/eyes-closed resting-state task. This design was motivated by two main factors. First, previous studies have reported conflicting accounts of the effect of hyperoxia on the EEG in humans who had their eyes open (Croal et al., 2015; Seo et al., 2007; Sheng et al., 2017) and those who had their eyes closed (Kaskinoro et al., 2010). Second, we hypothesized that hyperoxia would affect the state transition caused by opening and closing the eyes (Berger, 1929). We found that hyperoxia was associated with decreases in the power (amplitude) of brain oscillations in the alpha and beta bands when the eyes were open but was not associated with any changes in power while the eyes were closed. We also found that hyperoxia was associated with decreases in the detection

($P_{episode}$) of alpha, beta, and gamma oscillations, and an increase in the detections of delta oscillations when the eyes were closed. Although we did observe increases in low-frequency oscillations detected in the eyes-closed condition, it is important to note that oscillations of that frequency (< 2 Hz) are almost never detected during waking activity, with the increase representing a shift from ~ 0 – 1% detection. If the delta oscillation is not normally present in this brain state, then what is the significance of the detected increase? This combined with the lack of a similar effect in the following study together suggests that hyperoxia may have no significant impact on low-frequency oscillations in awake humans, whether the eyes are opened or closed. We also found that hyperoxia was associated with an enhancement in the transition from the eyes-open ('activated') state to the eyes-closed ('deactivated') state, where the alpha synchronization caused by closing the eyes was enhanced for both the power and the detections of alpha oscillations (specifically around ~8 Hz) by ~ 15%. Lastly, we also observed a similar effect under hyperoxia on the epoch length of detected alpha oscillations, such that the time alpha oscillations persisted above threshold was longer in the eyes-closed condition (where alpha oscillations are already high) but shorter in eyes-open condition (where alpha oscillations are already low). This interesting result shows that in certain conditions, hyperoxia may have the effect of increasing high-frequency activity rather than decreasing it, because in the eyes-closed condition, although neither the power nor detections of alpha oscillations were affected, they became more consistent under hyperoxia, rather than less consistent. Although it was non-significant, both the power and detections of the eyes-closed condition (Figure 2.3C and Figure 2.4C) do show trends towards an increase of oscillations specifically around 8 Hz. This observation suggests that it may be premature to conclude that hyperoxia necessarily decreases alpha oscillations per se. Indeed, most EEG experiments instruct their participants to keep their

eyes open, and so without an explicit test of the effect of hyperoxia on known generators of the alpha rhythm (thalamus) during eyes-closed waking rest, it is difficult to conclude with certainty that hyperoxia is only associated with decreases in the alpha-band. To summarize, it may be the case that hyperoxia enhances both the neural processes which cause synchronization of alpha oscillations when the eyes are closed and those which cause the desynchronization of alpha oscillations when they are opened.

4.3 Summary of Experiment 2 Results

In experiment 2, I examined the relationship between oxygen administration and sleep states as well as sleep oscillations in humans who were taking a 90-minute nap. The design of this experiment was motivated by the fact that previous experiments (Hauer et al., 2018) seemed to indicate that the effect of hyperoxia was specific to NREM sleep. Human sleep always enters NREM first, and proceeds to REM after 60-90 minutes in the sleeping period. Therefore, to examine the effect of hyperoxia on the NREM sleep state, only the first 90 minutes of the sleep cycle needed to be observed.

We hypothesized that similarly to the previous research in rats, hyperoxia would be associated with increases in the time spent in NREM sleep compared to REM sleep, and potentially enhancing low-frequency sleep oscillations. Instead, we observed that hyperoxia appears to have no effect on sleep patterns in humans and likely has no effect on low-frequency oscillations in the EEG. In the N2 and SWS stages, we observed decreases in the power of slow oscillations and theta oscillations, but there was no effect in terms of detections (via $P_{episode}$) for either slow oscillations or theta oscillations. As already discussed, the $P_{episode}$ measure represents the contribution of consistently oscillatory neural activity, as opposed to transient fluctuations in the EEG. For this reason, it seems reasonable to conclude that the decreases observed in the

power measure are due to some non-oscillatory contribution, and that in reality there is no effect of hyperoxia on low-frequency oscillations in the SWS stage. In the N2 stage however, we did observe an increase in theta oscillations, but not slow waves, which may represent an effect of hyperoxia to enhance the initiation of deep sleep. Returning to the SWS stage, we observed a decrease in sleep spindles at one electrode, and in the N1 and wake stages, we observed decreases in both the power and $P_{episode}$ of ~8 Hz alpha oscillations, albeit the effects were not as pronounced as in experiment 1. As we will discuss below, if these effects on high-frequency oscillations prove to be reproducible, it would suggest a role for the thalamus in the brain's response to hyperoxia.

4.4 Relevance of the combined results to cognitive neuroscience

In Chapter 1, I hypothesized that the effect of hyperoxia in both the eyes-opened and eyes-closed conditions would conform to a generalized 'slowing' of the EEG spectrum, increasing the power and detection of low-frequency oscillations, and biasing the brain towards lower-frequency states. Our results demonstrate that hyperoxia does decrease alpha and beta oscillations in awake humans, especially when the eyes are opened, and potentially also in the light stages of sleep. However, the evidence for the corresponding increase in slow oscillations is less convincing. Hyperoxia was associated with a small increase in the $P_{episode}$ of delta oscillations when the eyes were closed, but not when the eyes were opened, and was also associated with an increase in theta oscillations in the N2 stage, but not in the SWS stage, or the Wake stage, which is analogous to the eyes-closed condition of the previous study. These disparate effects suggest that the effects of hyperoxia on neural activity reported in the human and rat literature may represent completely different processes.

Both alpha oscillations (Goldman et al., 2002; Larson et al., 1998) and sleep spindles (Mircea Steriade, 2003) are thought to be generated in the thalamus and use thalamocortical projections to induce the cortical oscillations which we measure in the EEG. During sleep, it is known that the connections between the thalamus and cortex become inhibited, to block external stimuli from reaching the cortex (Brown et al., 2012). As already discussed in Chapter 1, thalamocortical neurons become increasingly hyperpolarized and therefore less responsive during the transition from N2 to SWS. It is unlikely that the same process which inhibits alpha oscillations and sleep spindles through the thalamus would also generate an increase in neocortically-generated slow oscillations (Steriade, 2003). Thus, if we assume that the deactivated state observed in anesthetized rats and the NREM activity observed in the naturally sleeping rat is analogous to the SWS stage in humans, then it does not appear that the reported effects of hyperoxia on rat and human neural activity are being mediated by the same processes. However, if we assume that the deactivated and NREM states are more analogous to N2 sleep, then it is possible that an increase in TC activity could produce both a decrease in alpha oscillations in waking states, and an increase in theta oscillations in sleeping states. A simple way to test this hypothesis would be to record from TC neurons in anesthetized and naturally sleeping rats under hyperoxia and normoxia. An increase in TC spiking which corresponds in time with the increased time spent in deactivated or NREM states would support this hypothesis.

An alternative hypothesis is that the effects of hyperoxia observed in sleeping rats is primarily due to the impact of hyperoxia on midbrain structures such as the hippocampus and are therefore unlikely to be detectable in the EEG, and that the effects of hyperoxia observed in awake humans is due to the effect of hyperoxia to enhance glucose metabolism in the thalamus. This is based on three points of evidence. First, in awake humans hyperoxia decreased the power

and detection of alpha oscillations, which are known to be inversely correlated with glucose metabolism in the thalamus (Larson et al., 1998). Second, in sleeping humans hyperoxia decreased sleep spindles, which are generated by TC neurons (Gennaro & Ferrara, 2003). Third, in sleeping humans hyperoxia decreased the detection of alpha oscillations but only in the light stages of sleep, and not in the deep stages of sleep, where the thalamus is hyperpolarized and disconnected from the cortex (Brown et al., 2012) and therefrom from the EEG system. One way to test this hypothesis would be to examine the activity of the hippocampus and thalamus with fMRI under hyperoxia and normoxia, and in awake and sleeping humans. If the hypothesis is correct, hyperoxia will be associated with increased signaling in the hippocampus during sleep, but not while awake, and will also be associated with increased signaling in the thalamus in both awake and sleeping humans.

One of the main aims of this thesis was to test whether the neural correlates of hyperoxia would be consistent with the effects claimed by recreational providers of oxygen. A synchronization of alpha oscillations is often related to a state of attentional inhibition (Sokoliuk & VanRullen, 2016; Thut et al., 2006). Thus, a decrease in alpha oscillations, especially while the eyes are opened, suggests that there may certainly be a perceivable effect on certain measures of attention and wakefulness. However, our experiments did not directly test whether the decreases in alpha oscillations are related to any changes in cognitive performance, and so we cannot conclusively say whether the use of supplemental oxygen will provide benefits to attention. A further aim of this research was to test whether hyperoxia would have the effect of disrupting or abolishing REM sleep in humans. Hyperoxia has been evaluated for a litany of possible dangers (Hafner et al., 2015; Owens, 2013) but the disruption of REM sleep was, to my knowledge, not one of the variables so far examined. Although we did not observe REM sleep in

many subjects, the lack of any difference in sleep state timings between the hyperoxic and normoxic groups suggests that this concern is minimal. In sum, the use of supplemental oxygen has here been shown to cause no drastic changes to the overall state of neural oscillation dynamics in the brain during waking or sleeping, and therefore will probably not pose a danger to consumers.

Methodologically speaking, our results also demonstrate the utility of the BOSC method compared to standard measurements of spectral power. In experiment 1, the $P_{episode}$ measure proved to be more sensitive than the power measure, detecting small differences in the prevalence of delta oscillations and beta oscillations where the power measure found none. More importantly, the $P_{episode}$ measure has an easily interpretable meaning (proportion of time an oscillation was detected) and scales evenly across frequencies, allowing for a more understandable interpretation of the results. For example, it is more interpretable to say that hyperoxia decreased the detection of alpha oscillations from 20% to 18%, than to say that it decreased the spectral power from 5.8 μV^2 to 5.7 $\mu V^2/Hz$. The $P_{episode}$ measure also has the advantage of being less sensitive to transient fluctuations in the EEG which may be mistaken for an oscillation by the FFT or Wavelet methods. In experiment 2, large decreases in the power of low-frequency oscillations were observed in the N2 and SWS stage, a paradoxical finding which directly contradicted our hypothesis. However, no such decrease was visible in the $P_{episode}$ measure, suggesting that the decreases observed in spectral power, although unexplained, probably do not represent decreases in the power of consistent theta and delta-band neural oscillations. Lastly, our results demonstrate that the BOSC methodology can be used to gather additional information about oscillations, such as the length of time that they persist above threshold. In sum, our studies demonstrate the utility of applying power and duration thresholds

to obtained power values, the dangers of not doing so, and provide researchers with new tools to examine, ever-more precisely, neural oscillations.

4.5 Limitations of the research and future aims

There are some limitations to our results which should be addressed. The main aim of chapter 2 was to test if hyperoxia could lead to cognitive benefits in healthy adults, but we did not specifically test a cognitive function. One recent study (Sheng et al., 2017) did actually test subjects on a visual ERP task while providing either 100% oxygen or regular air, and while they did find changes in the amplitude of the P1 and N1 ERP components (indexes of visual processing), this did not translate to a behavioral advantage. Future studies could employ a design similar to our first experiment, but test participants on a battery of cognitive tasks instead of an eyes-opened/eyes-closed task. If it is found that hyperoxia both decreases alpha oscillations, and increases behavioral performance, and these variables are found to be correlated on a trial by trial basis, then there will be very strong evidence for the claims of recreational oxygen providers to improve attention. Secondly, the main aim of chapter 3 was to directly replicate the effect of hyperoxia on the sleep states of naturally sleeping rats, which was that NREM states were enhanced *relative to REM states*. Due to the fact that REM sleep is usually not observed until the second sleep cycle of the sleeping period (Lee-Chiong, 2005) we only observed REM sleep in 5 subjects, and thus could not directly compare the relative time spent in REM and NREM over several cycles. Furthermore, the time of day that participants came in to participate in the study (12:00pm to 2:00pm) may have caused their sleep patterns to be more heterogeneous than during regular nightly sleep. Indeed, out of the 22 participants who completed both sessions of experiment 2, only 9 participants entered SWS during the 90-minute period in both sessions. It is possible that the increase of time spent in NREM sleep in naturally

sleeping rats actually represents a disruption to REM sleep in those animals. If that was the case, then our design may not have been able to properly assess the relative time spent in REM sleep, as compared to NREM sleep, throughout the night. Future studies could replicate our results with full-night sleep recordings, which would provide significantly more power to detect neural changes and ensure that both REM and NREM sleep stages are fully considered.

In chapter 3 I hypothesized that an algorithmic scoring process using the BOSC $P_{episode}$ values would be able to replicate the accuracy of a manual scorer. The justification behind this is that the method by which sleep stages are scored largely relies on a percentage detection score for various oscillatory waveforms from the EEG (Berry et al., 2013). Therefore, it would be possible to directly implement these definitions into the scoring algorithm, because $P_{episode}$ is also a percent detection score. The algorithm was able to detect the correct sleep stage most of the time (61%) but this is not sufficient accuracy to replace an expert scorer. The percentages for each frequency band used by the BOSC scoring algorithm were chosen so as to make as direct a comparison as possible with our manual scorers. However, another approach, which could improve the accuracy of the BOSC algorithm, would be to use a machine learning approach to train the percentage values using a large number of datasets which already have expert scoring. Future studies could test such a trained BOSC scoring algorithm on newly collected sleep data and compare to novice and expert manual scorers.

Lastly, further investigation could be conducted on some areas of this research. First, Hyperoxia was not found in our studies to induce any consistent changes in breathing rate despite the increased supply of oxygen, suggesting that the breathing rate measure may not have been sufficient to detect the physiological impact of oxygen. Future studies could examine a more precise relationship between the effect of hyperoxia on neural oscillations and cerebral

oxygenation using more precise methodological techniques, such as the measurement of end-tidal O_2 and CO_2, as well as more direct measures of cerebral oxygenation, such as with some kind of functional spectroscopy. Second, the decreases in alpha and beta oscillations were found to be centered around more frontal electrodes, rather than the posterior distribution commonly reported with alpha differences. This discrepancy likely suggests that any effect of hyperoxia on alpha oscillations is mediated through a source that is distinct from the thalamocortical circuit which creates the posterior alpha oscillation. Future studies could make use of source localization techniques in EEG, or alternatively make use of neuroimaging techniques such as MEG which have a finer spatial resolution to examine whether the alpha decreases are explained by a more frontal source.

4.6 Summary and Conclusion

To conclude, our results support the hypothesis that hyperoxia has a measurable effect on the neural oscillations and brain states of awake humans, which may be associated with enhancements in cognitive functioning. However, our results do not provide conclusive evidence for the hypothesis that hyperoxia affects sleep states and sleep oscillations in humans. The importance of this finding is that it demonstrates that the effects of hyperoxia on the brain are complex and cannot be explained as a simple 'slowing' phenomenon which applies across the entire frequency spectrum. Rather, our results suggest that hyperoxia has disparate effects on several bands of neural oscillations implicating the hippocampus, thalamus, and visual cortex, and suggest future avenues of research. The findings of these studies will allow users of supplemental oxygen, whether for therapeutic or recreational purposes, to understand the effects that supplemental oxygen has on the brain and will guide future research on the relationship between oxygen metabolism in the brain and sleep states and sleep oscillations.

References

Adrian, E. D., & Matthews, B. H. C. (1934a). The berger rhythm: Potential changes from the occipital lobes in man. *Brain*, *57*(4), 355–385. https://doi.org/10.1093/brain/57.4.355

Adrian, E. D., & Matthews, B. H. C. (1934b). The interpretation of potential waves in the cortex. *The Journal of Physiology*, *81*(4), 440–471. https://doi.org/10.1113/jphysiol.1934.sp003147

Areza-fegyveres, R., Kairalla, R. a, Carvalho, C. R. R., & Nitrini, R. (2010). Cognition and chronic hypoxia in pulmonary diseases. *Dement Neuropsychol*, *4*(1), 14–22.

Asada, H., Fukuda, Y., Tsunoda, S., Yamaguchi, M., & Tonoike, M. (1999). Frontal midline theta rhythms reflect alternative activation of prefrontal cortex and anterior cingulate cortex in humans. *Neuroscience Letters*, *274*(1), 29–32. https://doi.org/10.1016/S0304-3940(99)00679-5

Atienza, M., Cantero, J. L., & Escera, C. (2001). Auditory information processing during human sleep as revealed by event-related brain potentials. *Clinical Neurophysiology*, *112*(11), 2031–2045. https://doi.org/10.1016/S1388-2457(01)00650-2

Bangash, M. F., Xie, A., Skatrud, J. B., Reichmuth, K. J., Barczi, S. R., & Morgan, B. J. (2008). Cerebrovascular response to arousal from NREM and REM sleep. *Sleep*, *\textbf{31}*(3), 321–327.

Başar, E., Başar-Eroglu, C., Karakaş, S., & Schürmann, M. (2001). Gamma, alpha, delta, and theta oscillations govern cognitive processes. *International Journal of Psychophysiology*, *39*(2–3), 241–248. https://doi.org/10.1016/S0167-8760(00)00145-8

Bastos, A. M., Vezoli, J., Bosman, C. A., Schoffelen, J.-M., Oostenveld, R., Dowdall, J. R., … Fries, P. (2015). Visual Areas Exert Feedforward and Feedback Influences through Distinct Frequency Channels. *Neuron*, *85*(2), 390–401. https://doi.org/10.1016/j.neuron.2014.12.018

Batterink, L. J., Creery, J. D., & Paller, K. A. (2016). Phase of Spontaneous Slow Oscillations during Sleep Influences Memory-Related Processing of Auditory Cues. *The Journal of Neuroscience : The Official Journal of the Society for Neuroscience*, *36*(4), 1401–1409. https://doi.org/10.1523/JNEUROSCI.3175-15.2016

Bélanger, M., Allaman, I., & Magistretti, P. J. (2011). Brain energy metabolism: Focus on Astrocyte-neuron metabolic cooperation. *Cell Metabolism*, *14*(6), 724–738. https://doi.org/10.1016/j.cmet.2011.08.016

Benchenane, K., Tiesinga, P. H., & Battaglia, F. P. (2011). Oscillations in the prefrontal cortex: A gateway to memory and attention. *Current Opinion in Neurobiology*, *21*(3), 475–485. https://doi.org/10.1016/j.conb.2011.01.004

Berger, H. (1929). Über das Elektrenkephalogramm des Menschen. *Archiv Für Psychiatrie Und Nervenkrankheiten*, *87*(1), 527–570. https://doi.org/10.1007/BF01797193

Bergø, G. W., & Tyssebotn, I. (1995). Effect of exposure to oxygen at 101 and 150 kPa on the cerebral circulation and oxygen supply in conscious rats. *European Journal of Applied Physiology and Occupational Physiology*, *71*(6), 475–484. https://doi.org/10.1007/BF00238548

Berry, R. B., Brooks, R., Gamaldo, C. E., Harding, S. M., Marcus, C. L., & Vaughn, B. V. (2013). *The AASM Manual for the Scoring of Sleep and Associated Events*. *American Academy of Sleep Medicine* (Vol. 53). American Academy of Sleep Medicine. https://doi.org/10.1017/CBO9781107415324.004

Berssenbrugge, Dempsey, Iber, Skatrud, & Wilson. (1983). Mechanisms Of Hypoxia Induced Periodic Breathing During Sleep In Humans. *J Physiol*, *343*, 507.

Bew, S. A., Field, L. M., Droste, D. W., & Razis, P. (1994). The effect of high concentrations of

inspired oxygen on middle cerebral artery blood velocity measured by transcranial Doppler. *Experimental Physiology*, *79*(4), 593–596.

Bitterman, H. (2009). Bench-to-bedside review: Oxygen as a drug. *Critical Care*, *13*(1), 205. https://doi.org/10.1186/cc7151

Bonnefond, M., & Jensen, O. (2013). The role of gamma and alpha oscillations for blocking out distraction. *Communicative and Integrative Biology*, *6*(1), 2–5. https://doi.org/10.4161/cib.22702

Borbély, A. A., & Tobler, I. (2011). Manifestations and functional implications of sleep homeostasis. *Handbook of Clinical Neurology*, *98*(C), 205–213. https://doi.org/10.1016/B978-0-444-52006-7.00013-7

Braun, A. R., Balkin, T. J., Wesenten, N. J., Carson, R. E., Varga, M., Baldwin, P., … Herscovitch, P. (1997). Regional cerebral blood flow throughout the sleep-wake cycle. An H2(15)O PET study. *Brain : A Journal of Neurology*, *120 (Pt 7*, 1173–1197. https://doi.org/10.1093/brain/120.7.1173

Brown, R. E., Basheer, R., McKenna, J. T., Strecker, R. E., & McCarley, R. W. (2012). Control of Sleep and Wakefulness. *Physiological Reviews*, *92*(3), 1087–1187. https://doi.org/10.1152/physrev.00032.2011

Busch, N. A., & VanRullen, R. (2010). Spontaneous EEG oscillations reveal periodic sampling of visual attention. *Proceedings of the National Academy of Sciences*, *107*(37), 16048–16053. https://doi.org/10.1073/pnas.1004801107

Busch, N. a, Dubois, J., & VanRullen, R. (2009). The phase of ongoing EEG oscillations predicts visual perception. *The Journal of Neuroscience : The Official Journal of the Society for Neuroscience*, *29*(24), 7869–7876. https://doi.org/10.1523/JNEUROSCI.0113-09.2009

Busija, D. W., Orr, J. a, Rankin, J. H., Liang, H. K., & Wagerle, L. C. (1980). Cerebral blood flow during normocapnic hyperoxia in the unanesthetized pony. *Journal of Applied Physiology: Respiratory, Environmental and Exercise Physiology*, *48*(1), 10–15. Retrieved from http://www.ncbi.nlm.nih.gov/pubmed/7353961

Buzsáki, G. (1998). Memory consolidation during sleep: a neurophysiological perspective. *Journal of Sleep Research*, *7 Suppl 1*, 17–23. https://doi.org/10.1046/j.1365-2869.7.s1.3.x, 10.1046/j.1365-2869.7.s1.3.x

Buzsáki, G. (2006). *Rhythms of the Brain*. *Rhythms of the Brain*. https://doi.org/10.1093/acprof:oso/9780195301069.001.0001

Buzsáki, G., & Draguhn, A. (2004). Neuronal oscillations in cortical networks. *Science (New York, N.Y.)*, *304*(5679), 1926–1929. https://doi.org/10.1126/science.1099745

Buzsáki, G., & Schomburg, E. W. (2015). What does gamma coherence tell us about inter-regional neural communication? *Nature Neuroscience*. https://doi.org/10.1038/nn.3952

Campbell, S. S., & Tobler, I. (1984). Animal Sleep : A Review of Sleep Duration Across Phylogeny. *Neuroscience and Behavioural Reviews*, *8*(1).

Caplan, J. B., Madsen, J. R., Raghavachari, S., & Kahana, M. J. (2001). Distinct Patterns of Brain Oscillations Underlie Two Basic Parameters of Human Maze Learning. *J Neurophysiol*, *86*(1), 368–380. Retrieved from http://jn.physiology.org.login.ezproxy.library.ualberta.ca/content/86/1/368.full.pdf+html

Cirelli, C., & Tononi, G. (2008). Is sleep essential? *PLoS Biology*, *6*(8), 1605–1611. https://doi.org/10.1371/journal.pbio.0060216

Clement, E. A., Richard, A., Thwaites, M., Ailon, J., Peters, S., & Dickson, C. T. (2008). Cyclic and Sleep-Like Spontaneous Alternations of Brain State Under Urethane Anaesthesia. *PLoS*

ONE, *3*(4), e2004. https://doi.org/10.1371/journal.pone.0002004

Cohen, M. X. (2014). Analyzing Neural Time Series Data: Theory and Practice. *MIT Press*, 600. https://doi.org/10.1017/CBO9781107415324.004

Colrain, I. M., Trinder, J., Fraser, G., & Wilson, G. V. (1987). Ventilation during sleep onset. *Journal of Applied Physiology (Bethesda, Md. : 1985)*, *63*(5), 2067–2074.

Croal, P. L., Hall, E. L., Driver, I. D., Brookes, M. J., Gowland, P. A., & Francis, S. T. (2015). The effect of isocapnic hyperoxia on neurophysiology as measured with MRI and MEG. *NeuroImage*, *105*, 323–331. https://doi.org/10.1016/j.neuroimage.2014.10.036

Dean, J. B., Mulkey, D. K., Henderson, R. a, Potter, S. J., & Putnam, R. W. (2004). Hyperoxia, reactive oxygen species, and hyperventilation: oxygen sensitivity of brain stem neurons. *Journal of Applied Physiology*, *96*(2), 784–791. https://doi.org/10.1152/japplphysiol.00892.2003

Dean, J. B., Mulkey, D. K., Iii, R. A. H., Potter, S. J., Putnam, R. W., Jay, B., … Hyperoxia, R. W. P. (2004). Oxygen Sensing in Health and Disease Hyperoxia , reactive oxygen species , and hyperventilation : oxygen sensitivity of brain stem neurons. *Journal of Applied Physiology*, *96*, 784–791. https://doi.org/10.1152/japplphysiol.00892.2003

Delorme, A., & Makeig, S. (2004). EEGLAB: An open source toolbox for analysis of single-trial EEG dynamics including independent component analysis. *Journal of Neuroscience Methods*, *134*(1), 9–21. https://doi.org/10.1016/j.jneumeth.2003.10.009

Desai, R., Tailor, A., & Bhatt, T. (2015). Effects of yoga on brain waves and structural activation: A review. *Complementary Therapies in Clinical Practice*, *21*(2), 112–118. https://doi.org/10.1016/j.ctcp.2015.02.002

Diekelmann, S., & Born, J. (2010). The memory function of sleep. *Nat.Rev.Neurosci.*, *11*(1471–

0048 (Electronic)), 114–126. https://doi.org/10.1038/nrn2762

Donner, T. H., & Siegel, M. (2011). A framework for local cortical oscillation patterns. *Trends in Cognitive Sciences*, *15*(5), 191–199. https://doi.org/10.1016/j.tics.2011.03.007

Dougherty, K., Cox, M. A., Ninomiya, T., Leopold, D. A., & Maier, A. (2015). Ongoing Alpha Activity in V1 Regulates Visually Driven Spiking Responses. *Cerebral Cortex (New York, N.Y. : 1991)*, bhv304. https://doi.org/10.1093/cercor/bhv304

Dunai, J., Wilkinson, M., & Trinder, J. (1996). Interaction of chemical and state effects on ventilation during sleep onset. *Journal of Applied Physiology (Bethesda, Md. : 1985)*, *81*(5), 2235–2243. https://doi.org/10.1152/jappl.1996.81.5.2235

Dunn, W. F., Nelson, S. B., & Hubmayr, R. D. (1991). Oxygen-induced Hypercarbia in Obstructive Pulmonary Disease. *Am Rev Respir Dis*, *144*, 526–530. https://doi.org/10.1164/ajrccm/144.3_Pt_1.526

Engel, A. K., & Fries, P. (2010). Beta-band oscillations-signalling the status quo? *Current Opinion in Neurobiology*, *20*(2), 156–165. https://doi.org/10.1016/j.conb.2010.02.015

Ferrara, M., & De Gennaro, L. (2001). How much sleep do we need? *Sleep Medicine Reviews*, *5*(2), 155–179. https://doi.org/10.1053/smrv.2000.0138

Ferrara, M., De Gennaro, L., & Bertini, M. (1999). Selective slow-wave sleep (SWS) deprivation and SWS rebound: do we need a fixed SWS amount per night? *Sleep Research Online : SRO*, *2*(1), 15–19. Retrieved from http://www.ncbi.nlm.nih.gov/pubmed/11382878

Fleetham, J., West, P., Mezon, B., Conway, W., Roth, T., & Kryger, M. (1982). Sleep, arousals, and oxygen desaturation in chronic obstructive pulmonary disease. The effect of oxygen therapy. *American Review of Respiratory Disease*, *126*(3), 429–433. Retrieved from http://www.scopus.com/inward/record.url?eid=2-s2.0-0019981541&partnerID=tZOtx3y1

Floyd, T. F., Clark, J. M., Gelfand, R., Detre, J. A., Ratcliffe, S., Guvakov, D., … Eckenhoff, R. G. (2003). Independent cerebral vasoconstrictive effects of hyperoxia and accompanying arterial hypocapnia at 1 ATA. *Journal of Applied Physiology*, *95*(6), 2453–2461. https://doi.org/10.1152/japplphysiol.00303.2003

Foxe, J. J., & Snyder, A. C. (2011). The role of alpha-band brain oscillations as a sensory suppression mechanism during selective attention. *Frontiers in Psychology*, *2*(JUL), 1–13. https://doi.org/10.3389/fpsyg.2011.00154

Fries, P. (2005). A mechanism for cognitive dynamics: Neuronal communication through neuronal coherence. *Trends in Cognitive Sciences*, *9*(10), 474–480. https://doi.org/10.1016/j.tics.2005.08.011

Fries, P. (2015). Rhythms for Cognition: Communication through Coherence. *Neuron*, *88*(1), 220–235. https://doi.org/10.1016/j.neuron.2015.09.034

Gennaro, L. De, & Ferrara, M. (2003). lJ Sleep spindles : an overview. *Sleep Medicine*, *7*(800), 422–440. https://doi.org/10.1016/S1087-0792(02)00116-8

Gips, B., van der Eerden, J. P. J. M., Jensen, O., & Foxe, J. (2016). A biologically plausible mechanism for neuronal coding organized by the phase of alpha oscillations. *European Journal of Neuroscience*, *44*(4), 2147–2161. https://doi.org/10.1111/ejn.13318

Goldman, R. I., Stern, J. M., Engel, J., & Cohen, M. S. (2002). Simultaneous EEG and fMRI of the alpha rhythm. *Neuroreport*, *13*(18), 2487–2492. https://doi.org/10.1097/00001756-200212200-00022

Gonçalves, S. I., De Munck, J. C., Pouwels, P. J. W., Schoonhoven, R., Kuijer, J. P. a, Maurits, N. M., … Lopes Da Silva, F. H. (2006). Correlating the alpha rhythm to BOLD using simultaneous EEG/fMRI: Inter-subject variability. *NeuroImage*, *30*(1), 203–213.

https://doi.org/10.1016/j.neuroimage.2005.09.062

Gratton, G., Coles, M. G. ., & Donchin, E. (1983). A new method for off-line removal of ocular artifact. *Electroencephalography and Clinical Neurophysiology*, *55*(4), 468–484. https://doi.org/10.1016/0013-4694(83)90135-9

Gray, C. M., König, P., Engel, A. K., & Singer, W. (1989). Oscillatory responses in cat visual cortex exhibit inter-columnar synchronization which reflects global stimulus properties. *Nature*, *338*(6213), 334–337. https://doi.org/10.1038/338334a0

Greene, R. W., & Frank, M. G. (2010). Slow Wave Activity During Sleep: Functional and Therapeutic Implications. *The Neuroscientist*, *16*(6), 618–633. https://doi.org/10.1177/1073858410377064

Güntekin, B., & Başar, E. (2016). Review of evoked and event-related delta responses in the human brain. *International Journal of Psychophysiology*, *103*, 43–52. https://doi.org/10.1016/j.ijpsycho.2015.02.001

Haegens, S., Cousijn, H., Wallis, G., Harrison, P. J., & Nobre, A. C. (2014). Inter- and intra-individual variability in alpha peak frequency. *NeuroImage*, *92*, 46–55. https://doi.org/10.1016/j.neuroimage.2014.01.049

Haegens, S., Luther, L., & Jensen, O. (2012). Somatosensory Anticipatory Alpha Activity Increases to Suppress Distracting Input. Retrieved from http://www.mitpressjournals.org.login.ezproxy.library.ualberta.ca/doi/abs/10.1162/jocn_a_00164

Hafner, S., Beloncle, F., Koch, A., Radermacher, P., & Asfar, P. (2015). Hyperoxia in intensive care, emergency, and peri-operative medicine: Dr. Jekyll or Mr. Hyde? A 2015 update. *Annals of Intensive Care*, *5*(1), 42. https://doi.org/10.1186/s13613-015-0084-6

Hajak, G., Klingelhöfer, J., Schulz-Varszegi, M., Matzander, G., Sander, D., Conrad, B., & Rüther, E. (1994). Relationship between cerebral blood flow velocities and cerebral electrical activity in sleep. *Sleep*, *17*(1), 11–19. Retrieved from http://www.ncbi.nlm.nih.gov/pubmed/7910702

Hamrahi, H., Stephenson, R., Mahamed, S., Liao, K. Sen, & Horner, R. L. (2001). Physiological and Genomic Consequences of Intermittent Hypoxia: Selected Contribution: Regulation of sleep-wake states in response to intermittent hypoxic stimuli applied only in sleep. *J Appl Physiol*, *90*(6), 2490–2501. Retrieved from http://jap.physiology.org.login.ezproxy.library.ualberta.ca/content/90/6/2490.short

Hanslmayr, S., Aslan, A., Staudigl, T., Klimesch, W., Herrmann, C. S., & Bäuml, K. H. (2007). Prestimulus oscillations predict visual perception performance between and within subjects. *NeuroImage*, *37*(4), 1465–1473. https://doi.org/10.1016/j.neuroimage.2007.07.011

Hanslmayr, S., Staresina, B. P., & Bowman, H. (2016). Oscillations and Episodic Memory: Addressing the Synchronization/Desynchronization Conundrum. *Trends in Neurosciences*, *39*(1), 16–25. https://doi.org/10.1016/j.tins.2015.11.004

Harmony, T. (2013). The functional significance of delta oscillations in cognitive processing. *Frontiers in Integrative Neuroscience*, *7*(December), 1–10. https://doi.org/10.3389/fnint.2013.00083

Harvey, B. M., Vansteensel, M. J., Ferrier, C. H., Petridou, N., Zuiderbaan, W., Aarnoutse, E. J., … Dumoulin, S. O. (2013). Frequency specific spatial interactions in human electrocorticography: V1 alpha oscillations reflect surround suppression. *NeuroImage*, *65*, 424–432. https://doi.org/10.1016/j.neuroimage.2012.10.020

Hauer, B. E., Negash, B., Chan, K., Vuong, W., Colbourne, F., Pagliardini, S., & Dickson, C. T.

(2018). Hyperoxia Enhances Slow-wave Forebrain States in Urethane Anesthetized and Naturally Sleeping Rats. *J Neurophysiol*, (780).

Hofle, N., Paus, T., Reutens, D., Fiset, P., Gotman, J., Evans, A. C., & Jones, B. E. (1997). Regional cerebral blood flow changes as a function of delta and spindle activity during slow wave sleep in humans. *Journal Of Neuroscience*, *17*(12), 4800–4808.

Hughes, A. M., Whitten, T. A., Caplan, J. B., & Dickson, C. T. (2012). BOSC: a better oscillation detection method, extracts both sustained and transient rhythms from rat hippocampal recordings. *Hippocampus*, *22*(6), 1417–1428. https://doi.org/10.1002/hipo.20979

Jann, K., Dierks, T., Boesch, C., Kottlow, M., Strik, W., & Koenig, T. (2009). BOLD correlates of EEG alpha phase-locking and the fMRI default mode network. *NeuroImage*, *45*(3), 903–916. https://doi.org/10.1016/j.neuroimage.2009.01.001

Jensen, O., Gips, B., Bergmann, T. O., & Bonnefond, M. (2014). Temporal coding organized by coupled alpha and gamma oscillations prioritize visual processing. *Trends in Neurosciences*, *37*(7), 357–369. https://doi.org/10.1016/j.tins.2014.04.001

Jensen, O., & Mazaheri, A. (2010). Shaping functional architecture by oscillatory alpha activity: gating by inhibition. *Frontiers in Human Neuroscience*, *4*(November), 186. https://doi.org/10.3389/fnhum.2010.00186

Kaskinoro, K., Maksimow, A., Laitio, R., Scheinin, H., & Jääskeläinen, S. (2010). Normobaric hyperoxia does not induce significant electroencephalogram changes in healthy male subjects: 7AP4-5. *European Journal of Anaesthesiology (EJA)*, *27*(47), 121–122. Retrieved from http://journals.lww.com/ejanaesthesiology/Fulltext/2010/06121/Normobaric_hyperoxia_doe

s_not_induce_significant.390.aspx

Kety, S. S., & Schmidt, C. F. (1948). The effects of altered arterial tensions of carbon dioxide and oxygen on cerebral blood flow and oxygen consumption of normal young men. *Journal of Clinical Investigation*, *27*(4), 484–492. https://doi.org/10.1172/JCI101995

Kim, H.-J., Park, H.-K., Lim, D.-W., Choi, M.-H., Kim, H.-J., Lee, I.-H., … Chung, S.-C. (2013). Effects of oxygen concentration and flow rate on cognitive ability and physiological responses in the elderly. *Neural Regeneration Research*, *8*(3), 264–269. https://doi.org/10.3969/j.issn.1673-5374.2013.03.009

Kim, H.-S., Choi, M.-H., Baek, J., Park, S., Lee, J., Jeong, U., … Chung, S. (2015). Effects of 92% oxygen administration on cognitive performance and physiological changes of intellectually and developmentally disabled people. *Journal of Physiological Anthropology*, *34*(1), 3. https://doi.org/10.1186/s40101-015-0043-9

Kizuk, S. A. D., & Mathewson, K. E. (2017). Power and phase of alpha oscillations reveal an interaction between spatial and temporal visual attention. *Journal of Cognitive Neuroscience*.

Kizuk, S. A. D., Vuong, W., Maclean, J., Dickson, C. T., & Mathewson, K. E. (n.d.). *Oxygen_ManuscriptDraft_Psychophysiology_SDK_tosubmit*.

Klimesch, W. (2012). Alpha-band oscillations, attention, and controlled access to stored information. *Trends in Cognitive Sciences*, *16*(12), 606–617. https://doi.org/10.1016/j.tics.2012.10.007

Klimesch, W., Sauseng, P., & Hanslmayr, S. (2007). EEG alpha oscillations: The inhibition-timing hypothesis. *Brain Research Reviews*, *53*(1), 63–88. https://doi.org/10.1016/j.brainresrev.2006.06.003

Klimesch, W., Sauseng, P., Hanslmayr, S., Gruber, W., & Freunberger, R. (2007). Event-related phase reorganization may explain evoked neural dynamics. *Neuroscience and Biobehavioral Reviews*, *31*(7), 1003–1016. https://doi.org/10.1016/j.neubiorev.2007.03.005

Knyazev, G. G. (2012). EEG delta oscillations as a correlate of basic homeostatic and motivational processes. *Neuroscience and Biobehavioral Reviews*, *36*(1), 677–695. https://doi.org/10.1016/j.neubiorev.2011.10.002

Kumaria, A., & Tolias, C. M. (2009). Normobaric hyperoxia therapy for traumatic brain injury and stroke: A review. *British Journal of Neurosurgery*, *23*(6), 576–584. https://doi.org/10.3109/02688690903050352

Lahiri, S., Mokashi, A., Mulligan, E., & Nishino, T. (1981). Comparison of aortic and carotid chemoreceptor responses to hypercapnia and hypoxia. *J Appl Physiol*, *51*(1), 55–61. Retrieved from http://jap.physiology.org.login.ezproxy.library.ualberta.ca/content/51/1/55.abstract

Landau, A. N., & Fries, P. (2012). Attention samples stimuli rhythmically. *Current Biology*, *22*(11), 1000–1004. https://doi.org/10.1016/j.cub.2012.03.054

Larson, C. L., Davidson, R. J., Abercrombie, H. C., Ward, R. T., Schaefer, S. M., Jackson, D. C., … Perlman, S. B. (1998). Relations between PET-derived measures of thalamic glucose metabolism and EEG alpha power. *Psychophysiology*, *35*(2), 162–169. https://doi.org/10.1017/S0048577298001620

Lee-Chiong, T. (2005). *Sleep: A Comprehensive Handbook*. https://doi.org/10.1002/0471751723

Lévy, P., Pépin, J. L., Arnaud, C., Tamisier, R., Borel, J. C., Dematteis, M., … Ribuot, C. (2008). Intermittent hypoxia and sleep-disordered breathing: Current concepts and perspectives. *European Respiratory Journal*, *32*(4), 1082–1095.

https://doi.org/10.1183/09031936.00013308

Loftus, G. R., & Masson, M. E. J. (1994). Using confidence intervals in within-subject designs. *Psychonomic Bulletin and Review*, *1*(4), 476–490. https://doi.org/10.3758/BF03210951

Lopes da Silva, F. (2013). EEG and MEG: Relevance to neuroscience. *Neuron*, *80*(5), 1112–1128. https://doi.org/10.1016/j.neuron.2013.10.017

Lopes da Silva, F. H., van Lierop, T. H. M. T., Schrijer, C. F., & Storm van Leeuwen, W. (1973). Organization of thalamic and cortical alpha rhythms: Spectra and coherences. *Electroencephalography and Clinical Neurophysiology*, *35*(6), 627–639. https://doi.org/10.1016/0013-4694(73)90216-2

Loredo, J. S., Ancoli-Israel, S., Kim, E.-J., Lim, W. J., & Dimsdale, J. E. (2006). Effect of Continuous Positive Airway Pressure Versus Supplemental Oxygen on Sleep Quality in Obstructive Sleep Apnea: A Placebo-CPAP−Controlled Study. *Sleep*, *29*(4), 564–571. https://doi.org/10.1093/sleep/29.4.564

Lu, J., Dai, G., Egi, Y., Huang, S., Kwon, S. J., Lo, E. H., & Kim, Y. R. (2009). Characterization of cerebrovascular responses to hyperoxia and hypercapnia using MRI in rat. *NeuroImage*, *45*(4), 1126–1134. https://doi.org/10.1016/j.neuroimage.2008.11.037

Luck, S. J. (2005). An Introduction to the Event-Related Potential Technique.

Lund, V. E., Kentala, E., Scheinin, H., Klossner, J., Helenius, H., Sariola-Heinonen, K., & Jalonen, J. (1999). Heart rate variability in healthy volunteers during normobaric and hyperbaric hyperoxia. *Acta Physiologica Scandinavica*, *167*(1), 29–35. https://doi.org/10.1046/j.1365-201x.1999.00581.x

Lundqvist, M., Rose, J., Herman, P., Brincat, S. L. L., Buschman, T. J. J., & Miller, E. K. K. (2016). Gamma and Beta Bursts Underlie Working Memory. *Neuron*, *90*(1).

https://doi.org/10.1016/j.neuron.2016.02.028

Macey, P. M., Woo, M. A., & Harper, R. M. (2007). Hyperoxic brain effects are normalized by addition of CO2. *PLoS Medicine*, *4*(5), 0828–0835. https://doi.org/10.1371/journal.pmed.0040173

Magistretti, P. J., & Allaman, I. (2015). A Cellular Perspective on Brain Energy Metabolism and Functional Imaging. *Neuron*, *86*(4), 883–901. https://doi.org/10.1016/j.neuron.2015.03.035

Makeig, S., & Onton, J. (2011). ERP Features and EEG Dynamics. *The Oxford Handbook of Event-Related Potential Components*, (July), 1–37. https://doi.org/10.1093/oxfordhb/9780195374148.013.0035

Marczak, M., & Pokorski, M. (2004). Oxygen breathing and ventilation. *Journal of Physiology and Pharmacology*, *55*(1 I), 127–134.

Marin, J. M., Carrizo, S. J., Vicente, E., & Agusti, A. G. N. (2005). Long-term cardiovascular outcomes in men with obstructive sleep apnoea-hypopnoea with or without treatment with continuous positive airway pressure: an observational study. *Lancet*, *365*(9464), 1046–1053. https://doi.org/10.1016/S0140-6736(05)71141-7

Mathewson, K. E., Gratton, G., Fabiani, M., Beck, D. M., & Ro, T. (2009). To see or not to see: prestimulus alpha phase predicts visual awareness. *The Journal of Neuroscience*, *29*(9), 2725–2732. https://doi.org/10.1523/JNEUROSCI.3963-08.2009

Mathewson, K. E., Lleras, A., Beck, D. M., Fabiani, M., Ro, T., & Gratton, G. (2011a). Pulsed out of awareness: EEG alpha oscillations represent a pulsed-inhibition of ongoing cortical processing. *Frontiers in Psychology*, *2*(MAY), 1–15. https://doi.org/10.3389/fpsyg.2011.00099

Mathewson, K. E., Lleras, A., Beck, D. M., Fabiani, M., Ro, T., & Gratton, G. (2011b). Pulsed

out of awareness: EEG alpha oscillations represent a pulsed-inhibition of ongoing cortical processing. *Frontiers in Psychology*, *2*(MAY), 1–15. https://doi.org/10.3389/fpsyg.2011.00099

Mazaheri, A., Nieuwenhuis, I. L. C., Van Dijk, H., & Jensen, O. (2009). Prestimulus alpha and mu activity predicts failure to inhibit motor responses. *Human Brain Mapping*, *30*(6), 1791–1800. https://doi.org/10.1002/hbm.20763

Mehta, V., Vasu, T. S., Phillips, B., & Chung, F. (2013). Obstructive sleep apnea and oxygen therapy: a systematic review of the literature and meta-analysis. *Journal of Clinical Sleep Medicine*, *9*(3), 271–279. https://doi.org/10.5664/jcsm.2500

Michalareas, G., Vezoli, J., van Pelt, S., Schoffelen, J. M., Kennedy, H., & Fries, P. (2016). Alpha-Beta and Gamma Rhythms Subserve Feedback and Feedforward Influences among Human Visual Cortical Areas. *Neuron*, *89*(2), 384–397. https://doi.org/10.1016/j.neuron.2015.12.018

Miller, R. (2013). *Cortico-hippocampal interplay and the representation of contexts in the brain* (Vol. 17). Springer Science & Business Media.

Mircea Steriade, R. W. M. (2005). *Brain Control of Wakefulness and Sleep*. Boston, MA: Springer US. https://doi.org/10.1007/b102230

Mitchell, D. J., McNaughton, N., Flanagan, D., & Kirk, I. J. (2008). Frontal-midline theta from the perspective of hippocampal "theta." *Progress in Neurobiology*, *86*(3), 156–185. https://doi.org/10.1016/j.pneurobio.2008.09.005

Mortola, J. P. (2007). Hypoxia and circadian patterns. *Respiratory Physiology and Neurobiology*, *158*(2–3), 274–279. https://doi.org/10.1016/j.resp.2007.02.005

Moss, M. C., Scholey, A. B., & Wesnes, K. (1998). Oxygen administration selectively enhances

cognitive performance in healthy young adults: a placebo-controlled double-blind crossover study. *Psychopharmacology*, *138*(1), 27–33. https://doi.org/10.1007/s002130050641

Neuper, C., Wörtz, M., & Pfurtscheller, G. (2006). Chapter 14 ERD/ERS patterns reflecting sensorimotor activation and deactivation. *Progress in Brain Research*, *159*, 211–222. https://doi.org/10.1016/S0079-6123(06)59014-4

Ong, J. L., Lo, J. C., Chee, N. I. Y. N., Santostasi, G., Paller, K. A., Zee, P. C., & Chee, M. W. L. (2016). Effects of phase-locked acoustic stimulation during a nap on EEG spectra and declarative memory consolidation. *Sleep Medicine*, *20*, 88–97. https://doi.org/10.1016/j.sleep.2015.10.016

Osipov, G. V, Kurths, J., & Zhou, C. (2009). *Synchronization in Oscillatory Networks*. (C. Bertelle, G. H. E. Duchamp, & H. Kadri-Dahmani, Eds.). Berlin, Heidelberg: Springer Berlin Heidelberg. https://doi.org/10.1007/978-3-540-88073-8

Owens, R. L. (2013). Supplemental Oxygen Needs During Sleep. Who Benefits? *Respiratory Care*, *58*(1), 32–47. https://doi.org/10.4187/respcare.01988

Pack, a I., Cola, M. F., Goldszmidt, a, Ogilvie, M. D., & Gottschalk, a. (1992). Correlation between oscillations in ventilation and frequency content of the electroencephalogram. *Journal of Applied Physiology (Bethesda, Md. : 1985)*, *72*(3), 985–992. Retrieved from http://www.ncbi.nlm.nih.gov/pubmed/1568995

Pagliardini, S., Funk, G. D., & Dickson, C. T. (2013). Breathing and brain state: Urethane anesthesia as a model for natural sleep. *Respiratory Physiology and Neurobiology*, *188*(3), 324–332. https://doi.org/10.1016/j.resp.2013.05.035

Paller, K. A., & Voss, J. L. (2004). Memory reactivation and consolidation during sleep, 664–670. https://doi.org/10.1101/lm.75704.otherwise

Pfurtscheller, G., Stancák, A., & Neuper, C. (1996). Event-related synchronization (ERS) in the alpha band — an electrophysiological correlate of cortical idling: A review. *International Journal of Psychophysiology*, *24*(1–2), 39–46. https://doi.org/10.1016/S0167-8760(96)00066-9

Poe, G., Walsh, C., & Bjorness, T. (2010). Cognitive Neuroscience of Sleep. *Progress in Brain Research*, *185*, 1–19. https://doi.org/10.1016/B978-0-444-53702-7.00001-4

Polotsky, V. Y., Rubin, A. E., Balbir, A., Dean, T., Smith, P. L., Schwartz, A. R., & O'Donnell, C. P. (2006). Intermittent hypoxia causes REM sleep deficits and decreases EEG delta power in NREM sleep in the C57BL/6J mouse. *Sleep Medicine*, *7*(1), 7–16. https://doi.org/10.1016/j.sleep.2005.06.006

Pomper, U. (2014). *Functional significance of EEG beta-band oscillations in multisensory perception and selective attention*. Humboldt-Universität zu Berlin. https://doi.org/10.18452

Pomper, U., Keil, J., Foxe, J. J., & Senkowski, D. (2015a). Intersensory attention and temporal orienting operate in parallel and widely independent of each other in sensory and motor cortices, *00*(April), 1–34. https://doi.org/10.1002/hbm.22845

Pomper, U., Keil, J., Foxe, J. J., & Senkowski, D. (2015b). Intersensory selective attention and temporal orienting operate in parallel and are instantiated in spatially distinct sensory and motor cortices. *Human Brain Mapping*, *36*(8), 3246–3259.

Raichle, M. E. (2010). Two views of brain function. *Trends in Cognitive Sciences*, *14*(4), 180–190. https://doi.org/10.1016/j.tics.2010.01.008

Raichle, M. E. (2015). The Brain's Default Mode Network. *Annual Review of Neuroscience*, *38*(1), 433–447. https://doi.org/10.1146/annurev-neuro-071013-014030

Raichle, M. E., & Gusnard, D. a. (2002). Appraising the brain's energy budget. *Proceedings of*

the National Academy of Sciences of the United States of America, *99*(16), 10237–10239. https://doi.org/10.1073/pnas.172399499

Raichle, M. E., & Mintun, M. A. (2006). Brain Work and Brain Imaging. *Annual Review of Neuroscience*, *29*(1), 449–476. https://doi.org/10.1146/annurev.neuro.29.051605.112819

Rial, R. V., Nicolau, M. C., Gamundí, A., Akaârir, M., Aparicio, S., Garau, C., … Esteban, S. (2007). The trivial function of sleep. *Sleep Medicine Reviews*, *11*(4), 311–325. https://doi.org/10.1016/j.smrv.2007.03.001

Rizzuto, D. S., Madsen, J. R., Bromfield, E. B., Schulze-Bonhage, A., & Kahana, M. J. (2006). Human neocortical oscillations exhibit theta phase differences between encoding and retrieval. *NeuroImage*, *31*(3), 1352–1358. https://doi.org/10.1016/j.neuroimage.2006.01.009

Romei, V., Brodbeck, V., Michel, C., Amedi, A., Pascual-Leone, A., & Thut, G. (2008). Spontaneous fluctuations in posterior alpha-band EEG activity reflect variability in excitability of human visual areas. *Cerebral Cortex*, *18*(9), 2010–2018. https://doi.org/10.1093/cercor/bhm229

Roux, F., & Uhlhaas, P. J. (2014). Working memory and neural oscillations: Alpha-gamma versus theta-gamma codes for distinct WM information? *Trends in Cognitive Sciences*, *18*(1), 16–25. https://doi.org/10.1016/j.tics.2013.10.010

Samaha, J., Bauer, P., Cimaroli, S., & Postle, B. R. (2015). Top-down control of the phase of alpha-band oscillations as a mechanism for temporal prediction. *Proceedings of the National Academy of Sciences of the United States of America*, *112*(27), 8439–8444. https://doi.org/10.1073/pnas.1503686112

Saunamäki, T., Himanen, S.-L., Polo, O., & Jehkonen, M. (2009). Executive Dysfunction in Patients with Obstructive Sleep Apnea Syndrome. *European Neurology*, *62*(4), 237–242.

https://doi.org/10.1159/000232156

Sauseng, P., Klimesch, W., Gerloff, C., & Hummel, F. C. (2009). Spontaneous locally restricted EEG alpha activity determines cortical excitability in the motor cortex. *Neuropsychologia*, *47*(1), 284–288. https://doi.org/10.1016/j.neuropsychologia.2008.07.021

Schlesinger, M. F., & West, B. J. (1988). 1/f versus 1/fa noise. *Random Fluctuations and Pattern Growth: Experiments and Models*, 320–324.

Scholey, A. B., Moss, M. C., Neave, N., & Wesnes, K. (1999). Cognitive Performance, Hyperoxia, and Heart Rate Following Oxygen Administration in Healthy Young Adults. *Physiology & Behavior*, *67*(5), 783–789. https://doi.org/10.1016/S0031-9384(99)00183-3

Scholey, A. B., Moss, M. C., & Wesnes, K. (1998). Oxygen and cognitive performance: The temporal relationship between hyperoxia and enhanced memory. *Psychopharmacology*, *140*(1), 123–126. https://doi.org/10.1007/s002130050748

Schürmann, M., Başar-Eroglu, C., & Başar, E. (1997). Gamma responses in the EEG. *NeuroReport*, *8*(2), 531–534. https://doi.org/10.1097/00001756-199701200-00030

Seo, H. J., Bahk, W. M., Jun, T. Y., & Chae, J. H. (2007, February 1). The effect of oxygen inhalation on cognitive function and EEG in healthy adults. *Clinical Psychopharmacology and Neuroscience*. The Korean College of Neuropsychopharmacology. Retrieved from http://www.cpn.or.kr/journal/view.html?spage=25&volume=5&number=1

Shannahoff-Khalsa, D. (2007). Psychophysiological States: the Ultradian Dynamics of Mind-Body Interactions. *International Review of Neurobiology*, *80*(07), 1–220. https://doi.org/10.1016/S0074-7742(07)80001-8

Sheng, M., Liu, P., Mao, D., Ge, Y., & Lu, H. (2017). The impact of hyperoxia on brain activity: A resting-state and task-evoked electroencephalography (EEG) study. *PLoS ONE*, *12*(5), 1–

14. https://doi.org/10.1371/journal.pone.0176610

Shi, S., Qi, Z., Luo, Y., Ji, X., & Liu, K. (2016). Normobaric oxygen treatment in acute ischemic stroke: a clinical perspective. *Medical Gas Research*, *6*(3), 147. https://doi.org/10.4103/2045-9912.191360

Shibata, S., Iwasaki, K. I., Ogawa, Y., Kato, J., & Ogawa, S. (2005). Cardiovascular neuroregulation during acute exposure to 40, 70, and 100% oxygen at sea level. *Aviation Space and Environmental Medicine*, *76*(12), 1105–1110.

Siegel, J. M. (2001). The REM Sleep-Memory Consolidation Hypothesis. *Science*, *294*(5544), 1058–1063. https://doi.org/10.1126/science.1063049

Siegel, J. M. (2005). Clues to the functions of mammalian sleep. *Nature*, *437*(7063), 1264–1271. https://doi.org/10.1038/nature04285

Siegel, J. M. (2008). Do all animals sleep? *Trends in Neurosciences*, *31*(4), 208–213. https://doi.org/10.1016/j.tins.2008.02.001

Silva, F. L. da. (1991). Neural mechanisms underlying brain waves: from neural membranes to networks. *Electroencephalography and Clinical Neurophysiology*, *79*, 81–93. Retrieved from http://www.sciencedirect.com/science/article/pii/0013469491900445

Sokoliuk, R., & VanRullen, R. (2016). Global and local oscillatory entrainment of visual behavior across retinotopic space. *Scientific Reports*, *6*(April), 25132. https://doi.org/10.1038/srep25132

Sokoloff, L., Reivich, M., Kennedy, C., Rosiers, M. H. Des, Patlak, C. S., Pettigrew, K. D., … Shinohara, M. (1977). The [14 C]Deoxyglucose Method for the Measurement of Local Cerebral Glucose Utilization: Theory, Procedure, and Normal Values in the Conscious and Anesthetized Albino Rat. *Journal of Neurochemistry*, *28*(5), 897–916.

https://doi.org/10.1111/j.1471-4159.1977.tb10649.x

Spaak, E., Bonnefond, M., Maier, A., Leopold, D. A. A., & Jensen, O. (2012). Layer-Specific Entrainment of Gamma-Band Neural Activity by the Alpha Rhythm in Monkey Visual Cortex. *Current Biology*, *22*(24), 2313–2318. https://doi.org/10.1016/j.cub.2012.10.020

Spaak, E., de Lange, F. P., & Jensen, O. (2014). Local entrainment of α oscillations by visual stimuli causes cyclic modulation of perception. *The Journal of Neuroscience : The Official Journal of the Society for Neuroscience*, *34*(10), 3536–3544. https://doi.org/10.1523/JNEUROSCI.4385-13.2014

Srinivasan, R., Winter, W. R., & Nunez, P. L. (2006). Source analysis of EEG oscillations using high-resolution EEG and MEG, *159*, 29–42. https://doi.org/10.1016/S0079-6123(06)59003-X

Steriade, M. (2000). Corticothalamic resonance, states of vigilance and mentation. *Neuroscience*, *101*(2), 243–276. https://doi.org/10.1016/S0306-4522(00)00353-5

Steriade, M. (2003). The corticothalamic system in sleep. *Frontiers in Bioscience : A Journal and Virtual Library*, *8*, d878-99. https://doi.org/10.1016/j.neuroimage.2007.02.026

Steriade, M., & Amzica, F. (1998). Coalescence of sleep rhythms and their chronology in corticothalamic networks. *Sleep Research Online : SRO*, *1*(1), 1–10. Retrieved from http://www.ncbi.nlm.nih.gov/pubmed/11382851

Stickgold, R. (2005). Sleep-dependent memory consolidation. *Nature*, *437*(October). https://doi.org/10.1038/nature04286

Stoller, J. K., Panos, R. J., Krachman, S., Doherty, D. E., & Make, B. (2010). Oxygen therapy for patients with COPD: Current evidence and the long-term oxygen treatment trial. *Chest*, *138*(1), 179–187. https://doi.org/10.1378/chest.09-2555

Strauss, M., Sitt, J. D., King, J.-R., Elbaz, M., Azizi, L., Buiatti, M., … Dehaene, S. (2015). Disruption of hierarchical predictive coding during sleep. *Proceedings of the National Academy of Sciences of the United States of America*, *112*(11), E1353-62. https://doi.org/10.1073/pnas.1501026112

Thut, G., Nietzel, A., Brandt, S. a, & Pascual-Leone, A. (2006). Alpha-band electroencephalographic activity over occipital cortex indexes visuospatial attention bias and predicts visual target detection. *The Journal of Neuroscience : The Official Journal of the Society for Neuroscience*, *26*(37), 9494–9502. https://doi.org/10.1523/JNEUROSCI.0875-06.2006

Tononi, G., Edelman, G. M., & Sporns, O. (1998). Complexity and coherency: Integrating information in the brain. *Trends in Cognitive Sciences*, *2*(12), 474–484. https://doi.org/10.1016/S1364-6613(98)01259-5

Tsanov, M., Chah, E., Reilly, R., & O'Mara, S. M. (2014). Respiratory cycle entrainment of septal neurons mediates the fast coupling of sniffing rate and hippocampal theta rhythm. *European Journal of Neuroscience*, *39*(6), 957–974. https://doi.org/10.1111/ejn.12449

Von Stein, A., & Sarnthein, J. (2000). Different frequencies for different scales of cortical integration: From local gamma to long range alpha/theta synchronization. *International Journal of Psychophysiology*, *38*(3), 301–313. https://doi.org/10.1016/S0167-8760(00)00172-0

Walker, M. P., & Stickgold, R. (2004). Sleep-dependent learning and memory consolidation. *Neuron*, *44*(1), 121–133. https://doi.org/10.1016/j.neuron.2004.08.031

Walsh, C., Thimmesch, A. R., D'Achiardi, A., & Pierce, J. D. (2011). Oxygen Bar Effectiveness: A Randomized Quantitative Study. *Journal of Complementary and Integrative Medicine*,

8(1). https://doi.org/10.2202/1553-3840.1424

Waring, W. S., Thomson, A. J., Adwani, S. H., Rosseel, A. J., Potter, J. F., Webb, D. J., & Maxwell, S. R. J. (2003). Cardiovascular effects of acute oxygen administration in healthy adults. *J Cardiovasc Pharmacol*, *42*(2), 245–250. https://doi.org/10.1097/00005344-200308000-00014

Watson, N. A., Beards, S. C., Altaf, N., Kassner, A., & Jackson, A. (2000). The effect of hyperoxia on cerebral blood flow: A study in healthy volunteers using magnetic resonance phase-contrast angiography. *European Journal of Anaesthesiology*, *17*(3), 152–159. https://doi.org/10.1046/j.1365-2346.2000.00640.x

Whitten, T. A., Hughes, A. M., Dickson, C. T., & Caplan, J. B. (2011). A better oscillation detection method robustly extracts EEG rhythms across brain state changes: The human alpha rhythm as a test case. *NeuroImage*, *54*(2), 860–874. https://doi.org/10.1016/j.neuroimage.2010.08.064

Whitten, T. a, Martz, L. J., Guico, A., Gervais, N., & Dickson, C. T. (2009). Heat synch: inter- and independence of body-temperature fluctuations and brain-state alternations in urethane-anesthetized rats. *Journal of Neurophysiology*, *102*(3), 1647–1656. https://doi.org/10.1152/jn.00374.2009

Wilson, M. A., & McNaughton, B. L. (1994). Reactivation of hippocampal ensemble memories during sleep. *Science*, *265*(5172), 676–679. https://doi.org/10.1126/science.8036517

Winder, R., & Borrill, J. (1998). Fuels for memory: the role of oxygen and glucose in memory enhancement. *Psychopharmacology*, *136*(4), 349–356. Retrieved from http://www.ncbi.nlm.nih.gov/pubmed/9600580

Winter, O., Kok, A., Kenernans, J. L., & Elton, M. (1995). Auditory event-related potentials to

deviant stimuli during drowsiness and stage 2 sleep. *Electroencephalography and Clinical Neurophysiology/ Evoked Potentials*, *96*(5), 398–412. https://doi.org/10.1016/0168-5597(95)00030-V

Wu, Y. W., Tang, C. Y., Ng, J., Wong, E., Carpenter, D., & Tao, X. (2014). Effects of hyperoxia on resting state functional magnetic resonance imaging. https://doi.org/10.1097/WNR.0000000000000239

Xu, W., Chi, L., Row, B. W., Xu, R., Ke, Y., Xu, B., … Liu, R. (2004). Increased oxidative stress is associated with chronic intermittent hypoxia-mediated brain cortical neuronal cell apoptosis in a mouse model of sleep apnea. *Neuroscience*, *126*(2), 313–323. https://doi.org/10.1016/j.neuroscience.2004.03.055

Yackle, K., Schwarz, L. A., Kam, K., Sorokin, J. M., Huguenard, J. R., Feldman, J. L., … Krasnow, M. A. (2017). Breathing control center neurons that promote arousal in mice, *1415*(March), 1411–1415.